The Institute of Paper Chemistry

Appleton, Wisconsin

Doctor's Dissertation

The Diffusional Properties of Sodium Hydroxide

A. David Fary, Jr.

January, 1966

THE DIFFUSIONAL PROPERTIES OF SODIUM HYDROXIDE

A thesis submitted by

A. David Fary, Jr.

B.S. 1960, North Carolina State College
M.S. 1962, Lawrence College

in partial fulfillment of the requirements
of The Institute of Paper Chemistry
for the degree of Doctor of Philosophy
from Lawrence University,
Appleton, Wisconsin

January, 1966

TABLE OF CONTENTS

SUMMARY

Studies of the concentration-dependence of electrolyte diffusion have been made for quite a number of neutral electrolytes and for a few acids. These studies reveal that the diffusion of 1:1 electrolytes such as sodium chloride and potassium chloride are consistent with the Onsager-Fuoss theory at low concentrations and at 25°C. In addition, it has been found that hydrochloric acid diffusion is compatible with the Onsager-Fuoss theory at high concentrations. It was thus the main purpose of this thesis to investigate the premise that sodium hydroxide diffusion was reasonably consistent with the Onsager-Fuoss theory over a relatively wide range of concentration. Second, it was the objective of the thesis to determine why the diffusion of sodium hydroxide did not fit the Onsager-Fuoss theory if the above premise were found invalid. While much experimentation has been done concerning concentration-dependence of electrolyte diffusion, the temperature-dependence of diffusion has received essentially no consideration. The final purpose of the thesis was to study the temperature-dependence of sodium hydroxide diffusion in light of the reaction rate theory.

The "oil lye" method of sodium hydroxide purification was shown to be quite satisfactory for preparing solutions for physicochemical study if the procedure were slightly modified and the manipulations carried out in a controlled atmosphere.

From a comparison of the diffusion of sodium hydroxide at 25°C. with the predictions of the Onsager-Fuoss theory, it was shown that the premise of the applicability of the theory was invalid except at very low concentrations. It was shown also that the modified Hartley-Crank relationship, for solvent counter-diffusion, hydration effects, and solution viscosity changes, was not applicable except at low concentrations. At low concentrations, the Hartley-Crank

relationship showed that the sodium ion was hydrated as in other electrolytes but the hydroxide ion was not.

It was shown that sodium hydroxide conductivity data from the literature could be analyzed theoretically, up to three-tenths molal, by: (1) treating the ions individually and applying Kohlrausch's law, (2) applying the electrophoretic correction and Falkenhagen relaxation correction to the sodium ion, (3) applying only the relaxation correction to the hydroxide ion, and (4) utilizing the value of the distance of closest approach obtained from activity data. Above three-tenths molal, it was shown from conductivity data of sodium hydroxide that ion-pairs existed in solution and the extent of the phenomenon was calculated.

It was found that the extent of ion-pair formation calculated from conductivity data could be used in the modified Hartley-Crank relationship to calculate the diffusion coefficient of the ion-pair. A slight decrease, with increasing sodium hydroxide concentration, was shown for the calculated ion-pair diffusion coefficients. By considering the effects of size, shape, and diffusion mechanism, it was shown that the calculated values of the ion-pair diffusion coefficients were quite realistic. From nuclear magnetic resonance data in the literature, it was found that ion-pairs would be present in sodium hydroxide solution but not in potassium hydroxide solutions. Limited potassium hydroxide diffusion data from the literature showed that this electrolyte exhibited the characteristic minimum in the diffusion coefficient-concentration curve as expected from the N.M.R. data.

From the investigation of the diffusion of sodium hydroxide at 20, 30, and 35°C., it was shown that the general concentration-dependence effects exhibited at 25°C. were present at the other temperatures. The concentration-dependence did, however, tend to decrease with increasing temperature in the high concentration

range. By analyzing the temperature-dependence according to the reaction rate theory, it was shown that there were two regions of diffusion behavior with respect to temperature at a concentration of one-tenth normal. The region of highest activation energy was attributed to the existence of ion-pairs (42) and the lowest activation energy region being essentially free of ion-pairs. At seven-tenths normal, it was found that the activation energy tended to decrease slightly with increasing temperature. Comparison of the temperature-dependence of sodium chloride diffusion with that of sodium hydroxide showed that the sodium chloride activation energy was greater by as much as 1400 cal./mole. This difference was considered to be evidence for the existence of a Grotthus-type transfer mechanism (36) for sodium hydroxide diffusion in the absence of ion-pairs.

INTRODUCTION

Because of its tremendous industrial usage and importance, one would expect that the diffusional behavior of sodium hydroxide has been thoroughly investigated and discussed. However, a review of the literature showed that such was not the case. In fact, no experimental data on sodium hydroxide diffusion has been found in literature since 1904 (1). In addition, correspondence with the five major producers of sodium hydroxide showed that there were no unpublished data available either. While some data were available from the work of 1904, these results were obtained at 18°C., with limited temperature control, and utilizing a measurement method which gave integral diffusion coefficients instead of differential coefficients. At 18°C., the amount of auxiliary information available for theoretically analyzing diffusion data is quite negligible, if at all existent. Also, the diffusion data available for sodium hydroxide were of the integral type and were therefore not amenable to theoretical analysis.

In theoretically analyzing simple electrolyte diffusion, the theory of Onsager and Fuoss (2) has been the most successful and widely utilized. It is seen in Fig. 1 (3) and 2 (3) that the Onsager-Fuoss theory will predict diffusion coefficients with reasonable accuracy for potassium chloride and sodium chloride, particularly at low concentrations. In addition, it has been pointed out (4) that the diffusion of hydrochloric acid is predicted quite well at high concentrations but not so well at low concentrations. An additional consideration of electrolyte diffusion is the fact that there has been no accurate and detailed study of the temperature-dependence of diffusion in light of the reaction rate theory (5).

Because of the applicability of the Onsager-Fuoss theory to the diffusion of other electrolytes, it was felt that sodium hydroxide diffusion should be reasonably

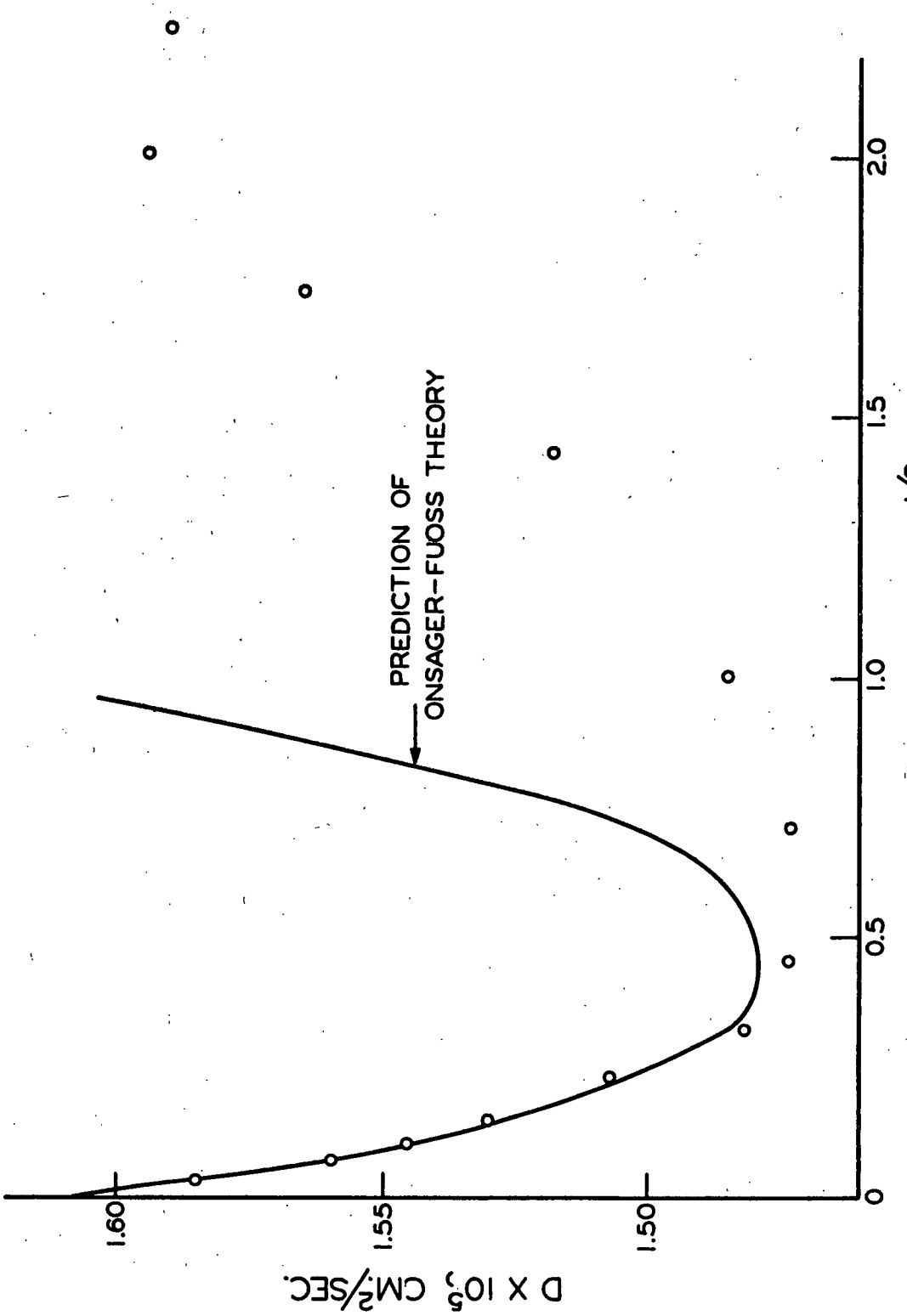

Figure 1. The Diffusion of Sodium Chloride at 25°C. (3)

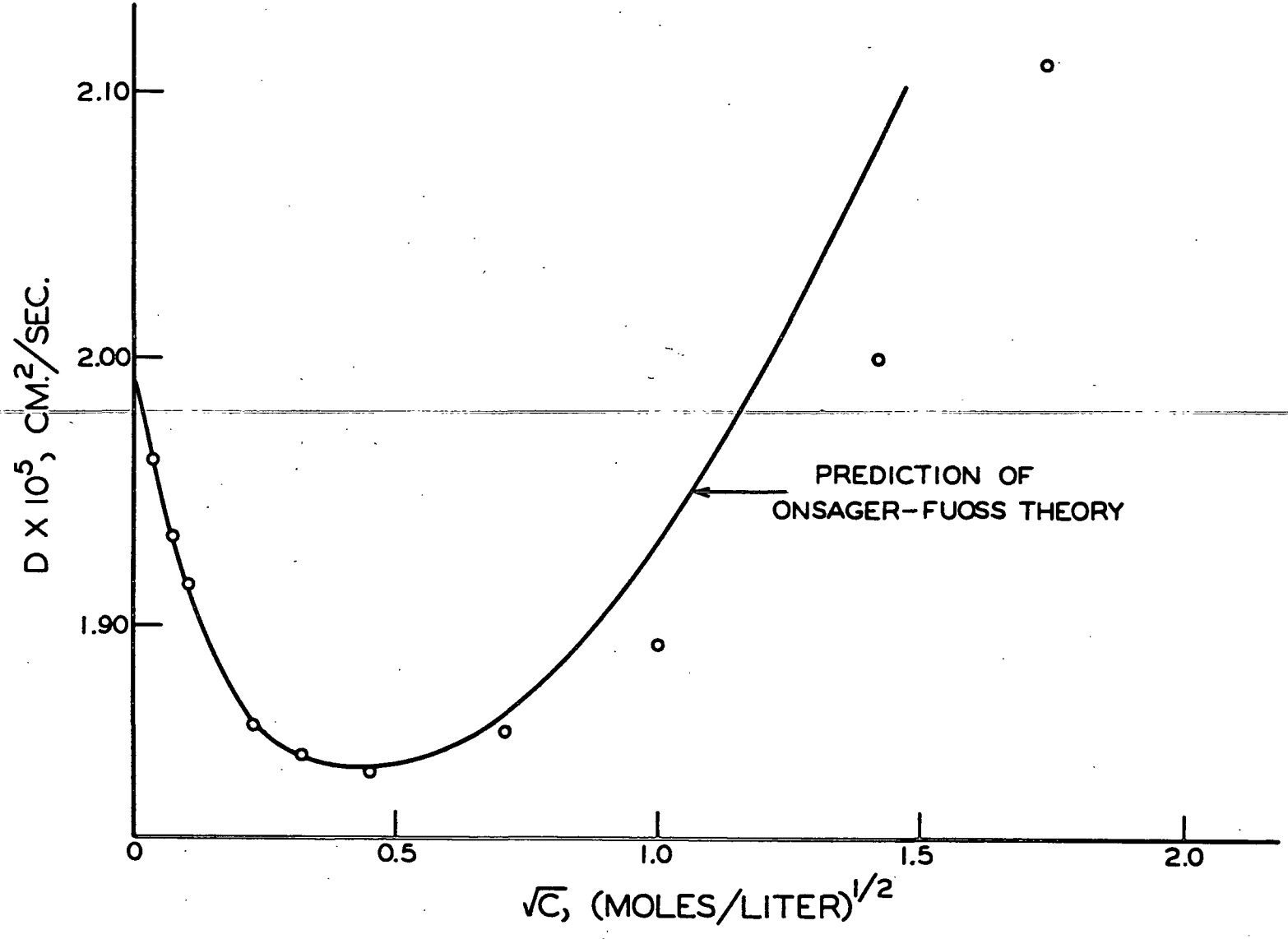

Figure 2. The Diffusion of Potassium Chloride at 25°C. (3)

consistent with the theory. This conclusion was arrived at because the chloride ion was present in both cases and was, therefore, not expected to be responsible for the compatibility of the acid diffusion with theory at high concentrations. Thus, due to the similarity of the hydronium and hydroxide ions in solution, the sodium hydroxide should behave in a reasonably ideal manner at the high end of the concentration range. Also, because of the presence of the sodium ion it would be expected that sodium hydroxide diffusion should coincide with the prediction of the Onsager-Fuoss theory at low concentrations.

The first objective of this study was to determine the validity of the premise that sodium hydroxide diffusion could be reasonably predicted from the Onsager-Fuoss theory. In addition, a second objective of the study was to determine why the diffusion of sodium hydroxide did not behave according to the Onsager-Fuoss theory if the original premise were not supported. Finally, an additional objective of this work was to investigate the temperature-dependence of sodium hydroxide diffusion in light of the reaction rate theory.

THE THEORIES OF DIFFUSION

ELECTROLYTE DIFFUSION THEORY

Attempts to predict the diffusion coefficients of electrolytes in aqueous solution have been in progress for many, many years. While there have been more attempts made than space would allow reporting here, the most successful, from the standpoint of recognition, were provided by Nernst (6), Debye and Hückel (7), and Onsager and Fuoss (2). In acknowledging these theories, it must be mentioned that in the latter two cases (7, 2) the primary concern was obtaining mathematical descriptions of the forces existing in electrolyte solutions. More recently, the work of Kirkwood (8) and of Mayer (9) has been concerned with a more rigorous statistical mechanical approach to solution theory. Although the "cluster theory" of Mayer (9) has been shown to be quite good for the prediction of activity coefficients in more concentrated solutions (10), it has been pointed out (11) that the "cluster theory" is not sufficiently developed for use in studying transport phenomena.

While not designed specifically for electrolytic phenomena, the so-called "theory of absolute rates" (12) has been adopted for use with electrolyte diffusion. Specifically, the theory is primarily concerned with the temperature-dependence of diffusion and considers the effect of concentration on diffusion to be limited to the variation of activity coefficient with concentration.

In the subsequent sections a brief review will be given of the chronological development of electrolyte transport theory. Although such a review might entail several volumes, consideration will be given to the works of Nernst, Debye and Hückel, and Onsager and Fuoss. To conclude the presentation of transport theory, a brief section on the absolute rate theory of diffusion will be presented with particular emphasis on the temperature effect on diffusion.

NERNST'S THEORY OF DIFFUSION

In the theory of Nernst, as developed by Robinson and Stokes (13) and Harned (14), for electrolyte diffusion, it was first assumed that for a single electrolyte

$$V = V_1 = V_2 \tag{1}$$

where the V's were the mean ionic velocity, cation velocity, and anion velocity, respectively. Or, more specifically, in order to maintain electroneutrality all of the ions must move at the same rate. The fluxes of ions are given by

$$J_1 = N_1 V_1 \text{ and } J_2 = N_2 V_2 \tag{2}$$

where the J's are fluxes and the N's are the molecules/cubic centimeter. To evaluate the mean ion velocity, the mobility, ω, is introduced such that

$$V = K_1 \omega_1 = K_2 \omega_2 \tag{3}$$

where the K's are the forces acting on the ions. These forces are related to the total force acting on an electroneutral ensemble of the electrolyte by

$$K = \nu_1 K_1 + \nu_2 K_2 \tag{4}$$

Here, the ν's represent the ions per molecule for the two ionic species. The force, K, acting on the ensemble is now defined as the negative of the gradient of chemical potential, $-\nabla\mu$. From this and Equations (3) and (4), it is possible to show that the mean velocity is given by

$$V = - \frac{\omega_1 \omega_2}{\nu_1 \omega_2 + \nu_2 \omega_1} \nabla\mu \tag{5}.$$

For an ideal solution, the chemical potential is given by

$$\mu = \mu^{\circ} + (\nu_1 + \nu_2)\, kT \ln N \tag{6}$$

where μ° is the chemical potential in a standard state. From this, the gradient of chemical potential is

$$\nabla\mu = (\nu_1 + \nu_2)\, kT \frac{\nabla N}{N} \tag{7}$$

A total flux, $\underline{J}$, may now be defined as

$$J = J_1 + J_2 = N_1 V_1 + N_2 V_2 \tag{8}$$

but from Equation (1), Equation (8) becomes

$$J = (N_1 + N_2)\, V = NV \tag{9}$$

or

$$J = - \frac{(\nu_1 + \nu_2)\omega_1\omega_2}{\nu_1\omega_2 + \nu_2\omega_1} kT\, \nabla N \tag{10}.$$

However, from Fick's law, the flux is defined by the diffusion coefficient according to

$$J = -D\nabla N \tag{11}.$$

Therefore,

$$D_o = \underset{n\to 0}{D} = \frac{(\nu_1 + \nu_2)\omega_1\omega_2}{\nu_1\omega_2 + \nu_2\omega_1} kT \tag{12}$$

which, when the mobilities are defined in terms of the conductivities, becomes

$$D_o = \frac{(\nu_1 + \nu_2)\lambda_1^{\circ}\lambda_2^{\circ}}{\nu_1 |Z_1| \left[\lambda_1^{\circ} + \lambda_2^{\circ}\right]} \frac{RT}{F^2} \tag{13}$$

where the mobility $\omega_i = \dfrac{\mathcal{N}\lambda}{|\underline{Z}_i| \underline{F}^2}$; $\mathcal{N}$ = Avogadro's number; $\underline{k} = \underline{R}/\mathcal{N}$. In Equation (13), the λ's are the equivalent conductances, the $\underline{Z}$'s are the valences per ion, and $\underline{F}$ is the Faraday (96,500 coulombs equiv.$^{-1}$).

If the solution is not ideal as shown by Equation (6), the chemical potential would be given by

$$\mu = \mu^{\circ} + (\nu_1 + \nu_2)\, kT \ln \zeta_{\pm} N \tag{14}$$

where $\zeta_{\pm}$ is the activity coefficient on the molecular scale. Thus,

$$\nabla\mu = (\nu_1 + \nu_2)\, kT \nabla \ln \zeta_{\pm} N \tag{15}$$

or

$$\nabla\mu = (\nu_1 + \nu_2)\, kT \left(1 + N \frac{\partial \ln \zeta_{\pm}}{\partial N}\right) \nabla N/N \tag{16}.$$

From Equations (5), (9), and (11) it is seen that the diffusion coefficient becomes

$$D = \frac{(\nu_1 + \nu_2)\omega_1\omega_2}{\nu_1\omega_2 + \nu_2\omega_1}\, kT \left(1 + N \frac{\partial \ln \zeta_{\pm}}{\partial N}\right) \tag{17}$$

or by (13)

$$D = \frac{(\nu_1 + \nu_2)\lambda_1^{\circ}\lambda_2^{\circ}}{\nu_1 |Z_1| (\lambda_1^{\circ} + \lambda_2^{\circ})}\, \frac{RT}{F^2} \left(1 + N \frac{\partial \ln \zeta_{\pm}}{\partial N}\right) \tag{18}.$$

In the above development it is first assumed that the diffusion coefficient is a constant for a particular electrolyte or that the development applies to the hypothetical diffusion at infinite dilution. Secondly, it is assumed that the deviation from the behavior at infinite dilution is due to the nonideality of the solution equilibrium properties as shown by Equation (14).

While not specifically part of the Nernst derivation, it is worthwhile to note one additional relationship. In Equation (11) it is shown that the flux, J, is given by

$$J = -D\nabla N \tag{11}$$

from Fick's first law. Since it is commonly recognized that the driving force

for diffusion is the gradient of the chemical potential rather than the gradient of concentration per se, Equation (11) may be written in the following form

$$J = -\mathfrak{M}\nabla\mu = -D\nabla N \qquad (19).$$

From this it is seen that

$$D = \left(\frac{\partial\mu}{\partial N}\right)\mathfrak{M} \qquad (20)$$

and Equation (17) may be put in the form

$$D = (\nu_1 + \nu_2)\frac{\mathfrak{M}}{N}\,kT\left(1 + N\frac{\partial \ln \zeta_{\pm}}{\partial N}\right) \qquad (21)$$

or, on a molar concentration scale

$$D = (\nu_1 + \nu_2)\frac{\overline{\mathfrak{M}}}{C}\,1000\,RT\left(1 + C\frac{\partial \ln y_{\pm}}{\partial C}\right) \qquad (22)$$

where $y_{\pm}$ is the mean molar ionic activity coefficient, C is in moles per liter, and $\overline{\mathfrak{M}} = \dfrac{C(\lambda_1^o\lambda_2^o)}{\nu_1|Z_1|(\lambda_1^o + \lambda_2^o)F^2}$.

One of the reasons why Equation (22) is written in this form is to note that from Equations (3) and (5) it is seen that the quantity $(\frac{\overline{\mathfrak{M}}}{C})$ in Equation (22) represents a mean ionic mobility. More specifically, $(\frac{\overline{\mathfrak{M}}}{C})$ represents the ionic mobility in a unit chemical potential field. This point was emphasized because the above derivation of the diffusion coefficient assumes that ion interaction plays no part in the variation of the diffusion coefficient with concentration. In subsequent derivation this mobility term will be adjusted to account for ion-pair interaction.

THE DEBYE-HÜCKEL THEORY

Although they were not the first to recognize the effect of electrostatic forces on the thermodynamic and irreversible properties of electrolyte solutions, Debye and Hückel (15, 16) were the first to make any successful mathematical treatment of the problem. Even though Debye and Hückel made no attempt to treat the problem of electrolyte diffusion they did consider the conduction of electrolytes. Thus, this section will be primarily concerned with the description of the forces existing in an electrolyte solution as presented by Debye and Hückel.

This theory is based first on the assumption that strong electrolytes are completely dissociated into ions. If there were no forces acting between ions, they would be randomly distributed in a solution. However, because of the forces between ions as partially described by Coulomb's Law, the probability of finding a positive ion in the vicinity of another positive ion is not as great as the probability of finding a negative ion in the vicinity of a positive ion. In order to account for the electrostatic interactions, Debye and Hückel found it necessary to calculate the average electrical potential ψ_i of a given ion in solution due to the other ions. To do this, the potential was related to the average charge density, ρ, in any region of the solution by Poisson's equation,

$$\nabla^2 \psi = - \frac{4\pi\rho}{D_i} \tag{23}$$

where D_i is the dielectric constant. In spherical co-ordinates, Equation (23) may be represented by

$$\frac{1}{r^2} \cdot \frac{d}{dr} \left(r^2 \frac{d\psi}{dr} \right) = - \frac{4\pi\rho}{D_i} \tag{24}$$

where r is the radial direction from an ion. The charge density in a particular region of solution may be represented by the product of the ions in that region and the charge per ion. The charge density would thus be given by

$$\rho = \sum N_i' q_i \tag{25}$$

where N_i' is the number of ions, i, of charge q_i in a region of potential ψ. To represent the number of ions, N_i', in a region of potential ψ, Debye and Hückel chose to use the Boltzmann distribution law in the form

$$N_i' = N_i e^{-q_i \psi / kT} \tag{26}$$

where the potential energy is given by $q_i \psi$. If Equations (25) and (26) are combined, the result is

$$\rho = \sum N_i q_i e^{-q_i \psi / kT} \tag{27}.$$

Debye and Hückel then assumed that the potential energy, $q_i \psi$, was much less than the average thermal energy, kT, and the exponential term in (27) was expanded to give

$$e^{-q_i \psi / kT} = 1 - \frac{q_i \psi}{kT} + \frac{1}{2!} \left(\frac{q_i \psi}{kT} \right)^2 - \frac{1}{3!} \left(\frac{q_i \psi}{kT} \right)^3 + \ldots \tag{28}.$$

All terms beyond the second were neglected, and ρ thus became

$$\rho = \sum N_i q_i - \frac{\psi}{kT} \sum N_i q_i^2 \tag{29}.$$

If q_i is represented by $Z_i \epsilon$, the first term of (29) vanishes by the requirement of over-all neutrality and the charge density is given by

$$\rho = - \frac{\psi \epsilon^2}{kT} \sum N_i Z_i^2 \tag{30}$$

where ϵ is the electronic charge and Z_i is the valence of the i ion.

In order to determine the average potential about ions in the solution, Equation (24) and (30) were combined to give

$$\frac{1}{r^2} \cdot \frac{d}{dr}\left(r^2 \frac{d\psi}{dr}\right) = \frac{4\pi\epsilon^2\psi}{D_i kT} \sum N_i Z_i^2 \qquad (31).$$

In order to simplify Equation (31), the following definition was made

$$b^2 = \frac{4\pi\epsilon^2}{D_i kT} \sum N_i Z_i^2 \qquad (32).$$

This reduced Equation (31) to

$$\frac{d}{dr}\left(r^2 \frac{d\psi}{dr}\right) = b^2 r^2 \psi \qquad (33)$$

which has the general solution

$$\psi_j = \frac{A}{r} e^{-br} \quad \frac{B}{r} \quad e^{br} \qquad (34)$$

Since ψ_j must vanish as r goes to infinity, B must be equal to zero. This gives

$$\psi = \frac{A}{r} e^{-br} \qquad (35).$$

Debye and Hückel reasoned that when $b = 0$, the concentration was zero, and hence the potential was that of a single ion in the absence of any other charges. Thus, Equation (35) became

$$\psi_j = \frac{Z\epsilon}{D_i r} e^{-br} \qquad (36).$$

This solution for the potential, however, assumed that each ion was a point charge and had no volume.

Later, Debye (17, 18) accounted for the volume of ions by observing that ψ in Equation (35) represented the potential of an ion and its atmosphere at some distance r from that ion. Thus, the potential could be written as

$$\psi_j(r) = \frac{Z_j\epsilon}{D_i r} + \psi^*(r) \qquad (37)$$

where the first term represented the potential at r due to the ionic charge $Z_j\epsilon$ and $\psi^*(r)$ represented the potential of the ionic atmosphere at this distance. If the ion were represented by a rigid sphere of diameter a_j or distance of closest approach of another ion then in order to insure a continuous field the gradient of the total potential $\partial\psi_j(r)/\partial r$, must be equal to the gradient of the potential of the ion alone, $\partial/\partial r(Z_j\epsilon/D_i r)$, when $r = a_j$. Thus, from Equation (35)

$$\frac{\partial\psi_j(r)}{\partial r} = -\frac{A}{r^2}(1 + br)\, e^{-br} \tag{38}$$

and

$$\frac{\partial}{\partial r}\left(\frac{Z_j\epsilon}{D_i r}\right) = -\frac{Z_j\epsilon}{D_i r^2} \tag{39}.$$

From Equations (38) and (39), the value of A was obtained, for $r = a_j$ as

$$A = \frac{Z_j\epsilon}{D_i} \cdot \frac{e^{ba_j}}{(1+ba_j)} \tag{40}.$$

Hence, the Debye-Hückel average potential about an ion was given by

$$\psi_j(r) = \frac{Z_j\epsilon e^{b(a_j-r)}}{D_i(1+ba_j)r} \tag{41}$$

when the ion was considered as a rigid sphere of diameter a_j.

Although they did not treat the problem of electrolyte diffusion, Debye and Hückel (18) did analyze electrolyte conduction in light of the above treatment. In so doing they recognized two electrostatic effects which would alter the mobility of ionic species in a solution subjected to external forces. These two phenomena are referred to as the electrophoretic effect and the relaxation effect (19). The electrophoretic effect arises from the fact that when an ion moves through a viscous medium there is a tendency for it to drag along solution

in its vicinity. Therefore, neighboring ions must move with or against the stream, and not in a stationary medium, depending on whether they are in the direction of the first ion or opposite. It is apparent that the effect is concentration-dependent and will thus produce an effect on the mobility of an ion in an irreversible process. The relaxation effect arises from the condition whereby the influence of an external force on an ion tends to disturb the symmetrical distribution of ions about a central ion in a solution at equilibrium. As a result of the external force, the central ion will tend to move out of a position of spherical symmetry with respect to its atmosphere and will thereby experience a restoring force. This restoring force would be expected to die away rapidly as a result of thermal motions of the ions which tend to reorganize the atmosphere of the ion under consideration. Thus, the relaxation effect tends to alter the ion mobility for a given external force and is, in addition, a concentration-dependent effect.

THE ONSAGER-FUOSS THEORY

The theoretical work of Onsager and Fuoss (2) was primarily an extension of the results of Debye and Hückel (7) with a more vigorous treatment of solution theory and the inclusion of an analysis of the diffusion process. Their general derivation (2, 20) for the description of irreversible processes, first, involved obtaining a distribution function which would describe the chance of finding two ions in two volume elements of solution, dV_1 and dV_2, at the same time. These volume elements are vector distances $\vec{r}_1$ and $\vec{r}_2$ from a point of reference. If two types of ions, i and j, were considered, the average bulk concentrations of these ions could be represented by N_i and N_j. In addition, N_{ji} was defined as the time average concentration of i ions in dV_2 in the vicinity of a single j ion in dV_1; likewise N_{ij} was the time average concentration of j ions in dV_1 in the

vicinity of an i ion in dV_2. Due to certain general considerations, N_{ji} and N_{ij} were represented by the vector functions

$$N_{ji} = N_{ji}(\vec{r}_1, \vec{r}_{21})$$

$$N_{ij} = N_{ij}(\vec{r}_2, \vec{r}_{12}) \tag{42}$$

where $\vec{r}_{21}$ and $\vec{r}_{12}$ were the vector distances between volume elements dV_1 and dV_2. As a result of the above definitions and probability considerations, Onsager and Fuoss showed that the desired distribution functions were given by

$$f_{ji}(\vec{r}_1, \vec{r}_{21}) = N_j N_{ji}(\vec{r}_1, \vec{r}_{21})$$

$$f_{ij}(\vec{r}_2, \vec{r}_{12}) = N_i N_{ij}(\vec{r}_2, \vec{r}_{12}) \tag{43}$$

and that

$$f_{ji}(\vec{r}_1, \vec{r}_{21}) = f_{ij}(\vec{r}_2, \vec{r}_{12}) \tag{44}$$

In these expressions, f_{ji} represents the concentration of i ions in the atmospheres of N_j ions of the type j. Thus, the first requirement for the description of irreversible processes was fulfilled.

The second requirement was that of evaluating the forces acting on the ions due to the presence of the ions themselves and to external forces.

By expressing the velocities of an i ion in the neighborhood of a j ion by

$$V_{ji} = V_{ji}(\vec{r}_1, \vec{r}_{21})$$

and similarly

$$V_{ij} = V_{ij}(\vec{r}_2, \vec{r}_{12}) \tag{45}$$

it was possible to relate the two velocities by use of the equation of continuity. Thus, as shown in (21), the following equation was derived

$$- \frac{\partial f_{ji}(\vec{r}_1, \vec{r}_{21})}{\partial t} = \nabla_1 \cdot (f_{ij} V_{ij}) + \nabla_2 \cdot (f_{ji} V_{ji}) = - \frac{\partial f_{ij}(\vec{r}_2, \vec{r}_{12})}{\partial t} \qquad (46).$$

In Equation (46), the subscripts 1 and 2 on the operators refer to differentiation with respect to the vectors $\vec{r}_1$ and $\vec{r}_2$. For the case of steady state, Equation (46) reduces to

$$\nabla_1 \cdot (f_{ij} V_{ij}) + \nabla_2 \cdot (f_{ji} V_{ji}) = 0 \qquad (47).$$

It is pointed out (21) that ions move as a result of external or internal forces on the ions, thermal motion, and bulk flow of the solution. The forces on the ions may be the result of an electric field, a concentration gradient, or electrostatic interaction of the ions. For an i ion exposed to a force K_i and having a mobility ω_i, the velocity of the ion will be $K_i \omega_i$. For an assumed diffusion coefficient per ion of $kT\omega_i$ and a concentration gradient ∇_{fi}, the total velocity, V_{ji}, is given by

$$V_{ji} = V(\vec{r}_2) + \omega_i (K_{ji} - kT\nabla_2 \ln f_{ji})$$

and

$$V_{ij} = V(\vec{r}_1) + \omega_j (K_{ij} - kT\nabla_1 \ln f_{ij}) \qquad (48)$$

where $V(\vec{r}_1)$ and $V(\vec{r}_2)$ and the bulk velocities of the solution at the points $\vec{r}_1$ and $\vec{r}_2$. If the velocities, V_{ji} and V_{ij}, in Equation (48) are utilized in Equation (47), the result is, for steady state,

$$\nabla_1 \cdot [f_{ij} V(\vec{r}_1) + \omega_j (f_{ij} K_{ij} - kT\nabla_1 f_{ij})] + \nabla_2 \cdot [f_{ji} V(\vec{r}_2) + \omega_i (f_{ji} K_{ji} - kT\nabla_2 f_{ji})] = 0 \qquad (49).$$

While Equation (49) is the general equation of continuity for a generalized irreversible process, the case of electrolyte diffusion may be treated in a

seemingly simpler manner. Such an analysis was made by Onsager and Fuoss (2) for diffusion in the following manner.

Due to the requirement, for the diffusion process, of over-all electroneutrality, the relaxation effect previously discussed would not exist for this case. Thus, the problem for diffusion would be to account for the electrophoretic effect on the mobility. This effect was evaluated by first defining the forces acting on the ions in a unit volume as

$$\sum_{j=1}^{s} N_j K_j = N_\sigma K_\sigma \qquad (50)$$

where N_j is the average concentration of j-ions, K_j is the force acting on each j-ion, N_σ is average total ion concentration, K_σ is the average force acting on each ion in solution, and s is the number of types of ions. These forces, for an equilibrium case, will be transferred to the N_o solvent molecules to give for the bulk properties

$$N_\sigma K_\sigma + N_o K_o = 0 \qquad (51).$$

However, if an element of volume dV is considered near a j-ion, the force acting on the ions in this volume will be different due to the change in concentration in dV as a result of the presence of the j-ion which produces an electrostatic attraction. Since the force on the solvent is unaffected by the electrostatic forces, it will remain as $N_o K_o dV$. Thus, there is a net force acting on the volume dV which is equal to

$$(N_{j\sigma} K_\sigma + N_o K_o)dV = (N_{j\sigma} - N_\sigma)K_\sigma dV \qquad (52).$$

Thus, in spherical co-ordinates, the force acting on a shell of solution at a distance r from the j-ion is

$$dF_j = 4\pi r^2 (N_{j\sigma} - N_\sigma) K_\sigma dr \qquad (53).$$

If the applicability of Stokes' equation is assumed, then the change in velocity dV_j of an ion due to the above form is

$$dV_j = \frac{dF_j}{6\pi\eta r} \qquad (54)$$

where η is the liquid viscosity and r is the radius of the ion's atmosphere. In order to evaluate the force in Equation (53) it is necessary to utilize the Boltzmann distribution from Equation (26) in an expanded form. This gives

$$N_{j\sigma} \approx N_\sigma \left\{ 1 - \frac{q_j \psi_j}{kT} + \frac{1}{2} \left(\frac{q_j \psi_j}{kT} \right)^2 \right\} \qquad (55)$$

where the potential, ψ_j, is equal to the function given in Equation (41); namely,

$$\psi_j = \frac{Z_j \epsilon e^{b(a_j - r)}}{D_k (1 + ba_j) r} \qquad (41).$$

When Equations (41), (55), and (53) are introduced into Equation (54), the limits of integration of the radius function are set at a_j to ∞, and the force $K_j = V/\omega_j$, the electrophoretic correction to the diffusion velocity of a 1-1 electrolyte, is given by

$$\Delta V_j = \frac{-2}{3\eta} \left(\frac{N_1 q_1}{\omega_1} + \frac{N_2 q_2}{\omega_2} \right) \frac{q_j V}{D_i kTb(1 + ba_j)} +$$

$$\frac{1}{3\eta} \left(\frac{N_1 q_1^2}{\omega_1} + \frac{N_2 q_2^2}{\omega_2} \right) \frac{v q_j^2}{(D_i kT)^2} \phi(ba) \qquad (56)$$

where

$$\phi(ba) = e^{2ba} Ei(2ba)/(1 + ba)^2$$

and

$$Ei(X) = \int_X^\infty e^{-t}\,\frac{dt}{t} = -0.5772 - \log X + X - \frac{X^2}{2.2!} + \frac{X^3}{3.3!} - \frac{X^4}{4.4!} + \frac{X^5}{5.5!} - \ldots$$

and $\underline{X} = 2\underline{ba}$.

For the simple electrolyte considered, the velocity correction in Equation (56) will influence the forces $\underline{K}_1$ and $\underline{K}_2$ by

$$K_j = \rho_j(V - \Delta V_j) \qquad (j = 1,2) \tag{57}$$

where $\rho_{\underline{j}} = 1/\omega_{\underline{j}}$. From Equation (4) and the definition of $\underline{K}$, it is seen that for a 1-1 electrolyte

$$-\nabla\mu = K = \nu_1\rho_1(V-\Delta V_1) + \nu_2\rho_2(V-\Delta V_2) \tag{58}$$

which may be employed along with Equation (56) to eliminate $\Delta\underline{V}_1$ and $\Delta\underline{V}_2$ and give

$$-\nabla\mu = V\left[\nu_1\rho_1 + \nu_2\rho_2 + (\rho_1 - \rho_2)^2\,\frac{\nu_1\nu_2}{(\nu_1+\nu_2)}\right.$$

$$\left.\frac{b}{6\pi\eta(1 + ba)} - \left(\frac{\nu_2\rho_1 + \nu_1\rho_2}{\nu_1 + \nu_2}\right)^2\,\frac{b^4\phi(ba)}{48\pi^2\eta N}\right] \tag{59}$$

where $\underline{N} = \underline{N}_1/\nu_1 = \underline{N}_2/\nu_2$. If Equation (59) is solved for $\underline{V}$ and is multiplied by $\underline{N}$, the result is the flux, $\underline{J}$. When second and higher order powers of $\Delta\underline{V}_1$ and $\Delta\underline{V}_2$ are neglected, one obtains

$$J = NV = -\mathfrak{M}\nabla\mu = -\left(\frac{N\omega_1\omega_2}{\nu_1\omega_2 + \nu_2\omega_1} + \Delta\mathfrak{M}\right)\nabla\mu \tag{60}$$

where

$$\Delta\mathfrak{M} = -\left(\frac{\omega_1 - \omega_2}{\nu_1\omega_2 + \nu_2\omega_1}\right)^2 \left(\frac{\nu_1\nu_2}{\nu_1 + \nu_2}\right) \frac{bN}{6\pi\eta(1 + ba)} +$$

$$\frac{(\nu_1\omega_1 + \nu_2\omega_2)}{(\nu_1 + \nu_2)(\nu_1\omega_2 + \nu_2\omega_1)^2} \quad \frac{b^4\phi(ba)}{48\pi^2\eta} .$$

If the concentration is expressed in moles per liter, and the mobility is given by $\omega_j = \frac{Cl \times 10^{-8}\lambda_j^o}{F|Z_j|\epsilon}$, $\Lambda^o = \lambda_1^o + \lambda_2^o$, then

$$\mathfrak{M} = 1.0741 \times 10^{-20} \frac{\lambda_1^o\lambda_2^o C}{\nu_1|Z_1|\Lambda^o} + \Delta\mathfrak{M}' + \Delta\mathfrak{M}'' \qquad (61)$$

where

$$\Delta\mathfrak{M}' = \frac{-(|Z_2|\lambda_1^o - |Z_1|\lambda_2^o)^2}{(\Lambda^o)^2|Z_1Z_2|(\nu_1 + \nu_2)} \cdot \frac{3.132 \times 10^{-19}}{\eta_o (D_iT)^{1/2}} \cdot \frac{C\sqrt{\Gamma}}{(1 + ba)}$$

$$\Gamma = C_1Z_1^2 + C_2Z_2^2 = 2C$$

$$\Delta\mathfrak{M}'' = \frac{(Z_2^2\lambda_1^o + Z_1^2\lambda_2^o)^2}{(\Lambda^o)^2} \cdot \frac{9.304 \times 10^{-13}}{\eta_o(D_iT)^2} \cdot C^2\,\phi(ba)$$

The function $\phi(ba)$ is given by the relationship in Equation (56). Previously, the diffusion coefficient was given by Equation (22) and thus for a 1-1 electrolyte becomes

$$D = 2000\,RT\,\frac{\mathfrak{M}}{C}\left(1 + C\,\frac{\partial \ln y\pm}{\partial C}\right) \qquad (62)$$

where the electrophoretic contribution to the diffusion coefficient is considered.

The derivation of Debye and Hückel and the extensions of Onsager and Fuoss involve a number of assumptions and limitations. One of the first assumptions is that the Boltzmann distribution function in Equation (26) may be applied.

This point was reviewed by Fowler (22) from a statistical mechanical approach and was concluded to be applicable for moderate concentrations. Fowler (22), however, questioned the use of a bulk average dielectric constant in the Poisson Equation, (24). This point is valid even in dilute solution. Fowler pointed out that although the use of such a dielectric constant was questionable, the error incurred by its use was not of a large magnitude.

Debye and Hückel also assumed that the potential energy, $q\psi$, in Equation (27) was small compared to the thermal energy, kT. This assumption would seem questionable for more concentrated solution since the potential function, ψ, is dependent on the distance of separation of ions. However, in an aqueous solution the possibility of hydration of ions might tend to provide sufficient ion separation to satisfy this condition.

Another point of question in the Debye-Hückel theory is the use of only the first two terms in the exponential expansion of Equation (28). Because of the change in sign of q_i as a result of both positive and negative ions, it can be shown that for all symmetrical electrolytes all odd-numbered terms of the expansion given by Equation (29) vanish. Also, due to the anticipated convergence of the series in Equation (28), the inclusion of the term $\frac{1}{3!}\left(\frac{\psi}{kT}\right)^3 \sum N_i q_i^4$ in Equation (29) was considered unnecessary.

An additional effect unaccounted for in the theory is that of ion-solvent interaction; or, more specifically, ion hydration. Such an effect would show up in the potential function of Equation (41) since hydration would probably affect the distance of closest approach, a_j. In addition, hydration, through a_j, would affect the integration limits of the differential velocity function of Equation (56).

One final consideration of the theory is that of the viscosity change at fairly high concentrations. This effect appears in the use of Stokes' Equation (54), to evaluate the velocity change due to the electrophoretic effect. While it might seem simple to account for the viscosity change by including the solution viscosity in Equation (61), the situation is not quite so simple. In the development of the electrophoretic effect for diffusion, consideration has been given to the volume force transfer between an ion and its atmosphere. Such a force transfer is part of the consideration of the theory of electrolyte solution viscosity. Thus, part of the viscosity correction is included in the theory of diffusion. Hence, replacing the solvent viscosity η_o, in Equation (61) with the solution viscosity would tend to overcompensate for the effect.

THE ABSOLUTE RATE THEORY OF DIFFUSION

In the application of the so-called absolute rate theory to the diffusion process (5), the primary result of this application is the relation of diffusion coefficient to temperature. The theory proceeds by evaluating the velocity of forward movement of solute across a 1 sq. cm. cross section in a concentration gradient as

$$V_f = \mathcal{N} C \lambda \tau \tag{63}$$

and the rate of movement in the backward direction as

$$V_b = \mathcal{N}(C + \lambda \frac{dc}{dx}) \lambda \tau \tag{64}$$

where $\mathcal{N}$ is Avogadro's number, C is concentration in moles/cc., λ is the distance between equilibrium positions of a solute molecule, and τ is the specific reaction rate for diffusion (the number of times a molecule moves from position to position per second). If the resultant flow is obtained as

$$V = -\eta \lambda^2 \tau \frac{dc}{dx} \tag{65}$$

then from Fick's law the diffusion coefficient becomes

$$D = \lambda^2 \tau \tag{66}.$$

According to the theory of absolute reaction rates, the rate constant τ is given by

$$\tau = \frac{kT}{h} \cdot \frac{F_{\ddagger}}{F_{*}} e^{-\epsilon_o/kT} \tag{67}$$

where $\underline{h}$ is Plank's constant, $\underline{F}_{\ddagger}$ and $\underline{F}_{*}$ are the partition functions of the system in the activated and normal states, and ϵ_o is the activation energy per molecule at 0°K. Equation (67) may also be written in the form

$$\tau = \frac{kT}{h} \cdot e^{\Delta S^{\ddagger}/R} \cdot e^{-\Delta H/RT} \tag{68}$$

where $\Delta\underline{S}$ and $\Delta\underline{H}$ are the entropy and enthalpy changes, respectively. Since diffusion involves a negligible volume change the diffusion coefficient becomes

$$D = e\lambda^2 \frac{kT}{h} e^{\Delta S^{\ddagger}/R} \cdot e^{-E/RT} \tag{69}$$

where $\underline{E}$ is the experimentally determined activation energy of diffusion.

For purposes of evaluating experimental data, Equation (69) is usually written in the form

$$D = Ae^{-E/RT} \tag{70}$$

where $\underline{A}$ is an assumed constant. Since both $\underline{A}$ and $\underline{E}$ may be evaluated experimentally, it thus is possible to evaluate approximately the entropy change due to the diffusion process.

The theory of absolute reaction rates for diffusion gives no consideration to the nonideality of the phenomenon or the interaction of ionic species. Thus, the use of this theory is limited to temperature dependence correlation where it has been shown to be applicable if comparisons are made at the same diffusion concentrations. In particular, the concept of activation energy of diffusion has been used to compare diffusion in aqueous and nonaqueous solutions. In addition, the concept of entropy of diffusion has been found to exhibit changes which give indications of the nature of the systems being investigated.

MATERIALS AND APPARATUS

MATERIALS

SODIUM HYDROXIDE

Preparation

Since reagent-grade sodium hydroxide pellets contain an insignificant (>0.01%) amount of impurities other than sodium carbonate, this was the reagent used as a starting material. The sodium carbonate impurities were removed by the "oil lye" method (23, 24) after modification, to produce an essentially carbonate-free stock solution. The "oil lye" method was modified because the amount of carbonate present after purification by this method ($\approx$0.15%) was thought to be excessive for physicochemical study.

The modified "oil lye" method consisted first of preparing a solution of sodium hydroxide which was saturated at approximately 100°C. By cooling the solution slowly to room temperature, a supersaturated solution resulted in which sodium carbonate was insoluble. The supersaturated solution was then filtered through a Gooch crucible containing a thick acid-washed asbestos mat to remove the precipitated sodium carbonate. By carrying out the filtration in a dry, CO_2-free atmosphere, some of the sodium hydroxide precipitated because of evaporation and there was no carbon dioxide contamination from the atmosphere. The filtrate was then diluted to approximately 3.5 normal to produce a stock solution and stored in a leached polyethylene bottle under a CO_2-free atmosphere.

Analysis

The carbonate content of the stock sodium hydroxide solution was determined by two methods in order to compare the results and insure greater accuracy in

the determination. Both methods are considered to be sufficiently accurate for analyzing solutions of low carbonate content.

With the so-called Winkler method (25) the total alkali of a sample was determined by titration with approximately 0.50N standard HCl to a mixed indicator (bromocresol green-methyl red) end point. The free hydroxide was then determined on a duplicate sample by precipitation of the carbonate with excess barium chloride and titration to a phenolphthalein end point with the standard acid. By subtracting the free hydroxide value from the total alkali, the amount of carbonate was obtained. Triplicate analyses by this method indicated that the stock NaOH solution contained an insignificant amount of carbonate (>0.01%) based on the total alkali.

Comparison analysis of the NaOH solution was carried out by the Warder method (24) in the following manner. A sample was titrated with 1N HCl until a phenolphthalein end point had almost been reached. The titration was then continued with 0.05N HCl to the end point and the two volumes recorded. At this point all of the hydroxide and one-half of the carbonate had been neutralized. A known excess of acid was subsequently added and the solution boiled for five minutes to expel all CO_2. After cooling the solution to room temperature, it was back titrated with standard base to determine the amount of acid consumed by the remaining bicarbonate. The portion of the excess acid that was consumed by the liberated free hydroxide represents one-half of the carbonate present in the solution. Triplicate analyses by the Warder method showed that the amount of carbonate present in the NaOH solution was approximately 0.01% (based on the total alkali).

WATER

The water used as solvent in the preparation of all of the solutions in this experimentation was prepared by a two-stage distillation procedure. Deionized water was used in the first stage of the still along with small amounts of sodium hydroxide and potassium permanganate. The distillate from this stage of the still passed through a condenser and into the flask of the second stage which contained a small amount of sulfuric acid. Distillate collected from the second stage was used for preparing solutions. Since this was a continuous operation, the first 1.5 liters obtained from the second stage, after distillation commenced, was discarded to insure maximum purity. The conductivity of this water was approximately 2×10^{-7} $(\text{ohm-cm.})^{-1}$ at 25°C. This procedure is quite similar to that discussed by Weissberger (26). The double distilled water was placed in a special flask fitted with an ascarite tube, boiled to remove any dissolved CO_2 in the water, and stored in the controlled atmosphere chamber.

STANDARD SOLUTIONS FOR ANALYSIS

In order to analyze all the sodium hydroxide solutions used in the diffusion experimentation, it was necessary to prepare volumetric standard acid and base solutions. Hydrochloric acid of approximately 0.5N was prepared by dilution of the concentrated reagent-grade acid. The above dilute acid was standardized by the use of freshly prepared, pure sodium carbonate using the technique of Pierce and Haenisch (27). Volumetric standard sodium hydroxide solution of 1/10N was prepared (23), and then standardized by comparison with the standard 0.5N hydrochloric acid.

Additional standard acids were prepared by diluting the above acid to the desired concentrations using calibrated pipets and volumetric flasks. A standard

1N hydrochloric acid solution was prepared by diluting concentrated acid and then comparing the diluted acid with the above standard base.

APPARATUS

RAYLEIGH DIFFUSIOMETER

The diffusiometer used for this work is a Beckman Spinco Model H electrophoresis-diffusion apparatus* with the optics arranged to give Rayleigh interference patterns. In essence, the apparatus is composed of four parts: a slit-source, schlieren lens, a Tiselius cell and mirror, and a camera assembly. To provide a greater light path length without requiring excessive space and thus increase the refractive sensitivity, the optical axis is folded and the light passes through the cell twice.

Light from a mercury vapor lamp is filtered by a Kodak Wratten filter 15 and a didymium filter to produce a monochromatic source of 546 mμ. The light then passes through a vertical slit and a schlieren lens before passing through the cell. A highly polished mirror is mounted in the constant temperature bath and returns the light through the cell into the schlieren lens again. From the schlieren lens, the light passes into the camera assembly where it is focused on the image plane.

For the condition where the diffusion cell contains a uniform liquid of refractive index quite close to that of the bath or there is no cell in the light path, the system is optically the same as a double slit interference set-up. In this type of set-up, the coherent monochromatic light source is split into two paths by impingement of the light on a double slit mask

*Beckman Instrument Company, Spinco Division, Palo Alto, California.

in front of the cell. One of the slits is in front of a channel of the U-shaped diffusion cell while the other slit is in front of the portion of the channel windows which extends into the bath and provides a reference light path. The result of the above set-up is a standard double slit interference pattern consisting of parallel lines of varying intensity, with the intensity decreasing slightly on both sides of a central line or fringe. This series of lines is due to the constructive and destructive interference of light waves bent by their interaction with the slit edges of the mask. When the diffusion cell contains a liquid of different refractive index from that in the reference path, the result is standard Rayleigh interference. For such a condition the central line or fringe is shifted, in a direction perpendicular to it, by an amount that is proportional to the difference in refractive index of the solution and reference. If a solution of varying concentration, or refractive index, is placed in the sample channel, the position of the central fringe will again be shifted by an amount proportional to the difference in refractive index between the solution path and reference path. However, the solution has a varying refractive index in the vertical direction of the cell and hence the central fringe, and all secondary fringes, will shift by a varying amount from point to point along the vertical cell direction. More specifically, the central and secondary fringes will shift one fringe unit when the product of the cell path and the refractive index difference is equal to the wavelength of incident light. The result of these fringe shifts will be a pattern such as that shown in Fig. 3.

DIFFUSION CELL

A Beckman Spinco Model H electrophoresis-diffusion cell of the Tiselius type was used in this experimentation. The top and bottom sections of the cell were made of crown glass. However, the center section was made from quartz (fused

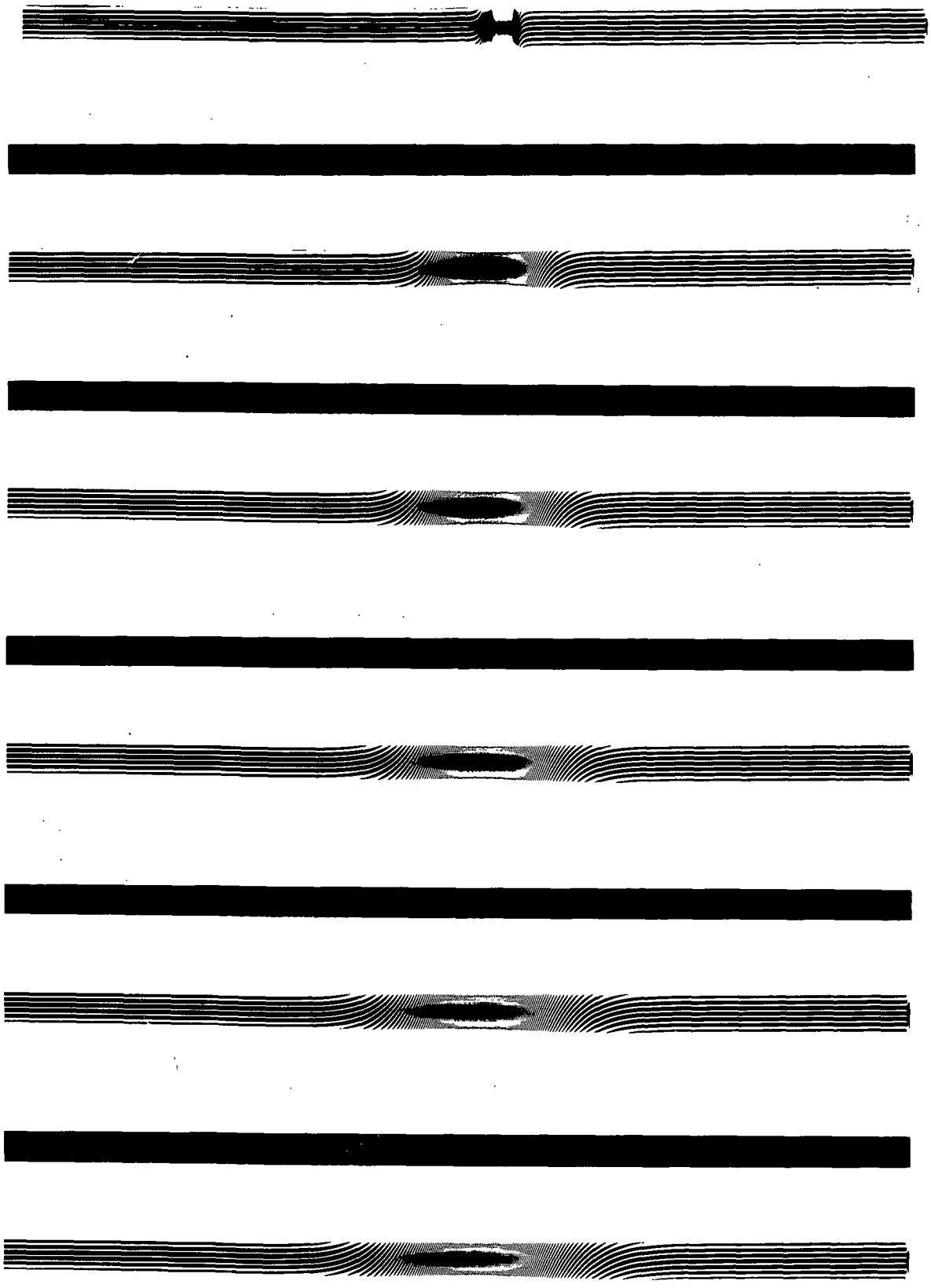

Figure 3. Photograph of Rayleigh Diffraction Pattern for a Diffusion Run

silica) because of its mechanical, thermal, and chemical resistance. This cell center section was the 11 milliliter size with the optical path being two times 2.50 centimeters since the light passes through the cell twice. The optical windows on the center section are extended laterally to provide, with the temperature bath liquid, a reference light path for the Rayleigh optics.

MICROCOMPARATOR

The instrument used for measuring the Rayleigh interferograms was a Wilder Model C Micro Projector. Measurement of the interferograms is affected by mounting the developed photographic plates on the transparent portion of the movable stage. The photographic image is then projected, by series of mirrors and a focusing lens, onto a Plexiglas viewing screen. Horizontal movement of the stage is adjusted by a two-inch micrometer screw. The stage is spring-loaded to maintain uniform contact with the screw point. In addition to the horizontal movement, the lateral movement is controlled by a one-inch micrometer screw with spring-loading being provided in this direction also. For adjusting the angular alignment of the photographic plates, the stage may be rotated through an angle of 20 to 30° in the horizontal plane by manipulation of a third screw mechanism.

CALIBRATION OF THE DIFFUSION CELL

In evaluating diffusion data from Rayleigh interferograms, it is assumed that the fringes are linear in all regions where there is no concentration gradient. For the above cell center section used in this experimentation, it was observed that the fringes were not linear for pictures taken of the cell containing only water (Fig. 4). To correct for this situation by use of a graph, such as Fig. 4, was felt to be unnecessarily tedious and hence a more direct method of correction was adopted.

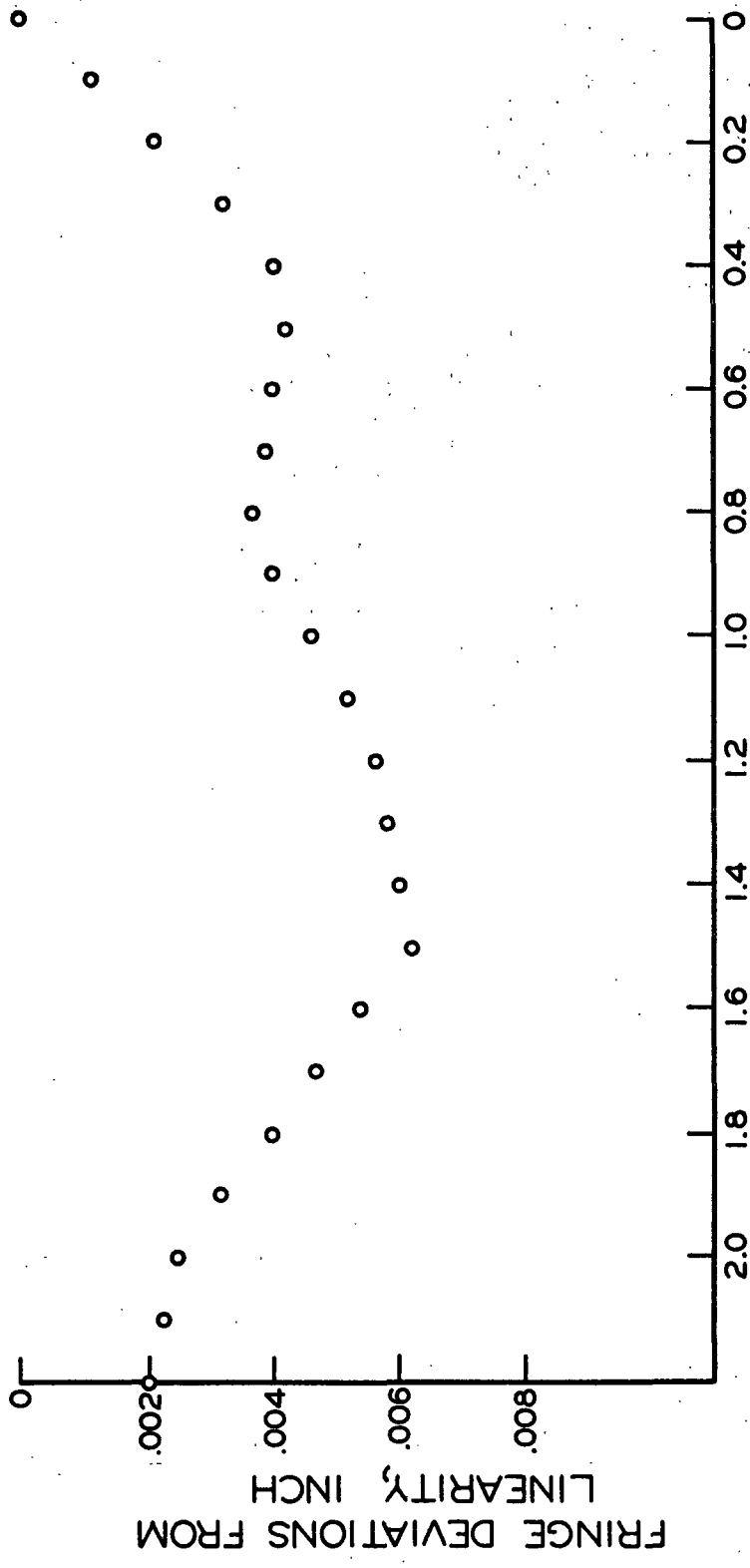

Figure 4. Deviations of the Rayleigh Fringes from Ideal Linearity

To make direct corrections for the nonlinearity of fringes for gradient-free interferograms, it was necessary to construct a uniform trace of the fringe irregularities by a method developed in co-operation with James Tostevin*. Such a trace was obtained by marking a scribe line on a photographic plate having gradient-free interferograms. By mounting a smoothly polished needle point gently against the photographic plate and in the microcomparator field of view, it was possible to obtain a trace of the fringe deviations as the stage of the microcomparator was moved horizontally along the interferogram. The microcomparator stage was moved by a multigeared synchronous motor and the comparator screen cross-hair was maintained at the center of a horizontal fringe by adjustment of the lateral micrometer screw. As a result of these operations, a continuous record of the center of a horizontal fringe as a function of longitudinal cell position was obtained for essentially the entire length of the diffusion cell center section. Traces such as described above were prepared periodically during this experimentation, particularly after the temperature bath was cleaned and the temperature changed.

CONTROLLED ATMOSPHERE CHAMBER

In order to prepare and handle electrolyte solutions under atmospheric conditions which were not conducive to contamination, it was necessary to manipulate these solutions in a chamber with a controlled atmosphere. The chamber was approximately 3 by 3 by 8 feet with a glass viewing port in the front of about 2 square feet. In the back of the chamber, numerous valve-controlled tube ports were available for providing vacuum, liquid, and gas supplies. Introduction of samples into the chamber was affected through a small port compartment at one end

*Thesis student, The Institute of Paper Chemistry.

of the main chamber. This small compartment could be opened to the exterior by a small door, for inserting samples without affecting the interior. The exterior opening could then be closed and the compartment evacuated to remove most of the exterior atmospheric gases which had entered. Subsequently, the samples could be placed into the main chamber by opening the interior door on the entry compartment. Once the samples were in the port compartment, they were manipulated with rubber gloves fitted to the chamber body.

Because of a minor leak in the chamber which could not be detected, it was necessary to maintain a slight positive gas pressure of approximately one-half inch of water to prevent contamination from the exterior atmosphere. The gas used for maintaining the positive pressure was obtained by partially purifying compressed air. To remove carbon dioxide, air was bubbled successively through two gas washing bottles containing 28% solutions of potassium hydroxide (24). Since this treatment rendered the resulting gas essentially saturated with water vapor, the moisture was removed by bubbling the water-saturated gas through concentrated sulfuric acid. Final treatment of the gas was accomplished by passing it through a large drying tube filled with drierite and ascarite adsorbents. Since the principal gaseous impurity of concern was carbon dioxide, an adsorption trap was fashioned for removing from the chamber atmosphere any carbon dioxide that might have been admitted during the transfer of samples from the outside. The adsorption trap consisted of an ascarite and drierite-filled Plexiglas cylinder which was covered at each end with fine mesh wire and a coarse Plexiglas grate. To insure that all the gas in the chamber was passed through the trap to effect CO_2 adsorption, the trap was attached to the exhaust of a squirrel-cage blower. This arrangement provided excellent circulation of the gas in the chamber and it was found that operation of the blower and trap for

approximately thirty minutes would remove all measurable carbon dioxide from the atmosphere. The interior atmosphere was tested for the existence of carbon dioxide by leaving a saturated barium hydroxide solution exposed for 48 hours.

EXPERIMENTAL PROCEDURE

PREPARATION OF SOLUTIONS

Solutions used in this study were all prepared in the controlled atmosphere chamber. The sample containers were placed in the chamber and the atmosphere conditioned for at least two hours before any solutions were prepared. Because of the difficulty of handling pipets in the chamber with rubber gloves, all the solutions were prepared to approximate concentrations and analyzed at a later date. The solutions of various concentrations were obtained by diluting the stock sodium hydroxide with carbon dioxide-free distilled water. Pipets of varying sizes were used with a rubber bulb pipetter to deliver quantities of stock NaOH solution, which would give the desired concentration, to 100-milliliter volumetric flasks where dilution was accomplished. Once a sample had been prepared, it was divided into two approximately equal parts; one part was used for the diffusion run while the other part was available for volumetric analysis.

ANALYSIS OF SOLUTIONS

All of the solutions prepared in the above manner were volumetrically analyzed to determine accurately the sodium hydroxide concentrations. Because of the precautions taken in handling the stock sodium hydroxide solution, no analyses for carbonate content were performed on the diffusion run samples. The analyses for sodium hydroxide content were performed by titrating a known volume of sample, delivered from one of the calibrated pipets, with standard hydrochloric acid solution. A five-milliliter microburet was used for delivering the acid and the titration was extended to a bromocresol green-methyl red mixed indicator end point. To reduce carbon dioxide adsorption during exposure

of the samples to the atmosphere, a gentle stream of nitrogen was maintained over the neck of the titration flasks during the course of each analysis. The bromocresol green-methyl red indicator was used for these analyses since no indicator blank is required and the end point is essentially unaffected by minute amounts of carbonate.

TRANSFER OF SOLUTIONS

The portions of the above-prepared solutions which were to be used in diffusion experimentation were placed in specially designed transfer vessels while still inside the controlled atmosphere chamber. Essentially, the transfer vessels consisted of standard 125-ml. polyethylene wash bottles which had been fitted with inlet tubes in the caps. To insure that the solutions were not contaminated after preparation, the transfer vessels were leached in several changes of distilled water for six weeks. Once the solutions were placed in the transfer vessels, the outlet and inlet tubes were clamped shut. Thus, the solutions could be prepared and transferred to the diffusion apparatus without being exposed to possible contamination from the atmosphere. With the above transfer apparatus, a slight pressure from a nitrogen source to the inlet tube would force the solution out of the delivery tube into any desired container.

DIFFUSION EXPERIMENTS

FILLING THE CELL

Once the solutions had been prepared for use in a diffusion experiment, the cell was assembled according to the Beckman Spinco Model H Instrument Instruction Manual. The extension tubes from both cell channels were then closed with rubber stoppers having 3-mm. glass inlets; the right channel having one inlet and the left channel two inlets. One of the inlets on the left channel was connected by

tygon tubing to a small drying tube containing ascarite. The other left channel inlet was fitted with a short section of tygon tubing which could be closed with a pinch clamp. An identical inlet arrangement was fitted to the stopper on the right channel. These two inlets were what might be termed "filling inlets."

The assembled cell, fitted with rubber stoppers, was flushed with nitrogen to remove any carbon dioxide by inserting a 12-inch needle from a nitrogen tank into the left filling inlet, and allowing the gas to flow for approximately one hour. After flushing the cell with nitrogen, the outlet of the transfer vessel having the most concentrated solution was attached to the needle inserted in the left channel of the cell. Solution was then forced out of the transfer vessel, through the needle and into the diffusion cell. The solution was added slowly to the cell until the level in the two channels was approximately at the middle of the cell center section. At this point the bottom section of the cell was displaced so that the level in the right channel would not rise and additional solution was added to the left channel until it had been adequately filled. The cell and its supporting rack were then placed in the constant temperature bath and allowed to equilibrate for fifteen minutes. In the meantime, a motor-driven 20-ml. syringe was filled with the less concentrated solution by attaching a section of tygon tubing from the second transfer vessel to the syringe. This procedure allowed the syringe to be filled without exposing the solution to the atmosphere. The cell and rack were positioned properly in the bath and a second needle, of smaller bore, was inserted through the filling inlet of the right channel to a position very slightly above the liquid level in this channel. After attaching the section of tygon tubing from the syringe to the second needle, the syringe motor was activated and the less dense solution delicately layered above the more dense solution. During addition of this solution, the needle point was gently raised as the liquid level rose, always maintaining the needle

point slightly under the liquid surface. This second or less concentrated solution was added until the liquid level in the right arm was slightly above (approximately 1/16 inch) the level in the left arm. After the solutions have been allowed to equilibrate for 15 minutes, the bottom section of the cell was aligned so that a continuous column of liquid existed in a U-shape.

SHARPENING THE BOUNDARY

Once the U-shaped cell had been properly filled, it was then essential to remove as much of the mixed region existing between the phases as possible. While the "layering" technique described above will produce in many cases very small regions of mixing, it was always felt that better results would be obtained by reducing the region of nonuniformity existing between the two solutions. Sharpening of the boundary was accomplished by lowering the point of the "layering" needle to a spot at the approximate center of the cell center section and reversing the syringe drive-motor. Solution was withdrawn at a rate of approximately 1 to 2 ml. per minute until the boundary separating the two solutions was almost the desired size. At this point the rate of solution withdrawal was reduced to an amount that would just maintain the boundary in a stationary state. This condition was maintained for several minutes during which time the "linear" portions of the Rayleigh fringes reached a state of equilibrium. If this equilibrium period was not allowed, the theoretically linear portions of the fringes would change their curvature and consequently the calibration curve would not be applicable for early pictures. However, proper equilibration resulted in fringes whose semi-straight portions are not time-dependent.

PHOTOGRAPHING THE EXPERIMENTS

Once the diffusion cell had been assembled, filled, and the boundary sharpened, the sodium hydroxide movement was recorded by photographing the

Rayleigh interference patterns at various time intervals. The camera assembly is such that the interference images are focused on the film plane. Pictures were obtained by simply inserting a loaded film holder into the holder insert and exposing the film for the desired period of time with the timing device on the instrument. For the work under consideration, it was found that Kodak type IV-G Spectroscopic photographic plates provided the best conditions of graininess and contrast. The exposure times were 16 seconds. This exposure was arrived at by trial-and-error experimentation using the diffusion cell filled with water. In addition to the Rayleigh patterns, the schlieren patterns for a diaphragm angle of 90° were also photographed. The patterns, which were solid black bands, served the purpose of preliminarily lining up each of the Rayleigh patterns.

The exposed photographic plates were developed in Kodak D-19 developer for 2 minutes and then placed in Kodak fix solution for five minutes to remove undeveloped chemicals. After developing, the plates were washed continuously for two hours.

MEASURING THE RAYLEIGH FRINGES

The Rayleigh interferograms obtained during the diffusion run are quite similar to those shown in Fig. 3, with the exception that the regions of curved fringes may be of different width. In order to determine diffusion coefficients from the interferograms, it is necessary to measure the distances between fringe centers, in the region of curved fringes, along a line parallel to the horizontal portions of the fringes. This would be the task if the cell optics were perfect; however, this is not the case and modifications must be made.

In a previous section the optical imperfections of the system were discussed and the calibration of the cell was described. This calibration plate, or scribe

record, was used to make the measurements necessary for determining diffusion coefficients. If some type of calibration technique were not used for these measurements, the positions of the fringe centers would be in error. Also, the alignment of the photographic plate on the microcomparator stage could be incorrect and this would produce an additional error in the fringe measurement. While an error due to lack of calibration would not be very sizable for fringes in the center of the boundary, the inaccuracies incurred at the outer fringes could be 20% or more (30). The error induced by improper alignment would be sizable for essentially the whole boundary.

The alignment and measurement technique described in this section was developed in co-operation with James Tostevin. In measuring photographs from a particular diffusion run, the plate with the calibration curve was placed on the microcomparator stage and fastened in place with double-faced masking tape. The plate was then aligned by rotating the stage until the edge of the projected solid schlieren image remained parallel to the screen cross-hair as the stage was moved horizontally. Once the reference plate was positioned, the observation plate, having the interferograms from the run, was placed above the reference plate and properly fastened. Fastening was accomplished by placing a small metal rod (1/4 x 1/4 x 6 inches) across the observation plate; the rod having small pieces of double-faced tape attached to it to secure the observation plate. One end of the rod was connected to a small magnet, on the metal stage, in such a manner that a point of rotation was established for the rod. The opposite end of the rod was pressure loaded against the end of a micrometer screw. With the observation plate arranged in this manner, it could be aligned properly by manipulation of the micrometer screw. However, in this position, only one of the photographic plates would be in focus at once. Therefore, the observation plate was

put in focus and a microscope slide was placed over the scribe line of the reference plate to bring it into focus.

After the reference and observation plates had been secured and the reference plate aligned, the observation plate was initially aligned by comparing the parallelism of its solid schlieren image with that of the reference plate and then making adjustments accordingly. This alignment was subsequently checked by comparing the horizontal portion of the observation-plate fringes with those of the reference plate by use of two cross-hairs on the comparator viewing screen. The above operations were performed on the first picture of each diffusion run for the purpose of determining the fractional fringe shift. The integral number of fringes shifted was obtained by simply counting the number of fringes which a cross-hair intersected in passing horizontally across a boundary.

Since the shift of Rayleigh fringes is the product of the refractive index difference between solutions of any two concentrations and the path length through the solutions, it is readily seen that the shift could entail some fractional fringe if the above product is different from a multiple of the wavelength of light. Because the boundary region is smallest for the initial photograph in a diffusion run, this photograph was used for determining the fractional fringe.

To determine the fractional fringe for a particular diffusion run, it was necessary to position one of the comparator-screen cross-hairs on the center of a horizontal fringe of the observation plate and to position the other, or bottom, cross-hair on the scribe line of the reference plate. This initial positioning was for fringes on the more concentrated side of the boundary. After positioning, the stage was moved horizontally until the straight portions of the fringes on the less concentrated side of the boundary were visible on the comparator screen.

The bottom cross-hair was then positioned on the scribe line, if it were not in that position. By adjusting the bottom cross-hair to coincide with the scribe line, the plate was in the position it would be if the optics were perfect. After the bottom cross-hair was positioned, a reading was then recorded from the lateral micrometer screw. The image on the comparator was then moved down until the top cross-hair was centered on the first horizontal fringe and the lateral micrometer reading recorded again. The difference in these two readings represented the absolute portion a fringe had shifted. By measuring the distance between two horizontal whole fringes, it was then straightforward to compute the ratio of the partial shift distance to the shift of a whole fringe. In order to provide a third check on the alignment of the observation plate, the fractional fringe shift was determined at several positions along the horizontal portions of the fringes on the solvent, or less concentrated, side of the boundary.

Once the fractional fringe had been determined on the first picture of a diffusion run, the observation plate was moved so that a later picture in the run might be viewed and measured. Pictures for measurement were selected on the basis of fringe separation in the boundary region and total boundary width. It was desired to have fringe separation such that the individual fringes were distinctly resolved. However, the boundary width had to be limited because the micrometer screw adjusting the horizontal travel was only two inches long. After selecting the pictures to be measured, the observation plate was properly aligned on a particular picture in the manner described for determining the fractional fringe. Measurement was initiated by moving along a particular horizontal fringe until a curved fringe was intersected. The bottom cross-hair was adjusted to the scribe line and the top cross-hair centered on the fringe. After recording the position on the horizontal micrometer screw, the stage was moved until another fringe had been intersected and the orientation process of

the cross-hair was repeated. This sequence of positioning the cross-hairs, recording the micrometer reading, and moving to the intersection of another fringe was repeated until all the positions of the boundary had been recorded. The number of such positions to be recorded usually amounted to seventy-five to one hundred. In addition, it was necessary to measure four or five pictures for each run; with each picture corresponding to a particular period of diffusion from the time of sharp boundary formation.

ANALYSIS OF FRINGE DATA

CALCULATION OF DIFFUSION COEFFICIENTS

For the case of unrestricted diffusion in a rectangular cell from an initially sharp boundary between two solutions of a homogeneous and single solute, one may use Fick's second law of diffusion in the form

$$\partial C/\partial t = D\partial^2 C/\partial x^2 \tag{71}$$

for predicting solute concentration as a function of time and distance from the boundary. In this case, the position $\underline{x} = 0$ is taken as the boundary and the $\underline{x}$ axis is positive in the downward direction. The diffusion coefficient, $\underline{D}$, here is assumed to be a constant for a particular solute. Initial and boundary conditions for this physical set-up would be

$$\begin{aligned} C &= C_A(t = 0, -\infty < x < 0) \quad \text{less concentrated} \\ C &= C_B(t = 0,\ 0 < x < \infty) \quad \text{more concentrated} \end{aligned} \tag{72}$$

and

$$\begin{aligned} C &\rightarrow C_A(t > 0,\ x \rightarrow -\infty) \\ C &\rightarrow C_B(t > 0,\ x \rightarrow \infty) \end{aligned} \tag{73}.$$

The solution of Equation (71) for the above initial and boundary conditions is

$$g(C) = \frac{2(C-\bar{C})}{\Delta C} = \frac{2}{\sqrt{\pi}} \int_0^{(x/2\sqrt{Dt})} e^{-\beta^2}\, d\beta \tag{74}$$

where $\bar{\underline{C}} = (\underline{C}_A + \underline{C}_B)/2$ and $\Delta\underline{C} = \underline{C}_B - \underline{C}_A$. From the physical relationships of the Rayleigh interference system, $\underline{g}(\underline{C})$, or $2(\underline{C}-\bar{\underline{C}})/\Delta\underline{C}$ may be equated to $2\underline{j}-\underline{J}/\underline{J}$ (28), where $\underline{J}$ is the total number of fringes and $\underline{j}$ is a fringe corresponding to concentration $\underline{C}$. This relationship is valid since the refractive index is a linear function of concentration; a condition quite closely approached for $\Delta\underline{C}$ of 0.10$\underline{N}$

or less as shown in Fig. 5 (29). If $x/2(Dt)^{1/2}$ is defined as Z, the right side of Equation (74) becomes the well-known error function

$$H(Z) = \frac{2}{\sqrt{\pi}} \int_0^Z e^{-\beta^2} \, d\beta \qquad (75);$$

therefore

$$H(Z) = (2j - J)/J \qquad (76).$$

From this it can be seen that for a diffusion system of J fringes one can calculate an $H(Z)$ value for each fringe in the system. By use of probability tables, the values of Z may be obtained from the calculated value of $H(Z)$.

If the position of the center of the boundary were known, it would be a simple matter to calculate the diffusion coefficient, D, by use of the above definition of Z. However, since the original boundary center is not known, we can utilize the differences in position of fringes and the definition of Z to arrive at the following relationship.

$$(X_i - X_k)/(Z_i - Z_k) = 2M\sqrt{Dt} \qquad (77)$$

In this case, M is the magnification factor of the optical system and the subscripts, i and k, denote two different fringes. If the diffusion coefficient were truly a constant, the fringe numbers to be paired, i and k, could be any two, with the only consideration being the accuracy of determining the quantity, $(X_i - X_k)$. Longsworth (28) considered the situation and concluded that the proper pairing would be that of maintaining the fringe-number difference, $(i-k)$, constant. In this case, the diffusion coefficient is evaluated as

$$\frac{1}{n} \sum_1^n \left(\frac{X_{J-j} - X_{J/2+j}}{Z_{J-j} - Z_{J/2+j}} \right) = 2M\sqrt{Dt} \qquad (78)$$

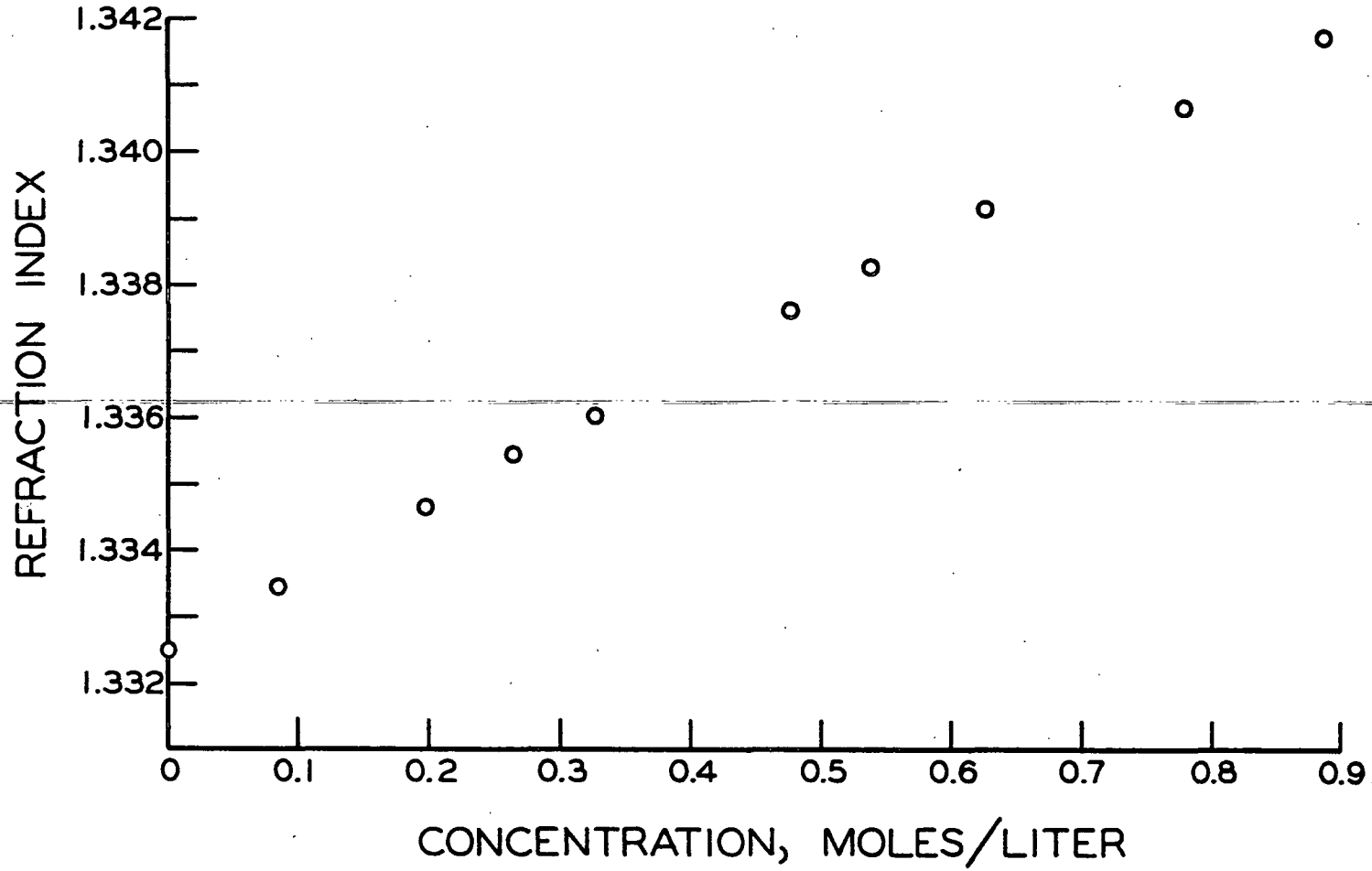

Figure 5. The Refractive Index of Sodium Hydroxide Solutions (29)

where the subscripts are the same as above. By doing this, advantage was taken of averaging the fringe differences.

In actuality, almost no solutes have constant diffusion coefficients; therefore, additional procedures must be added to account for this nonideality. It was noted by Longsworth (28) that some diffusion boundaries were skewed from the assumed Gaussian distribution of concentration gradient. To account for this skewness, Creeth (31), utilizing treatment for Gouy optics by Gosting and Fujita (32), developed the mathematics of concentration-dependent diffusion for a Rayleigh optical system. Briefly, the treatment consisted of expressing the diffusion coefficient and the refractive index as polynomial functions of concentration and solving Fick's second law in the form

$$\partial C/\partial t = \partial/\partial x \cdot (D\partial C/\partial x) \qquad (79).$$

The result of Creeth's analysis showed that, except for strong second-order concentration dependence effects, the differential diffusion coefficient corresponding to the mean concentration could be calculated by symmetrically pairing fringes about the Fringe $J/2$. In addition, the analysis showed that second-order effects were proportional to $(\Delta C/2)^2$ and by proper choice of ΔC these effects would become negligible.

Realizing the above conditions for proper analysis of fringe data, the present experimentation was carried out such that ΔC was never greater than $0.10M$ for any of the diffusion experiments. As a result of this, second-order effects were essentially eliminated because of the magnitude of $(\Delta C/2)^2$. In addition, the differential diffusion coefficient, $D_{\overline{C}}$, for the mean concentration was calculated by symmetrical pairing of fringes about the central fringe, $J/2$. For this condition a diffusion coefficient, $D'_{\overline{C}}$ was calculated for each diffusion time by

$$\frac{1}{n}\sum_{1}^{n}\left(\frac{X_{J-j} - X_j}{Z_{J-j} - Z_j}\right) = 2M\sqrt{D_C' t'} = \bar{Y}_t \qquad (80)$$

where the X's are the comparator readings for the two particular fringes and n is equal to $J/2$. Since the accuracy of the comparator measurements are not as good for the outer fringes by virtue of their angle from the horizontal base, $\bar{Y}_t$ values were calculated for n, n-2, n-4, etc., pairings. In the calculations, a pair of the innermost fringes and a pair of the outermost fringes were dropped from each of the successive calculations, thereby accounting for the n, n-2, n-4, etc., pairings per calculation. The inner pairings were dropped because the most probable error in a comparator reading would be a greater percentage of the position differences of inner paired fringes than of outer paired fringes. As a result of these successive calculations of $\bar{Y}_t$, the various values of $\bar{Y}_t$ would approach a value which was constant to the fourth decimal place. It is seen that the diffusion coefficient, D_C', can be calculated by use of Equation (80).

In all these calculations, the quantities t' and D_C' have been used instead of t and D_C. This condition exists because t and D_C refer to a diffusion coefficient calculated on a time scale which starts when there exists in the diffusion cell an infinitely sharp boundary. In actuality it is difficult to determine the base line for such a time scale; hence, the base line of the time scale for each diffusion experiment was taken as the time of the first photographic exposure. Thus, each exposure time, or diffusion time, was incorrect by some amount Δt. It can be shown (33) that for the above condition the actual diffusion coefficient, D_C, is related to the apparent one, D_C', by the relationship

$$D_C' = D_C\left[1 + \frac{\Delta t}{t'}\right] \qquad (81).$$

Thus, it is seen that by calculating an apparent diffusion coefficient, $\underline{D}_{\underline{C}}'$, for each apparent time, or photograph, the actual differential diffusion coefficient was determined by a regression of $\underline{D}_{\underline{C}}'$ on $1/\underline{t}'$. A typical plot of $\underline{D}_{\underline{C}}'$ versus $1/\underline{t}'$ is shown in Fig. 6. The value of the $\underline{D}_{\underline{C}}$ is determined by extrapolation of $1/\underline{t}'$ to zero.

ANALYSIS OF ASSUMED LINEAR CONCENTRATION DEPENDENCE OF DIFFUSION

In the extended analysis of Creeth (31) for concentration-dependent systems, it is shown that the deviations of a diffusion boundary from a Gaussian distribution of concentration gradients may be represented by complex functions of $\underline{Z}$. If $\underline{Z}^*$ represents an idealized position on the gradient distribution curve and $\underline{Z}$ represents the actual position, the difference between these two quantities may be represented by

$$Z - Z^* = \left(\frac{\Delta C}{2}\right)\left[a_1 U(Z^*) - k_1 R(Z^*)\right] + \left(\frac{\Delta C}{2}\right)^2 \left[\frac{a_1^2}{2} W(Z^*) - a_1 k_1 V(Z^*) + a_2 U(Z^*)H(Z^*) + \frac{k_1^2}{2} S(Z^*) - k_2 T(Z^*)\right] + \ldots \quad (82)$$

where $\underline{a}_1$, $\underline{a}_2$, $\underline{k}_1$, and $\underline{k}_2$ are polynomial coefficients in the assumed refractive index-concentration and diffusion coefficient-concentration functions. The other quantities in Equation (82), $\underline{H}(\underline{Z}^*)$, $\underline{U}(\underline{Z}^*)$, $\underline{R}(\underline{Z}^*)$, $\underline{W}(\underline{Z}^*)$, $\underline{V}(\underline{Z}^*)$, $\underline{S}(\underline{Z}^*)$, and $\underline{T}(\underline{Z}^*)$, are complex functions of the error function or its derivative. If it is assumed that the second-order concentration effects are negligible, Equation (82) is reduced to

$$Z - Z^* = \left(\frac{\Delta C}{2}\right)\left[a_1 U(Z^*) - k_1 R(Z^*)\right] \quad (83).$$

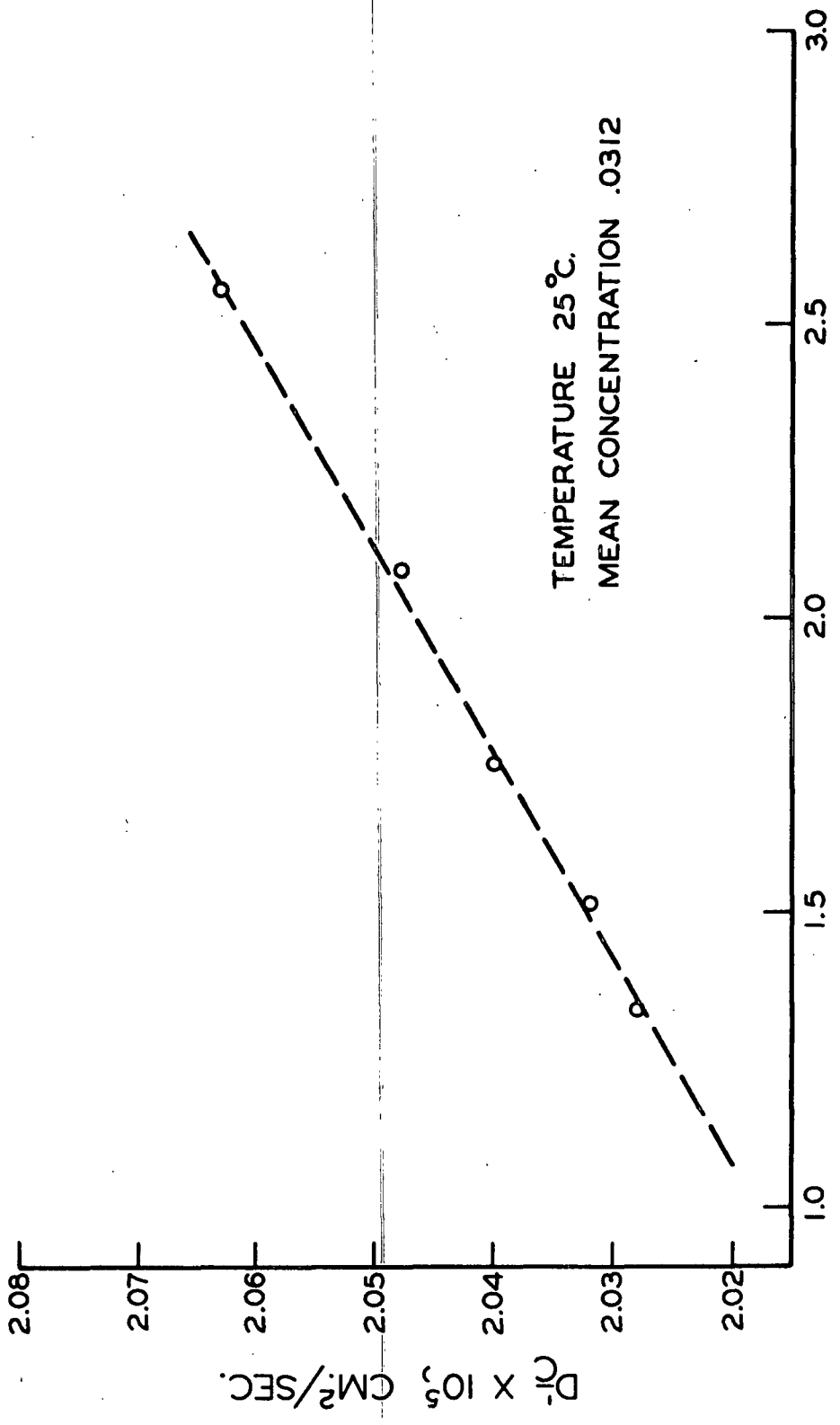

Figure 6. A Typical Zero-Time Correction Plot for Diffusion of Sodium Hydroxide

This could be considered a good assumption for the present experimentation because the quantity $(\Delta C/2)^2$ was purposely kept small. In addition, it is seen from Fig. 5 that for the concentration increments used in this experimentation, 0.10N, the deviations from linearity would be quite small. Thus, Equation (83) may be reduced, for two fringes, j_1 and j_2, to

$$(Z_2-Z_1) - (Z_2^* - Z_1^*) = -k_1 \left(\frac{\Delta C}{2}\right) \left[R(Z_2^*) - R(Z_1^*)\right] \qquad (84).$$

Since the Function $R(Z^*)$ is symmetrical about the Fringe $J/2$, it can be seen that Equation (84) will be most operative for the condition where the Fringes j_1 and j_2 are j_j and $j_{J/2+j}$. Recognizing that $\bar{Y}_t$ in Equation (80) is a characteristic quantity of a fringe pattern, it can be seen from the definition of Z that (Z_2-Z_1) may be replaced by $(X_2-X_1)/\bar{Y}_t$, where X_2 and X_1 are comparator readings. Thus, Equation (84) becomes

$$\frac{\left(X_{(J/2+j)} - X_j\right)}{\bar{Y}_t} - \left[Z^*_{(J/2+j)} - Z_j^*\right] = -k_1 \left(\frac{\Delta C}{2}\right) \left[R\left(Z^*_{(J/2+j)}\right) - R(Z_j^*)\right] \qquad (85).$$

The Function $R(Z^*)$ has been shown by Creeth (31) to be given by

$$R(Z^*) = -\frac{1}{4H'(Z^*)} \left\{2\left[H(Z^*)\right]^2 + 2Z^*H'(Z^*)\,H(Z^*) + \left[H'(Z^*)\right]^2 - 2\right\} \qquad (86)$$

where $H(Z^*)$ is given by Equation (75) and $H'(Z^*)$ is the derivative. Values of Z^* for a particular fringe are obtained through the use of Equations (75) and (76) and the error function probability tables (30).

From the above presentation it is seen that the only unknown quantity in Equation (85) is k_1. This, therefore, may be obtained from a plot of the left side of Equation (85) versus $R(Z^*)$.

RESULTS AND DISCUSSION

DIFFUSION OF SODIUM HYDROXIDE AT 25°C.

The diffusion runs, at 25.00 ± 0.01°C., were carried out according to the procedure given in a previous section. Fringe positions were measured from the resulting photographs (such as Fig. 3) and the data analyzed according to the previously described method of Creeth (31). Because of the large number of arithmetic manipulations involved in the data analysis, a computer program was developed for use with an IBM 1620-II computer. Results of the computer analysis may be found in Table I and are shown graphically in Appendix I. The results in the figures indicate the zero-time correction discussed in a previous section. In addition, Fig. 7 shows the validity of the Creeth method of calculation since the refractive index gradient is essentially a linear function of concentration. This is concluded from the fact that the refractive index gradient, $J/\Delta C$, would be linear over the one-tenth normal concentration range of each diffusion run.

The series of apparent diffusion coefficients for each run were correlated by a second computer program which carried out the zero-time corrections by a standard linear extrapolation procedure of $D'_{\overline{C}}$ vs. $1/t'$ to infinite time. From these correlations, the differential diffusion coefficients corresponding to the various mean concentrations were obtained. The standard error of the extrapolated diffusion coefficients in all this work ranged from 3.2×10^{-8} to 7.9×10^{-8}. The results for 25°C. are found in Table II.

The results of Table II are shown graphically in Fig. 8 using the normal graphical co-ordinates of differential diffusion coefficient and square root of concentration. According to the original premise of this study, it was hypothesized that the diffusional behavior of sodium hydroxide would be reasonably consistent with the Onsager-Fuoss Theory. At first observation, the

TABLE I

RESULTS OF SODIUM HYDROXIDE DIFFUSION

Temperature = 25.00 ± 0.01°C.

Apparent Diffusion Coefficient, sq.cm./sec.	Reciprocal Time, $sec.^{-1}$
Mean Concentration = 0.0312N	
2.063×10^{-5}	2.564×10^{-4}
2.048	2.083
2.040	1.719
2.033	1.515
2.028	1.333
Mean Concentration = 0.0515N	
2.308×10^{-5}	2.778×10^{-4}
2.230	2.083
2.178	1.667
2.141	1.389
2.123	1.235
Mean Concentration = 0.1026N	
1.960×10^{-5}	2.083×10^{-4}
1.952	1.754
1.949	1.515
1.946	1.333
1.937	1.191
Mean Concentration = 0.3014N	
1.946×10^{-5}	2.193×10^{-4}
1.923	1.736
1.905	1.418
1.898	1.272
1.889	1.142
Mean Concentration = 0.7035N	
1.849×10^{-5}	1.852×10^{-4}
1.837	1.522
1.825	1.333
1.822	1.191
1.814	1.072

TABLE I (Continued)

RESULTS OF SODIUM HYDROXIDE DIFFUSION

Temperature = 25.00 ± 0.01°C.

Apparent Diffusion Coefficient, sq.cm./sec.	Reciprocal Time, $sec.^{-1}$
Mean Concentration = 1.011N	
1.807×10^{-5}	2.381×10^{-4}
1.794	1.852
1.782	1.515
1.778	1.282
1.770	1.149
Mean Concentration = 2.178N	
1.748×10^{-5}	1.389×10^{-4}
1.742	1.190
1.737	1.111
1.735	1.042
1.733	0.980

TABLE II

DIFFERENTIAL DIFFUSION COEFFICIENTS OF SODIUM HYDROXIDE

Temperature = 25.00°C.

Mean Concentration, mole/l.	Differential Diffusion Coefficient, sq.cm./sec.
0.03120	1.990×10^{-5}
0.05149	1.975
0.1026	1.913
0.3015	1.829
0.7035	1.778
1.010	1.739
2.178	1.696
Standard deviation = ± 0.1%	Standard error = $\pm 3.2 \times 10^{-8}$ to 7.9×10^{-8}

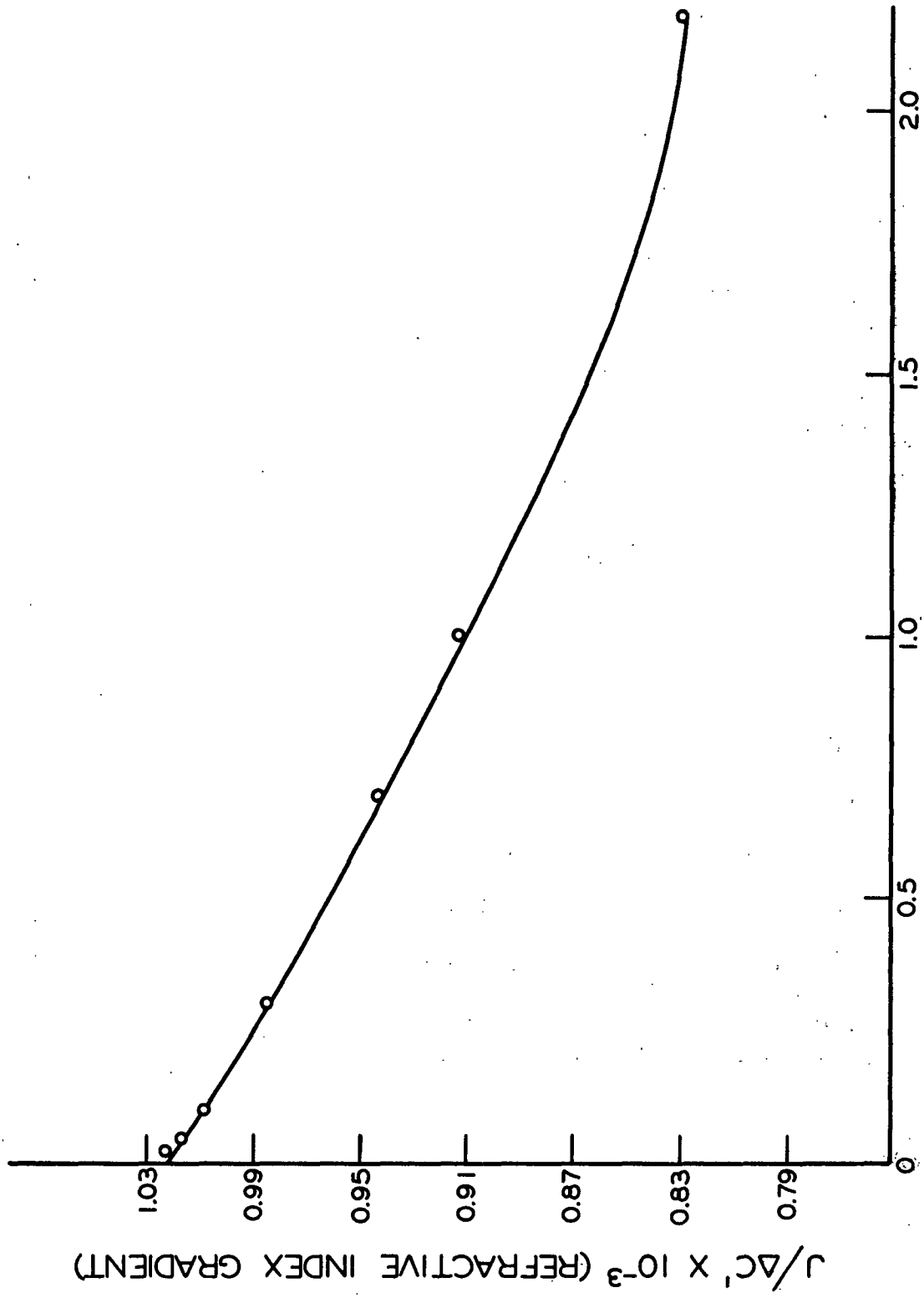

Figure 7. The Refractive Index Gradient of Sodium Hydroxide Solutions as Determined from Rayleigh Pictures of Diffusion Runs

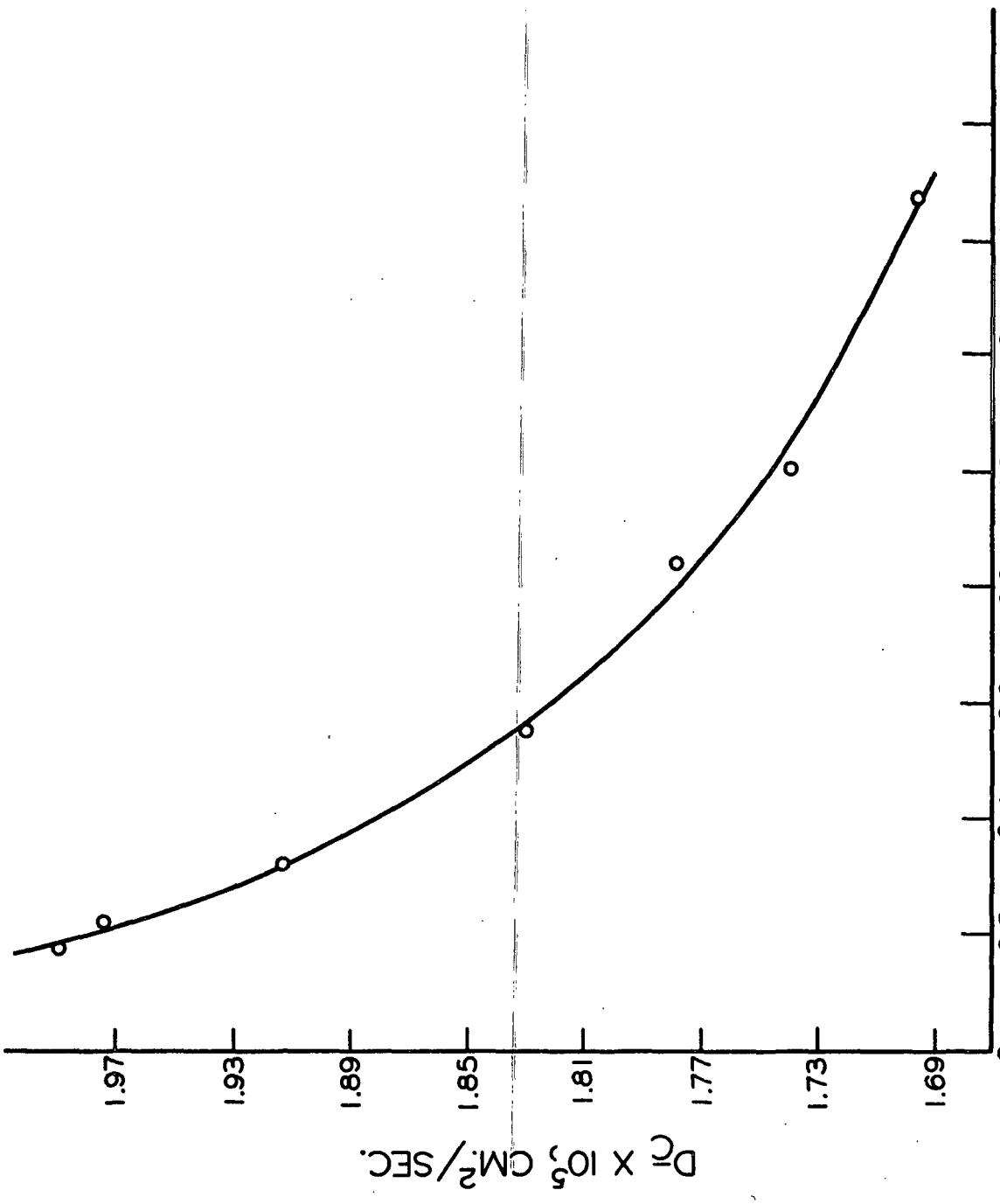

Figure 8. The Diffusion Coefficients of Sodium Hydroxide at 25°C.

concentration-dependence of sodium hydroxide seems to be consistent with the behavior of sodium chloride and potassium chloride shown in earlier figures. However, closer examination of Fig. 8 shows that while the diffusion coefficient seems to be approaching a minimum, the concentration range is considerably different. In addition, it is quite apparent that the diffusion coefficient of sodium hydroxide is considerably higher than the diffusion coefficient of sodium chloride even though the two electrolytes should be of comparable size. In assessing the situation, it was found that the diffusivity of hydrochloric acid (34, 35) is extremely high also. Thus, the difference in diffusivity of sodium chloride and sodium hydroxide must be due to the difference in anion mobility. From the literature, it was found that the hydronium and hydroxide ions both have extremely high mobilities (36, 37). This condition was first attributed, by Grotthus, to the existence of a molecular transport mechanism whereby either of the two ions may interact with a water molecule to liberate a comparable ion on the opposite side of the water molecule. By successive transformations such as this the complementary ion is pulled through the medium as a result of electrostatic forces arising from charge separations. While some changes have evolved in the physical picture of hydroxyl and hydronium ion transfer, a picture of the Grotthus mechanism similar to the brief one described above is generally accepted (36, 37).

In Fig. 9, the diffusion data for sodium hydroxide at 25°C. are shown in conjunction with the values of the diffusion coefficient predicted by the Onsager-Fuoss theory and the associated equations. The diffusion coefficient is given by

$$D = 2000\ RT \frac{\partial \bar{m}}{\partial C} \left(1 + C \frac{\partial \ln y_{\pm}}{\partial C}\right) \qquad (62)$$

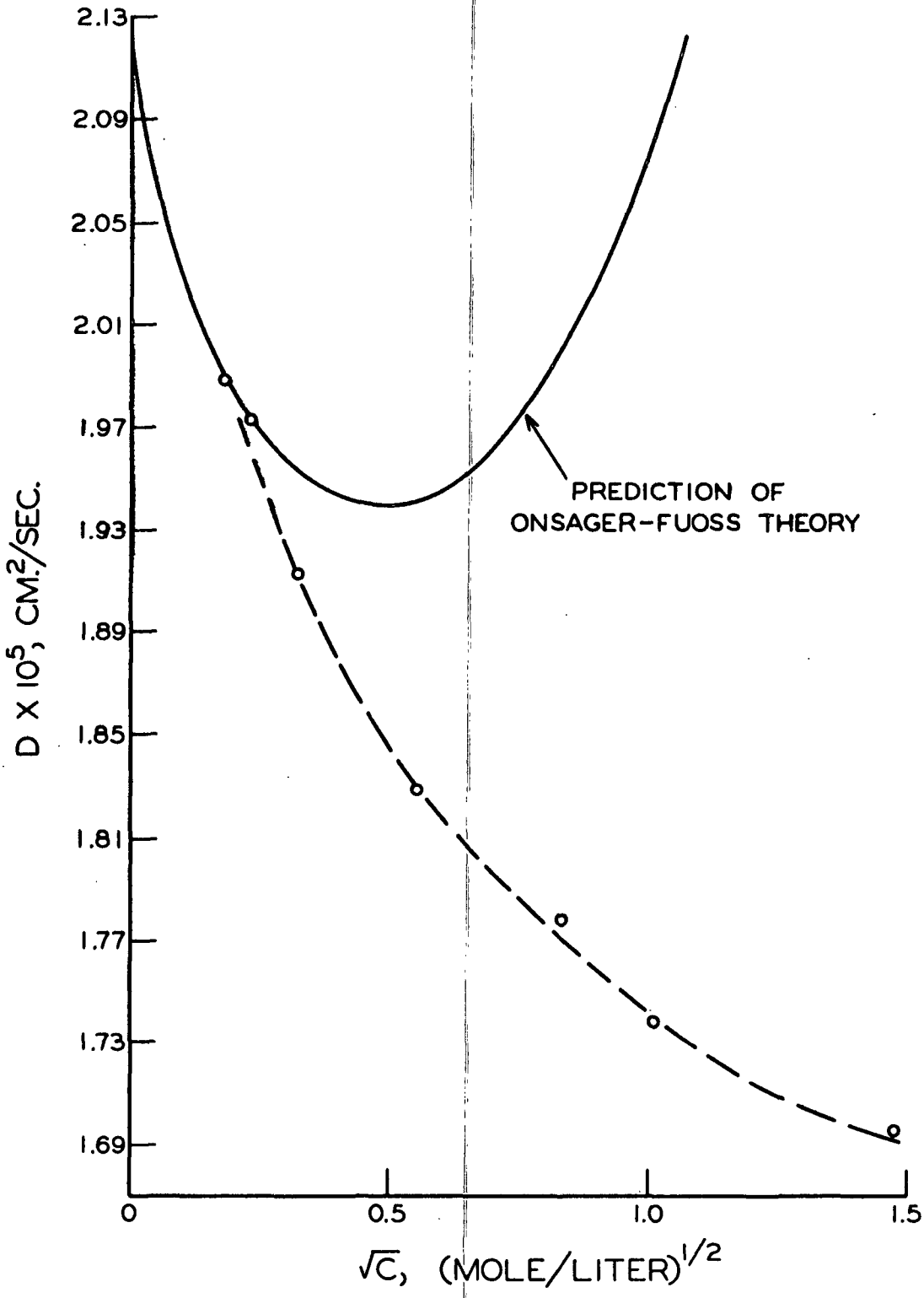

Figure 9. The Diffusion of Sodium Hydroxide at 25°C. Along with the Prediction of the Onsager-Fuoss Theory

where

$$\mathfrak{m} = 1.0741 \times 10^{-20} \frac{\lambda_1^o \lambda_2^o C}{\nu_1 |Z_1| \Lambda^o} + \Delta\mathfrak{m}' + \Delta\mathfrak{m}'' \qquad (61).$$

$$\Delta\mathfrak{m}' = - \frac{(|Z_2|\lambda_1^o - |Z_1|\lambda_2^o)^2}{(\Lambda^o)^2 |Z_1 Z_2| (\nu_1+\nu_2)} \cdot \frac{3.132 \times 10^{-19}}{\eta_o (D_i T)^{1/2}} \cdot \frac{C\sqrt{\Gamma}}{(1 + ba)}$$

$$\Gamma = C_1 Z_1^2 + C_2 Z_2^2$$

$$\Delta\mathfrak{m}'' = \frac{(Z_2^2 \lambda_1^o + Z_1^2 \lambda_2^o)^2}{(\Lambda^o)^2} \cdot \frac{9.304 \times 10^{-13}}{\eta_o (D_i T)^2} \cdot C^2 \, \phi(ba).$$

All of the symbols have been defined previously. Values of the dielectric constant, viscosity, ionic conductivity, and activity were obtained from Harned and Owen (38). In calculating the activity function, $(1 + \underline{C} \frac{\partial \ln \underline{y}\pm}{\partial \underline{C}})$, data from (38) were utilized along with an empirical equation of the type, $\ln \underline{y}\pm = \underline{A}\underline{C}^{\underline{B}} + \underline{D}\underline{C}$, as suggested by Harned (39).

It is apparent from Fig. 9 that the diffusion of sodium hydroxide is not comparable in concentration-dependence to sodium chloride or potassium chloride (Fig. 1 and 2). In fact, the behavior of sodium hydroxide diffusion is comparable to only one of the 1:1 electrolytes reported by Robinson and Stokes (34), namely ammonium nitrate. While ammonium nitrate is by no means as structurally simple as sodium hydroxide, it is nevertheless of interest to note the postulation given by Wishaw and Stokes to explain the results of ammonium nitrate diffusion measurements. To explain the behavior they observed, Wishaw and Stokes (40) postulated that ion-pairs were being formed. The concept of ion-pairs used by Wishaw and Stokes was the same as that introduced by Bjerrum (41, 42) to denote ion combinations due purely to electrostatic forces between ions

of opposite charge and not due to the formation of covalent bonds. To show the existence of ion-pairs, they proceeded to use the theoretical conductivity equation of Onsager and Fuoss (2) and Falkenhagen, et al. (43),

$$\Lambda_C = \left(\Lambda^o - \frac{82.5}{(DT)^{1/2}} \frac{\sqrt{C}}{1 + ba}\right) \left(1 + \frac{\Delta x}{x}\right) \eta_o/\eta \qquad (87)$$

in determining the degree of dissociation, α. They showed that, if C was replaced by $\alpha \cdot C$ in Equation (87), it was possible to calculate α by trial and error through the use of the relationship

$$\Lambda_e = \alpha \cdot \Lambda_{(\alpha \cdot C)} \qquad (88)$$

where Λ_e is the experimentally observed conductivity. Wishaw and Stokes (40) found that it was indeed possible to determine the extent of ion-pair formation by the use of Equations (87) and (88). Thus, it was considered possible that the extent of ion-pair formation in sodium hydroxide, if it existed, might be calculated from the conductivity data of Darken and Meier (44).

Before investigating the possibility of calculating the extent of ion-pair formation, two distinctive features had become apparent about the diffusion of sodium hydroxide. First, there was some unusual phenomenon causing the diffusivity of sodium hydroxide to be quite high in comparison to similar electrolytes; this phenomenon might be a Grotthus-type transfer mechanism. Secondly, the same phenomenon as above, a second phenomenon, or a combination of the two was causing sodium hydroxide to exhibit quite unusual concentration-dependence. Since a Grotthus-type transfer was considered quite likely to exist, the first feature of sodium hydroxide diffusion mentioned above was felt to be briefly explained. As a result of the diffusional behavior observed for ammonium nitrate by Wishaw and Stokes (40), it was considered quite possible that ion-pair formation was

occurring in the sodium hydroxide-water system even though it, in general, would not be suspected.

As discussed in more detail in Appendix II, it became apparent on first inspection that the theoretical conductivity relationships represented by Equations (87) and (88) were not applicable to the data of Darken and Meier (44). It was then concluded from the accepted physical picture of the system that in order for Equation (87) to be applicable the ions must be considered on an individual basis rather than in pairs. By considering the ions on an individual basis, one can account for the effects of the assumed Grotthus mechanism. For the sodium ion both the electrophoretic and relaxation effects would exist, but for the hydroxyl ion only the relaxation effect would exist due to the transfer mechanism. As pointed out in the Appendix, when the above reasoning was applied to the conductivity data the theoretical results coincided with the experimental results up to approximately 0.3M. Beyond this concentration the theoretical values were higher than the experimental values. This result is contrasted to that of applying Equation (87) to the data directly, instead of on an individual ion basis, in which the theoretically calculated results were considerably lower than the experimentally observed results. Since it was felt that Equation (87) should not predict quite low conductivity values for the composite ion case if it actually represented the physical picture, the results obtained by individually treating the ions were tentatively accepted. Thus, it was possible to utilize the individual ion method in conjunction with Equation (88) to determine the extent of ion-pair formation. The results of these calculations are presented in detail in Appendix II and are shown graphically in Fig. 10. While one might readily reject the idea of ion-pair formation in a 1:1 electrolyte such as sodium hydroxide, it is worthwhile to note from Fig. 10 that ion-pair formation is

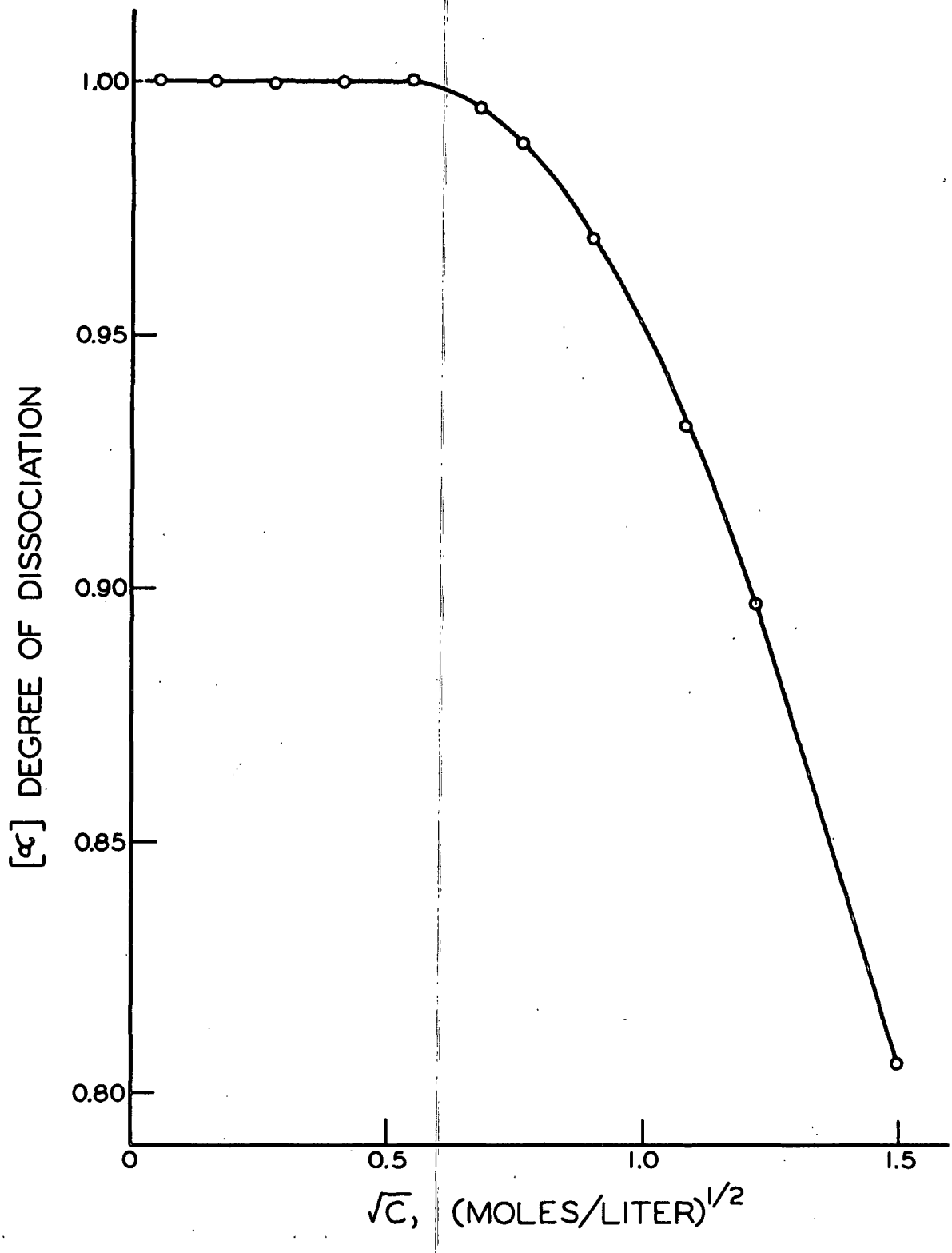

Figure 10. The Extent of Ion-Pair Formation for Sodium Hydroxide at 25°C. Calculated from Conductivity Data

predicted at a concentration region in which the diffusion coefficients of most other 1:1 electrolytes begin to increase.

Since the result of an analysis of conductivity data leads to the conclusion that ion-pairs are formed in the sodium hydroxide – water system, the next obvious investigation concerns the quantitative significance of ion-pair formation on sodium hydroxide diffusion. Even though the Onsager-Fuoss theory has been shown to predict the diffusional behavior of some electrolytes, there are a number of factors involved in electrolyte diffusion which the theory does not take into account; namely, countermovement of solvent, change in solution viscosity, and rigidly bound water of hydration. Agar (45) has extended the theoretical development of Hartley and Crank (46) for two-component diffusion and flow so that it will be applicable to an electrolyte diffusion system. The development of Agar (45) takes into account the countermovement of solvent molecules, the movement of a permanently bound layer of solvent molecules along with the ions, and the change in drag forces on the ions due to viscosity changes. This analysis led to the following equation relating the diffusivity to a number of other variables.

$$D = (D^{\circ} + \Delta_1 + \Delta_2)\,[1 - .018\ h^{*}m]\left[1 + .018\ m\left(\frac{\nu D^{*}_{H_2O}}{D^{\circ}} - \bar{n}\right)\right] \times \left(1 + m\,\frac{d\ \ln\ \gamma_{\pm}}{dm}\right)\ \eta_o/\eta \qquad (89)$$

In this equation, h^* is the moles of bound solvent per mole of electrolyte, m is the molality, Δ_1 and Δ_2 are the electrophoretic corrections, $D^{*}_{H_2O}$ is the self-diffusion coefficient of water, and D° is the diffusion coefficient of sodium hydroxide at zero concentration. Equation (89) may be simplified by combining the two middle brackets and neglecting $(.018\ h^{*}m)^2$ to give

$$D = (D^{\circ} + \Delta_1 + \Delta_2)\left[1 + .036m\left(\frac{D^*_{H_2O}}{D} - h^*\right)\right]\left(1 + m\frac{d \ln \gamma_{\pm}}{dm}\right)\eta_o/\eta \qquad (90)$$

Robinson and Stokes (47) have used Equation (90) to determine hydration numbers, h^*, for a series of electrolyte systems. In so doing, they have been able to determine hydration numbers for seven individual ions; among this group sodium ion has a hydration number of 0.70.

For the case of sodium hydroxide diffusion, it has been assumed, that because of the evidence for a Grotthus transfer mechanism, the sodium ion would be the only one having permanent hydration and h^* would be 0.70. Thus, Equation (90) was rearranged in the following manner to give

$$f(D)_{theo.} = 1 + .036m\left(\frac{D^*_{H_2O}}{D^{\circ}} - h^*\right) \qquad (91)$$

and

$$f(D) = \frac{D \cdot \eta}{D_{theo.} \cdot \eta_o} \qquad (92)$$

where $D_{theo.} = (D^{\circ} + \Delta_1 + \Delta_2)\left(1 + m\frac{d \ln \gamma_{\pm}}{dm}\right)$. In Fig. 11 the solid line represents a plot of Equation (91) which might be defined as the theoretical function of D, $f(D)_{theo.}$. If D in Equation (92) is now replaced by the observed value of the diffusion coefficient, $D_{ob.}$, it is then possible to calculate values of $f(D)$ which correspond to the actual diffusion behavior observed. The points in Fig. 11 represent the values calculated from Equation (92). It is to be noted that the slope of the straight line in the figure is dependent on the self-diffusion coefficient of water which is somewhat uncertain.

Since the calculated values of $f(D)$ from Equation (92) tend to approach those of Equation (91) as the molality approaches zero, the first reaction is to accept the fact that the hydroxyl ion is not hydrated. However, deviation of the $f(D)$ points below the line indicates from Equation (91) that the hydroxyl

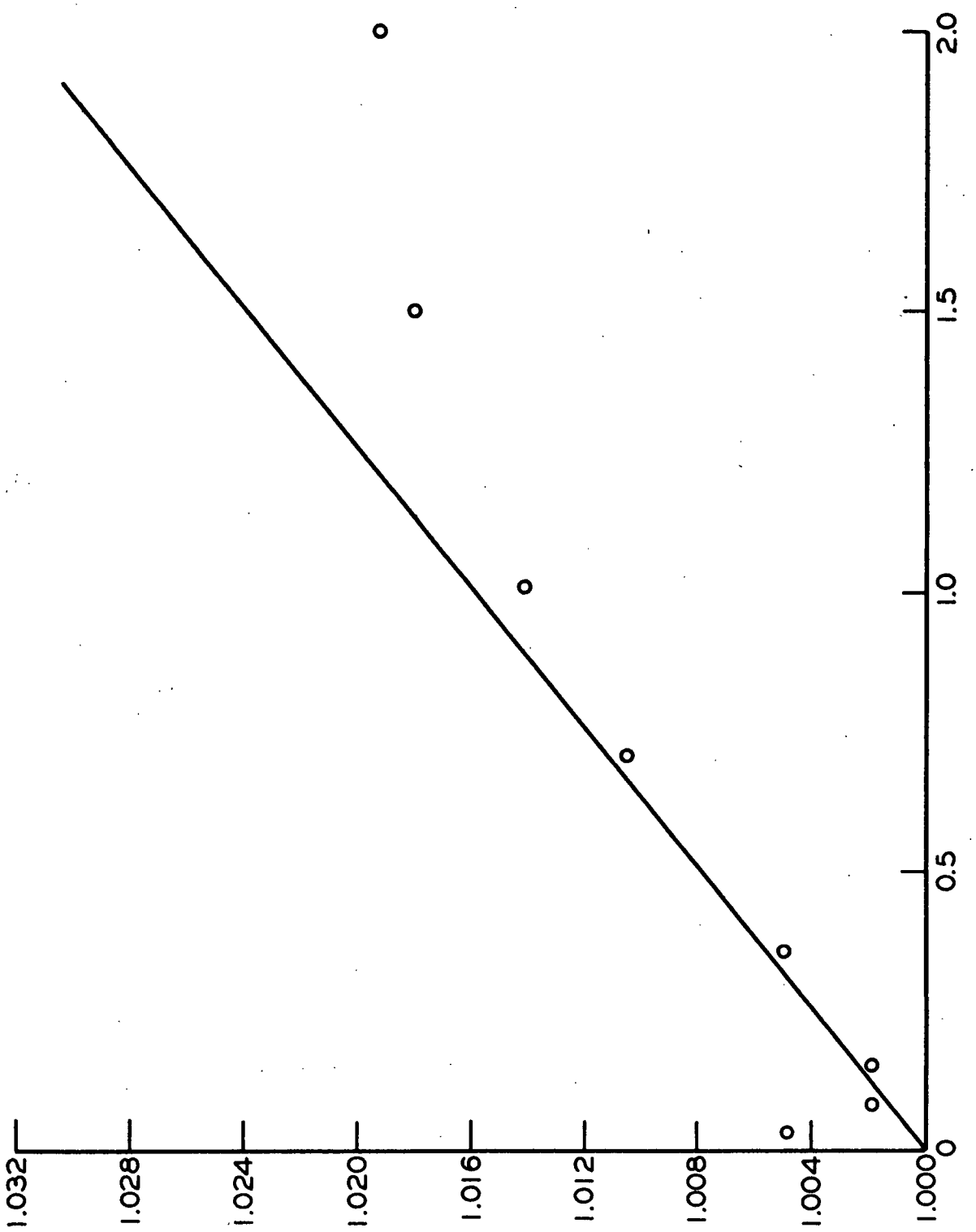

Figure 11. Results of the Application of the Hartley-Crank Relationship to Diffusion of Sodium Hydroxide at 25°C.

ion is taking up water of hydration as the molality increases. Consideration of the physical picture of this situation leads one to conclude that the probability of such an occurrence is rather small, since the ratio of water to hydroxide ion would be decreasing with increasing hydroxide concentration. An entirely different explanation of the results in Fig. 11 considers the deviations to be due to the formation of ion-pairs as previously discussed. For such a case it was shown by Wishaw and Stokes (40) and can be readily seen from Equation (90) that one may define a diffusion coefficient for the ion-pair and thus arrive at the following equation:

$$D = \left[1 + .036m\left(\frac{D^*_{H_2O}}{D^o} - h^*\right)\right]\left(1 + m\,\frac{d\ \ln\ \gamma_{\pm}}{dm}\right)$$
$$x(\alpha D_C + 2(1 - \alpha)\ D_{ip})\ \eta_o/\eta \qquad (93).$$

In this equation, α is the degree of dissociation, $\underline{D_C}$ is the limiting diffusion coefficient for ionized sodium hydroxide plus the two electrophoretic corrections, and $\underline{D_{ip}}$ is the diffusion coefficient for the ion-pair. Utilizing the values of α calculated from conductivity data, it was thus possible to calculate the diffusion coefficient of the ion-pair, $\underline{D_{ip}}$. The results of these calculations are given in Table III. By showing the existence of ion-pairs and calculating their diffusivities, it can be concluded from Fig. 11 that the hydroxyl ion is not hydrated since the points in this figure approach the theoretical line at low concentrations.

Reviewing the results presented in Table III, it is readily seen that the ion-pair diffusivities vary to only a slight degree. Such a result would, in general, indicate that the degree of dissociation, from which the ion-pair diffusivities were calculated, are reasonably consistent. When the magnitude of the ion-pair diffusivities are viewed, one wonders whether the values are

TABLE III

THE DIFFUSION COEFFICIENT OF ION-PAIRS

$\underline{m}$	α	$\underline{\underline{D}}_{ip}$
0.70	0.975	1.03×10^{-5}
1.00	0.951	1.01×10^{-5}
1.50	0.894	0.97×10^{-5}
2.00	0.833	0.95×10^{-5}

$$\left[\underline{\underline{D}}_{ip}\right]_{av.} = 0.99 \times 10^{-5}$$

realistic. If the two ions are assumed to be spheres of equal size because of the similarity of mass, the resulting ion-pair would have twice the volume of either of the ions. If an ion-pair represented a uniform sphere of twice the volume of an ion, the radius of this sphere would be approximately 1.26 times the radius of one of the ions. In actuality, an ion-pair would be more likely to exist as a prolate spheroid with an axial ratio of two. For such an irregular shape, the friction factor would be 1.048 (48). If the above two assumed factors were correct, the friction factor of an ion-pair would be 1.32 times that of an individual ion. In attempting to apply the above friction factor correction, an additional complication arises; namely, the effect of the assumed Grotthus-type transport mechanism. Thus, the friction factor correction cannot be applied directly to the sodium hydroxide diffusivity because it does not take into account the loss in diffusivity due to the elimination of the Grotthus mechanism. One possible solution to this dilemma is to assume, again because of similarity of mass, that the diffusivity of sodium hydroxide without the Grotthus mechanism is approximated by the diffusivity of sodium chloride or bromide. Using the diffusion coefficient of sodium chloride and applying the friction factor correction of 1.32, one obtains 1.14×10^{-5} for the diffusion coefficient of the ion-pair.

Having calculated the degree of ion-pair formation from a modification of the Onsager-Fuoss theory for conductance and also having calculated the diffusion coefficient of the ion-pair from the modified Hartley-Crank equation, there remained a very significant question. How realistic is the concept of ion-pair formation in aqueous sodium hydroxide solution? The author's attention was pointed to nuclear magnetic resonance measurements which determine the nature of a proton's atmosphere. Gutowsky and Saika (49) found that for hydrochloric acid and potassium hydroxide solutions the proton shift was a linear function of the fraction of protons in solution which theoretically should be associated with the hydronium and hydroxide ions. However, for sodium hydroxide the proton shift was not a linear function of the fraction of protons in the hydroxide ion over any significant portion of the concentration range studied, up to maximum solubility. They (49) concluded that the results for sodium hydroxide could be explained only by the formation of Na^+OH^- ion-pairs. Thus, the previously assumed existence of ion-pairs, as shown by the diffusion and conductivity data, appears to be substantiated by an essentially direct measurement. In addition to this evidence, it can be pointed out that the limited data on potassium hydroxide diffusion (50) show the characteristic minimum in the diffusion coefficient-concentration curve, a condition predicted by the N.M.R. spectral results. While the potassium hydroxide diffusion coefficients are of the integral type, the trends are sufficient to indicate the diffusion coefficient minimum.

THE TEMPERATURE DEPENDENCE OF SODIUM HYDROXIDE DIFFUSION

In addition to the diffusion measurements at 25°C. discussed in the previous section, measurement series were also made at 20, 30, and 35°C. The procedures used in making these measurements were the same as those used at 25°C. Results for the three temperatures are given in Tables IV, V, and VI and summarized in Table VII. The results from the last table are shown graphically in Fig. 12-14

TABLE IV

RESULTS OF SODIUM HYDROXIDE DIFFUSION

Temperature = 20.00 ± 0.01°C.

Apparent Diffusion Coefficient, sq.cm./sec.	Reciprocal Time, $sec.^{-1}$
Mean Concentration = 0.02783N	
1.809×10^{-5}	2.545×10^{-4}
1.788	1.754
1.782	1.383
1.778	1.287
1.775	1.191
Mean Concentration = 0.05440N	
1.734×10^{-5}	1.149×10^{-4}
1.731	1.075
1.728	1.025
1.728	0.980
1.730	0.939
Mean Concentration = 0.1028N	
1.712×10^{-5}	1.852×10^{-4}
1.705	1.515
1.701	1.333
1.700	1.191
1.695	1.075
Mean Concentration = 0.3181N	
1.636×10^{-5}	1.282×10^{-4}
1.633	1.111
1.631	1.010
1.631	1.952
1.629	0.901
Mean Concentration = 0.7413N	
1.547×10^{-5}	1.191×10^{-4}
1.546	1.075
1.544	0.980
1.544	0.926
1.542	0.877

TABLE V

RESULTS OF SODIUM HYDROXIDE DIFFUSION

Temperature = 30.06 ± 0.01°C.

Apparent Diffusion Coefficient, sq.cm./sec.	Reciprocal Time, $sec.^{-1}$
Mean Concentration = 0.02543N	
2.546×10^{-5}	3.745×10^{-4}
2.449	2.506
2.403	1.927
2.372	1.558
2.349	1.235
Mean Concentration = 0.03675N	
2.330×10^{-5}	4.105×10^{-4}
2.276	2.637
2.250	1.943
2.240	1.575
2.226	1.325
Mean Concentration = 0.08905N	
2.267×10^{-5}	1.805×10^{-4}
2.240	1.482
2.210	1.212
2.207	1.026
2.190	0.889
Mean Concentration = 0.2341N	
2.193×10^{-5}	3.086×10^{-4}
2.168	2.252
2.128	1.754
2.119	1.456
2.106	1.244
Mean Concentration = 0.5444N	
2.062×10^{-5}	1.852×10^{-4}
2.057	1.658
2.052	1.501
2.047	1.386
2.044	1.277
Mean Concentration = 1.1011N	
2.044×10^{-5}	2.381×10^{-4}
2.020	1.667
2.016	1.515
2.011	1.389
2.007	1.282

TABLE VI

RESULTS OF SODIUM HYDROXIDE DIFFUSION

Temperature = 35.00 ± 0.01°C.

Apparent Diffusion Coefficient, sq.cm./sec.	Reciprocal Time, $sec.^{-1}$
Mean Concentration = 0.02889N	
2.627×10^{-5}	4.065×10^{-4}
2.558	2.381
2.521	1.667
2.511	1.515
2.517	1.389
Mean Concentration = 0.05717N	
2.502×10^{-5}	2.222×10^{-4}
2.487	1.961
2.482	1.754
2.473	1.587
2.466	1.449
Mean Concentration = 0.09954N	
2.930×10^{-5}	3.030×10^{-4}
2.806	2.381
2.720	1.961
2.664	1.667
2.631	1.515
Mean Concentration = 0.3139N	
2.327×10^{-5}	1.667×10^{-4}
2.315	1.389
2.313	1.277
2.311	1.212
2.308	1.149
Mean Concentration = 0.7523N	
2.297×10^{-5}	2.381×10^{-4}
2.271	1.587
2.253	1.282
2.244	1.149
2.237	1.093

TABLE VII

DIFFERENTIAL DIFFUSION COEFFICIENTS OF SODIUM HYDROXIDE

Mean Concentration, moles/l.	Differential Diffusion Coefficient, sq.cm./sec.
Temperature = 20.00 ± 0.01°C.	
0.02783	1.746×10^{-5}
0.05440	1.707
0.1028	1.674
0.3181	1.615
0.7413	1.532
Temperature = 30.06 ± 0.01°C.	
0.02543	2.251×10^{-5}
0.03675	2.179
0.08905	2.117
0.2341	2.047
0.5444	2.002
1.101	1.964
Temperature = 35.00 ± 0.01°C.	
0.02889	2.448×10^{-5}
0.05717	2.402
0.09954	2.335
0.3139	2.267
0.7521	2.194

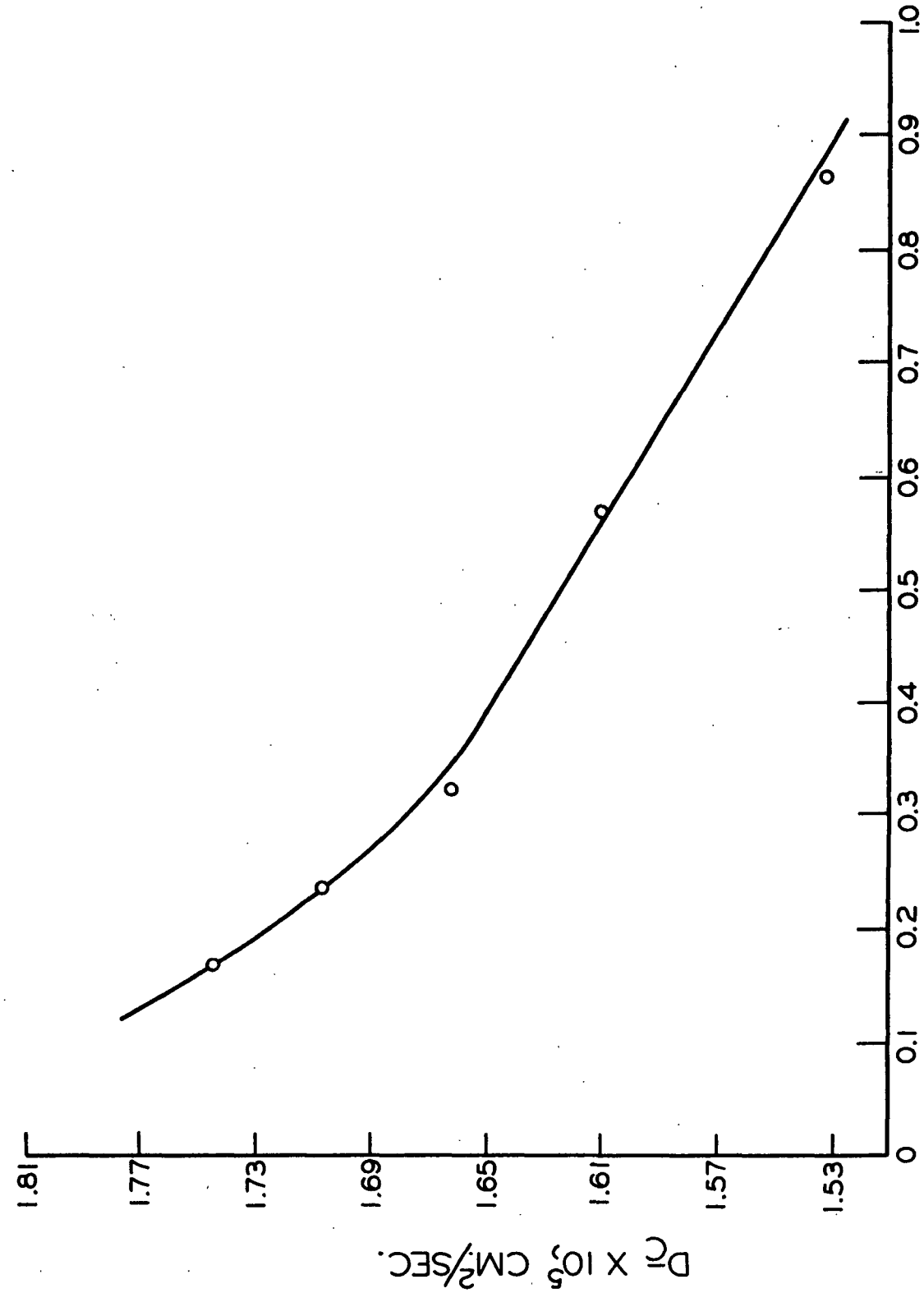

Figure 12. The Diffusion of Sodium Hydroxide at 20°C.

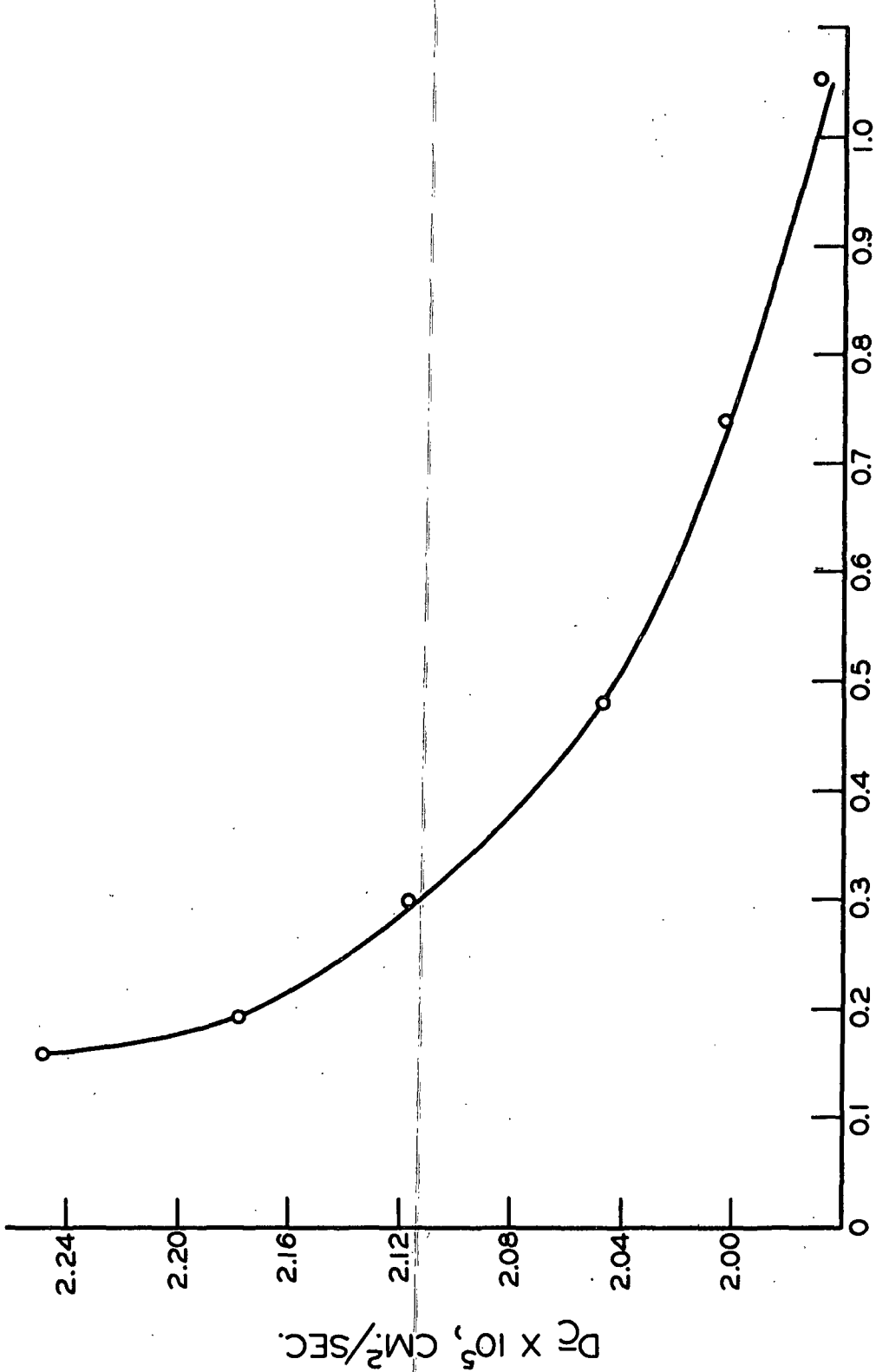

Figure 13. The Diffusion of Sodium Hydroxide at 30°C.

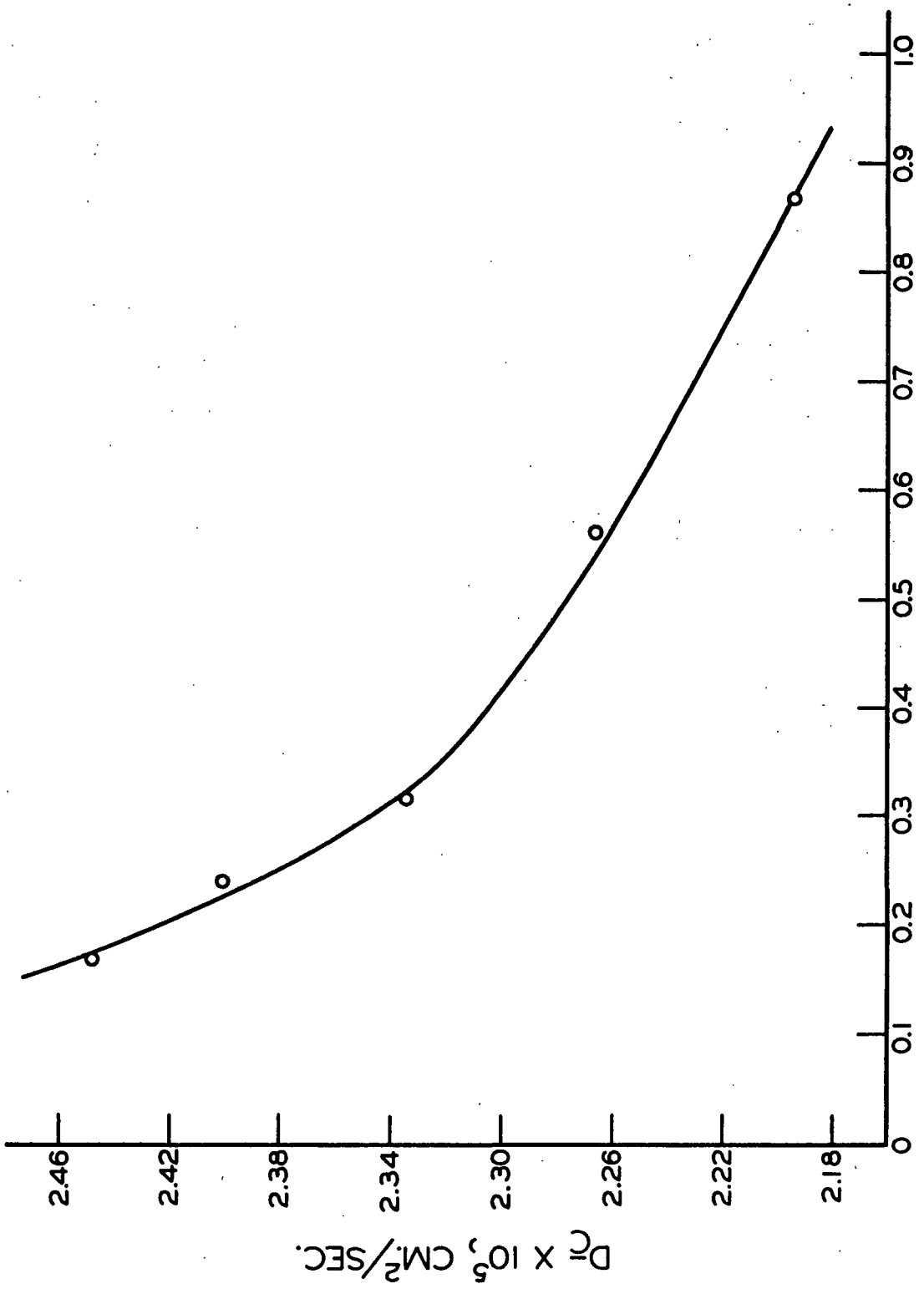

Figure 14. The Diffusion of Sodium Hydroxide at 35°C.

using the normal co-ordinates of diffusion coefficient and square root of concentration. In order to assess the consistency of the data, zero-time correction plots are presented in Appendix III. Since sufficient supplementary data are not available for a quantitative analysis of these results, it will be necessary to discuss them in qualitative terms. It becomes immediately apparent from Fig. 12-14 that the general concentration-dependence of sodium hydroxide diffusion is not radically changed by changes in temperature from 20 → 35°C. If one compares the concentration-dependence for each of the four temperatures investigated as shown in Fig. 15 it can be seen that the rate of change of diffusion coefficient with concentration, at a seven-tenths molar concentration, generally decreases with increasing temperature. In the previous section it was indicated that because of ion-pair formation sodium hydroxide did not exhibit the rather characteristic minimum in the diffusion coefficient-concentration curve. From the indication of ion-pair formation, one would expect the above effect of temperature on concentration-dependence based on the Bjerrum theory of ion-pair formation (41) as presented by Robinson and Stokes (51). According to the Bjerrum theory, the probability of ion-pair formation at a particular ion concentration is inversely proportional to the absolute temperature. This result arises from the fact that the forces tending to cause ion-pair formation, the electrostatic forces, are opposed by the thermal forces which give rise to Brownian motion; the thermal forces being proportional to the product of Boltzmann's constant and the absolute temperature.

In Table VIII and Fig. 16, the temperature-dependence of sodium hydroxide diffusion at two concentrations is shown along with that of sodium chloride. The usual co-ordinates of the log of the diffusion coefficient and the reciprocal of the absolute temperature are used in the figure. For sodium hydroxide at one-tenth normal it is seen that the activation energy, as indicated by the slope of

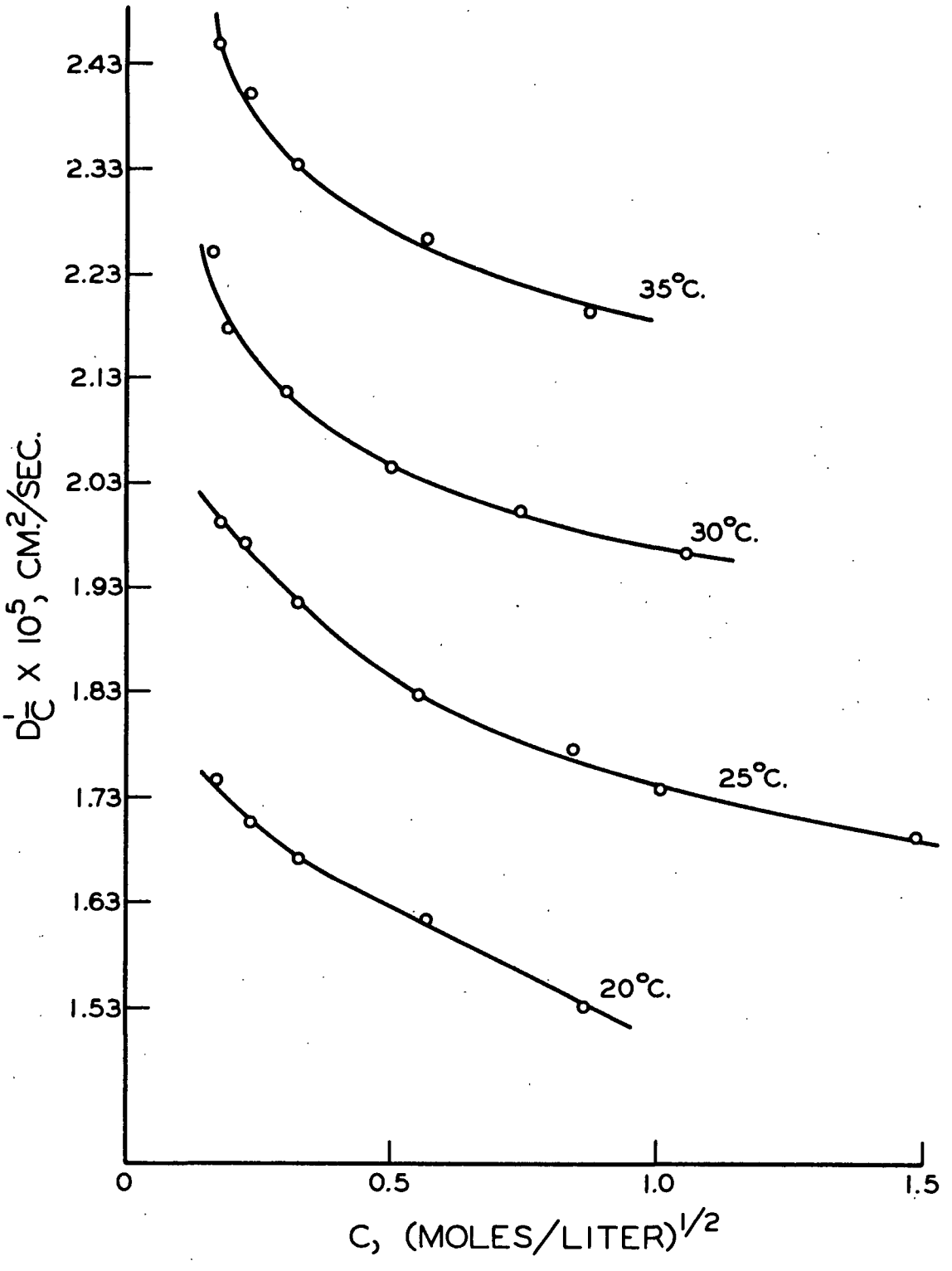

Figure 15. The Diffusion of Sodium Hydroxide at 20, 25, 30, 35°C.

TABLE VIII

TEMPERATURE DEPENDENCE OF DIFFUSION

t, °C.	$1/T$, °K^{-1}	$\log_{10}$ (D x 10^5)	D x 10^5
	Sodium Hydroxide ($\bar{C}$ = 0.10N)		
20.00	3.41 x 10^{-3}	0.224	1.673
25.00	3.35 x 10^{-3}	0.282	1.912
30.06	3.30 x 10^{-3}	0.324	2.111
35.00	3.25 x 10^{-3}	0.369	2.341
	Sodium Hydroxide ($\bar{C}$ = 0.70N)		
20.00	3.41 x 10^{-3}	0.188	1.543
25.00	3.35 x 10^{-3}	0.248	1.772
30.06	3.30 x 10^{-3}	0.299	1.992
35.00	3.25 x 10^{-3}	0.342	2.200
	Sodium Chloride[a] ($\bar{C}$ = 0.10N)		
10.0	3.53 x 10^{-3}	0.013	1.03
15.0	3.47 x 10^{-3}	0.076	1.19
20.0	3.41 x 10^{-3}	0.143	1.39
25.0	3.35 x 10^{-3}	0.207	1.61
30.0	3.30 x 10^{-3}	0.265	1.84

[a]Data from International Critical Tables (55).

the line, is essentially constant from 25 to 35°C. but is measurably higher between 20 and 25°C. as shown in Table IX.

TABLE IX

ACTIVATION ENERGY OF DIFFUSION

Solute	Temp. Range, °C.	$\bar{C}$	Activation Energy, cal./mole
NaOH	20-25	0.10	4700
NaOH	25-35	0.10	3700
NaOH	20-35	0.70	4300[a]
NaCl	10-30	0.10	5100

[a]For assumption of constant activation energy.

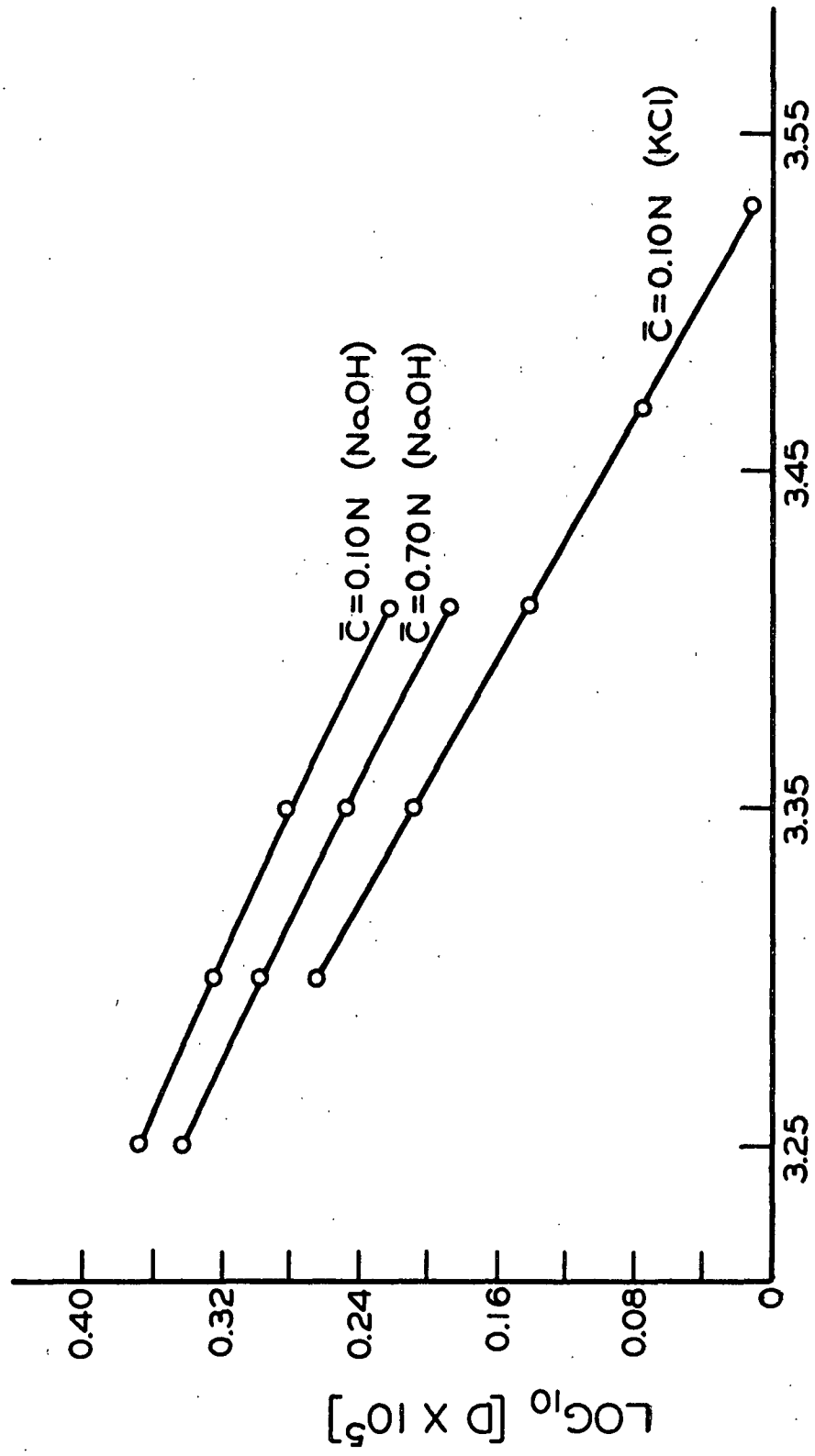

Figure 16. The Temperature-Dependence of Sodium Hydroxide and Sodium Chloride Diffusion

Specifically, the activation energy between 20 and 25°C. is 4700 cal./mole and between 25 and 35°C. is 3700 cal./mole. The difference between these two activation energies has been found to be statistically significant by regression analysis. While it is not possible to attach quantitative significance to the activation energies, they are of qualitative importance. According to Glasstone, Laidler, and Eyring (52), the activation energy is a measure of the energy required for a molecule to enter into a physical or chemical reaction. Thus, it is seen that sodium hydroxide requires more energy to diffuse in the 20 to 25°C. range than in the 25 to 35°C. range. Such a situation is consistent with the previously presented indication that ion-pair formation exists in sodium hydroxide solutions. In the previous section it was shown that at 25°C. ion-pair formation was expected in the 0.25 to 0.30N concentration range. It is thus conceivable that in the 20 to 25°C. range ion-pairs are being formed at a considerably lower concentration and because of their formation more energy is required for diffusion. Such an explanation is partially supported by the results of Wang (53) for the self-diffusion of water. Wang observed that from 10 to 50°C. the activation energy of self-diffusion of water was constant and therefore he concluded that the structure of water did not change appreciably with temperature in the range studied. His view of the structure of water was the same as that presented by Cross and co-workers (54) from Raman spectra experiments. Since the structure of water does not change over the temperature range of this investigation, the change in activation energy for diffusion must be due to a change in the diffusing species.

In Fig. 16, the temperature-dependence of sodium hydroxide diffusion at seven-tenths normal concentration is shown to be somewhat like that at one-tenth normal. The essential difference between the two concentrations is the region over which the different activation energies exist. At seven-tenths normal,

the average activation energy is 4300 cal./mole over the 20 to 35°C. temperature range. This activation energy is statistically significant from the activation energy between 25 and 35°C. at one-tenth normal. While the activation energy for a concentration of seven-tenths normal was presented as a constant, it should be noted that the data in Fig. 16 for this concentration actually describes a curve that is concave downward. Since it is not possible to analyze these data by regression statistics, it can be pointed out that one could not adjust the diffusion coefficients within their statistical confidence limits and eliminate the curvature. Although this curvature may be fortuitous, it does suggest the possibility that the activation energy is decreasing with increasing temperature. Such a change in activation energy, if real, would be consistent with the existence of ion-pairs and would be in the proper direction based on the Bjerrum theory (51).

In addition to the data on the temperature-dependence of sodium hydroxide diffusion, Fig. 16 shows this effect on sodium chloride; the data being taken from the International Critical Tables (55). It is apparent from the figure that the sodium chloride diffusion coefficient yields a linear temperature-dependence plot. This is contrasted to the partially curved plots of sodium hydroxide and suggests that, like the self-diffusion of water, the structure of the species and its surroundings are not affected by temperature. It is also to be noted that the activation energy for sodium chloride diffusion is 5100 cal./mole as compared to a range of 3700 to 4700 cal./mole for sodium hydroxide at one-tenth normal. Such a difference between the two solutes, which may amount to 1400 cal./mole and is statistically significant, suggests that the mechanism of diffusion is somewhat different for the two electrolytes when ion-pairs are not present. The possibility of a different mechanism of diffusion

for sodium hydroxide such as a Grotthus-type mechanism is thus indicated by the temperature-dependence as well as by the concentration-dependence discussed in the previous section.

CONCLUSIONS

It was shown that, by proper modification of the "oil lye" method of sodium hydroxide purification and manipulation of the material in a controlled atmosphere, a highly purified solution of sodium hydroxide could be prepared for physicochemical study.

Comparison of the diffusion of sodium hydroxide at 25°C. with the predictions of the Onsager-Fuoss theory showed that the original premise of the applicability of the theory was invalid except at very low concentrations. The diffusion of sodium hydroxide also does not coincide with the modified Hartley-Crank relationship, except at low concentrations. This relationship accounts for counterdiffusion of solvent, ionic hydration effects, and solution viscosity changes. From application of the Hartley-Crank relationship at low concentrations the sodium ion appeared to be hydrated normally but the hydroxide ion was not.

It was shown that sodium hydroxide conductivity data from the literature could be analyzed theoretically, up to three-tenths molal, by: (1) treating the ions individually and applying Kohlrausch's law, (2) applying the electrophoretic correction and Falkenhagen relaxation correction to the sodium ion, (3) applying only the relaxation correction to the hydroxide ion, and (4) utilizing the value of the distance of closest approach obtained from activity data. Above three-tenths molal, it was shown from the conductivity data that ion-pairs existed and the extent of this phenomenon was calculated.

From the calculated values of the extent of ion-pair formation it was possible to utilize the modified Hartley-Crank relationship to calculate the diffusion coefficient of the ion-pair. The ion-pair diffusion coefficients that were

calculated showed a slight decrease with increasing sodium hydroxide concentration. Consideration of the effects of size, shape, and diffusion mechanism of the ion-pairs showed that the calculated values of the ion-pair diffusion coefficients were quite realistic. In addition, nuclear magnetic resonance data in the literature shows that ion-pairs would be present in sodium hydroxide solutions but not in potassium hydroxide solutions. Limited data in the literature also showed that potassium hydroxide exhibited the characteristic minimum in the diffusion coefficient-concentration curve as expected from N.M.R. data.

An investigation of the diffusion of sodium hydroxide at 20, 30, and 35°C. showed that the general concentration-dependence effects exhibited at 25° were present at the other temperatures. One of the results of increasing the temperature was a reduction in the concentration-dependence of diffusion at the higher concentrations. From a presentation of the temperature-dependence according to the reaction rate theory, it was shown that there were two regions of diffusion behavior with respect to temperature; this effect being shown for one concentration. The region of highest activation energy was attributed to the existence of ion-pairs and the lowest activation energy region being considered essentially free of ion-pairs for a concentration of one-tenth normal. Comparison of the temperature-dependence of sodium chloride diffusion with that of sodium hydroxide showed that the activation energy of sodium chloride diffusion may be greater by as much as 400 to 1400 cal./mole at the same concentration. Such a difference was considered to be evidence for the existence of a Grotthus-type transport mechanism in sodium hydroxide diffusion in the absence of ion-pairs.

ACKNOWLEDGMENTS

I wish to express my thanks to the members of my thesis advisory committee, Dr. Harry D. Wilder, Dr. Donald D. Bump, and Dr. Howard S. Gardner, for their time, guidance, and encouragement during the progress of my thesis.

The willingness to listen, constructive criticism, and suggestions of my fellow students are gratefully acknowledged.

An additional note of thanks is in order for Dr. E. O. Dillingham and John A. Carlson for assistance in the use of the electrophoresis-diffusion apparatus. Also, my thanks to John J. Bachhuber for his many suggestions in the use of the IBM 1620-II computer. Finally, my appreciation is extended to Dr. R. W. Nelson for the use of his regression analysis computer program.

A special thanks goes to my wife, Janet, for her continual encouragement and for her help in the mechanics of preparing this dissertation.

NOMENCLATURE

a	the distance of closest approach for an electrolyte
$\mathring{a}$	the distance of closest approach, angstroms
a_j	diameter of an ion of species, j
a_1, a_2	constants in the Creeth concentration-dependence analysis
B_1, B_2, B	constants in the conductivity theory equation
b	reciprocal of the Debye length; defined by Equation (32)
C	concentration in moles per liter
D	diffusion coefficient at finite concentration
D'	apparent diffusion coefficient
$D_{\bar{C}}$	diffusion coefficient at a mean concentration
D_o	diffusion coefficient of electrolyte at infinite dilution
$D^*_{H_2O}$	self-diffusion coefficient of water
D_{ip}	diffusion coefficient of sodium hydroxide ion-pair
D_i	dielectric constant of the medium
E	activation energy per mole
e	base of the Naperian logarithm
F_*, $F_\ddagger$	partition functions of the normal and activated states
$f_{i,j}$	distribution of j ions in the atmosphere of i ions
F	Faraday, 96,500 coulombs/equivalent
H	enthalpy
$H(Z^*)$	error function, $H(Z^*) = \frac{2}{\sqrt{\pi}} \int_0^{Z} e^{-\beta^2} d\beta$
h	Plank's constant
h^*	the moles of bound solvent per mole of electrolyte (degree of hydration)
J	total number of Rayleigh fringes
J_i	fluxes of ion species, i

j specific Rayleigh fringe

K_i forces acting on ion specie, i

k Boltzmann constant

k_1, k_2 constants in the Creeth concentration-dependence analysis

M magnification factor of diffusion apparatus optical system

$\mathcal{m}$ complex function in the diffusion theory which is proportional to the diffusion coefficient by the realtionship $(\partial\mu/\partial n)\mathcal{m} = D$

m concentration in moles per 1000 grams of solvent

$\mathcal{n}$ Avogadro's number

N concentration in molecules per cc.

n_i number of ions of type i per cc.

n number of fringe pairs used in calculation of $\overline{Y}_t$

q_i charge on an ion of species, i

R the gas constant per mole

r radius of electric field around an ion

$\vec{r}_i$ radius vector about an ion of species, i

$\vec{r}_{i,j}$ radius vector between ions i and j

S entropy

T absolute temperature, °K.

t time, sec.

t' apparent time

$U(Z^*), R(Z^*), W(Z^*)$ complex function of the error function

V mean ionic velocity

V_1, V_2, etc. individual ion velocity

$V(\vec{r}_i)$ bulk velocity of the solution at the end of vector $\vec{r}_i$

$V(Z^*), S(Z^*), T(Z^*)$ complex functions of the error function

X co-ordinate on a Rayleigh interferogram

x direction co-ordinate in Fick's law

$\underline{y}_{\pm}$	mean molar activity coefficient
$\underline{Z}$	the probability co-ordinate, $\underline{X}/2(\underline{D}\underline{t})^{1/2}$
$\underline{Z}_{\underline{i}}$	the charge on ion, $\underline{i}$
α	the degree of dissociation of an electrolyte
$\gamma_{\pm}$	mean molal activity coefficient
Δ_1, Δ_2	electrophoretic correction terms
$\Delta\underline{t}$	zero-time correction
$\frac{\Delta x}{x}$	the relaxation correction
ϵ	the charge of an electron
ϵ_o	activation energy per molecule
$\zeta_{\pm}$	mean ionic activity coefficient on the molecular scale
η	viscosity of the solution
η_o	viscosity of the solvent
Λ^o	the equivalent conductivity of an electrolyte
$\Lambda_{(\alpha\underline{C})}$	equivalent conductivity calculated for particular values of α and $\underline{C}$
Λ_e	experimentally determined equivalent conductivity
λ	the distance between equilibrium positions of a diffusing particle (reaction rate theory)
$\lambda_{\underline{i}}$	equivalent conductivity of ion species, $\underline{i}$
μ	chemical potential
$\nu_{\underline{i}}$	ions of species $\underline{i}$ formed per molecule of electrolyte
ρ	the charge density in a particular region
τ	specific reaction rate for diffusion
ψ	the average electrical potential
$\omega_{\underline{i}}$	mobility of ion species, $\underline{i}$
∇	differential operator

LITERATURE CITED

1. Ölholm, L. W., Z. Physik. Chem. 50:309(1904).

2. Onsager, L., and Fuoss, R. M., J. Phys. Chem. 36:2689(1932).

3. Harned, H. S., and Owen, B. B. The physical chemistry of electrolyte solutions. 3rd ed. p. 254. New York, Reinhold Publishing Co., 1958.

4. Harned, H. S., and Owen, B. B. The physical chemistry of electrolyte solutions. 2nd ed. p. 181. New York, Reinhold Publishing Co., 1950.

5. Glasstone, S., Laidler, K. J., and Eyring, H. The theory of rate processes. p. 516. New York, McGraw-Hill Book Co., 1941.

6. Nernst, W., Z. Physik. Chem. 2:613(1888).

7. Debye, P., and Hückel, E., Physik. Z. 24:185, 305(1923).

8. Kirkwood, J. G., Chem. Rev. 19:275(1936).

9. Mayer, J. E., J. Chem. Phys. 18:1426(1950).

10. Porier, J. C., J. Chem. Phys. 21:972(1953).

11. Friedman, H. L. Ionic solution theory. p. 3. New York, Interscience, 1962.

12. Ref. (5), p. 555.

13. Robinson, R. A., and Stokes, R. H. Electrolyte solutions. 2nd ed. p. 286. London, Butterworth's Scientific Publ., 1959.

14. Harned, H. S., Chem. Rev. 40:461(1947).

15. Moore, W. J. Physical chemistry. p. 458. Englewood, New Jersey, Prentice-Hall, 1955.

16. Daniels, F., and Alberty, R. A. Physical chemistry. p. 483, 647. New York, John Wiley & Sons, 1958.

17. Ref. (3), p. 64.

18. Debye, P., and Hückel, E., Physik. Z. 24:305(1923).

19. Ref. (13), p. 133.

20. Ref. (3), p. 42.

21. Ref. (3), p. 48.

22. Fowler, R. H., Trans. Faraday Soc. 23:434(1927).

23. Pierce, W. C., and Haenisch, E. L. Quantitative analysis. p. 124. New York, John Wiley & Sons, 1948.

24. Han, J. E. S., and Chao, T. Y., Ind. Eng. Chem., Anal. Ed. 4:229(1932).

25. Ref. (23), p. 136, 138.

26. Weissberger, Arnold, ed. Physical methods of organic chemistry. Vol. I. Part I. 3rd ed. p. 136. New York, Interscience, 1959.

27. Ref. (23), p. 124-7, 130.

28. Longsworth, L. G., J. Am. Chem. Soc. 74:4155(1952).

29. Washburn, E. R., and Olsen, A. L., J. Am. Chem. Soc. 54:3212(1932).

30. Tables of probability functions. Washington, D. C., Federal Works Agency, Works Project Administration, Supt. of Documents, 1941.

31. Creeth, J. M., J. Am. Chem. Soc. 77:6428(1955).

32. Gosting, L. J., and Fujita, H., J. Am. Chem. Soc. 79:359(1957).

33. Longsworth, L. G., J. Am. Chem. Soc. 69:2510(1949).

34. Ref. (13), p. 515.

35. Ref. (3), p. 702.

36. Kortum, G., and Bocharis, J. O'M. Textbook of electrochemistry. p. 3, 204. New York, Elsevier Publishing Co., 1951.

37. Hamer, W. J., ed. The structure of electrolyte solutions. p. 67. New York, John Wiley & Sons, 1959.

38. Ref. (3), p. 159, 231, 498.

39. Harned, H. S., J. Am. Chem. Soc. 47:676(1925).

40. Wishaw, B. F., and Stokes, R. H., J. Am. Chem. Soc. 76:2065(1954).

41. Bjerrum, N., Kgl. Danske Videnskab. Selskäb. Math-fys. Medd. [9], 7:1-48 (1926).

42. Ref. (13), p. 50.

43. Falkenhagen, H., Leist, M., and Kelby, G., Ann. Phys., Lpz. [6], 11:51 (1952).

44. Darken, L. S., and Meier, H. F., J. Am. Chem. Soc. 64:621(1942).

45. Agar, J. N., University of Cambridge, unpublished work, 1950.

46. Hartley, G. S., and Crank, J., Trans. Faraday Soc. 45:80(1949).

47. Ref. (13), p. 331.

48. Alexander, A. E., and Johnson, P. Colloid science. p. 261. New York, Oxford University Press, 1949.

49. Gutowsky, H. S., and Saika, A., J. Chem. Phys. 21:1688(1953).

50. International Critical Tables, Vol. V. p. 68. New York, McGraw-Hill Book Co., 1929.

51. Ref. (13), p. 392.

52. Ref. (5), p. 2.

53. Wang, J. H., J. Am. Chem. Soc. 73:510(1951).

54. Cross, P. C., Barnham, J., and Leighton, P. A., J. Am. Chem. Soc. 59:1134 (1937).

55. International Critical Tables. Vol. V. p. 67. New York, McGraw-Hill Book Co., 1929.

56. Onsager, L., Physik. Z. 28:277(1927).

57. Stokes, R. H., J. Am. Chem. Soc. 76:1988(1954).

58. Ref. (13), p. 319.

59. Hückel, E., and Schaaf, H., Z. Physik. Chem. 21:326(1959).

60. Ref. (3), p. 150.

61. McBain, J. W., and Dawson, C. R., J. Am. Chem. Soc. 56:52(1934).

APPENDIX I

ZERO-TIME CORRECTION DATA FOR SODIUM HYDROXIDE DIFFUSION AT 25°C.

The zero-time correction data for all diffusion runs at 25°C. are shown in Fig. 17 to 23.

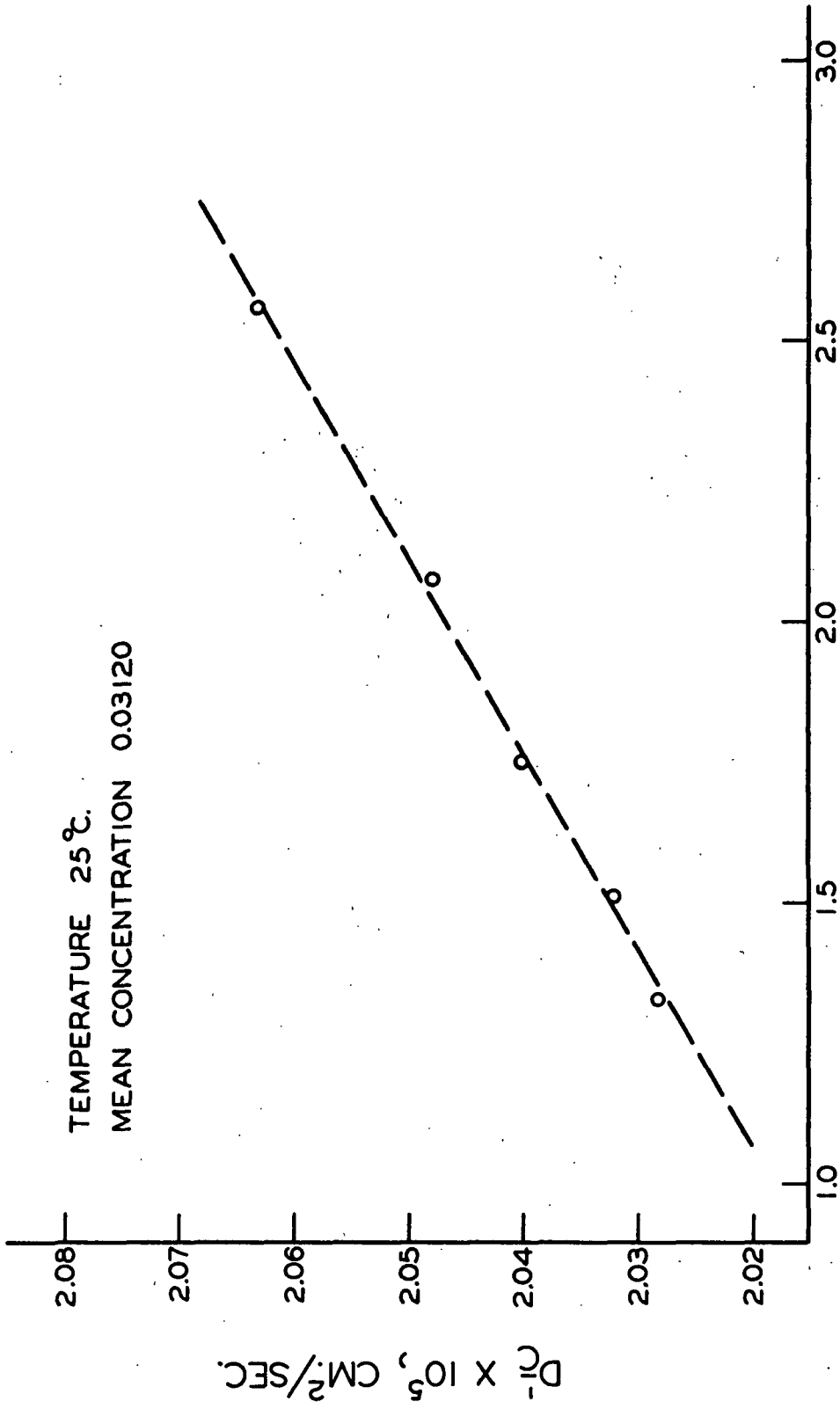

Figure 17. Zero-Time Correction for Diffusion at 25°C. at a Mean Concentration of 0.03120

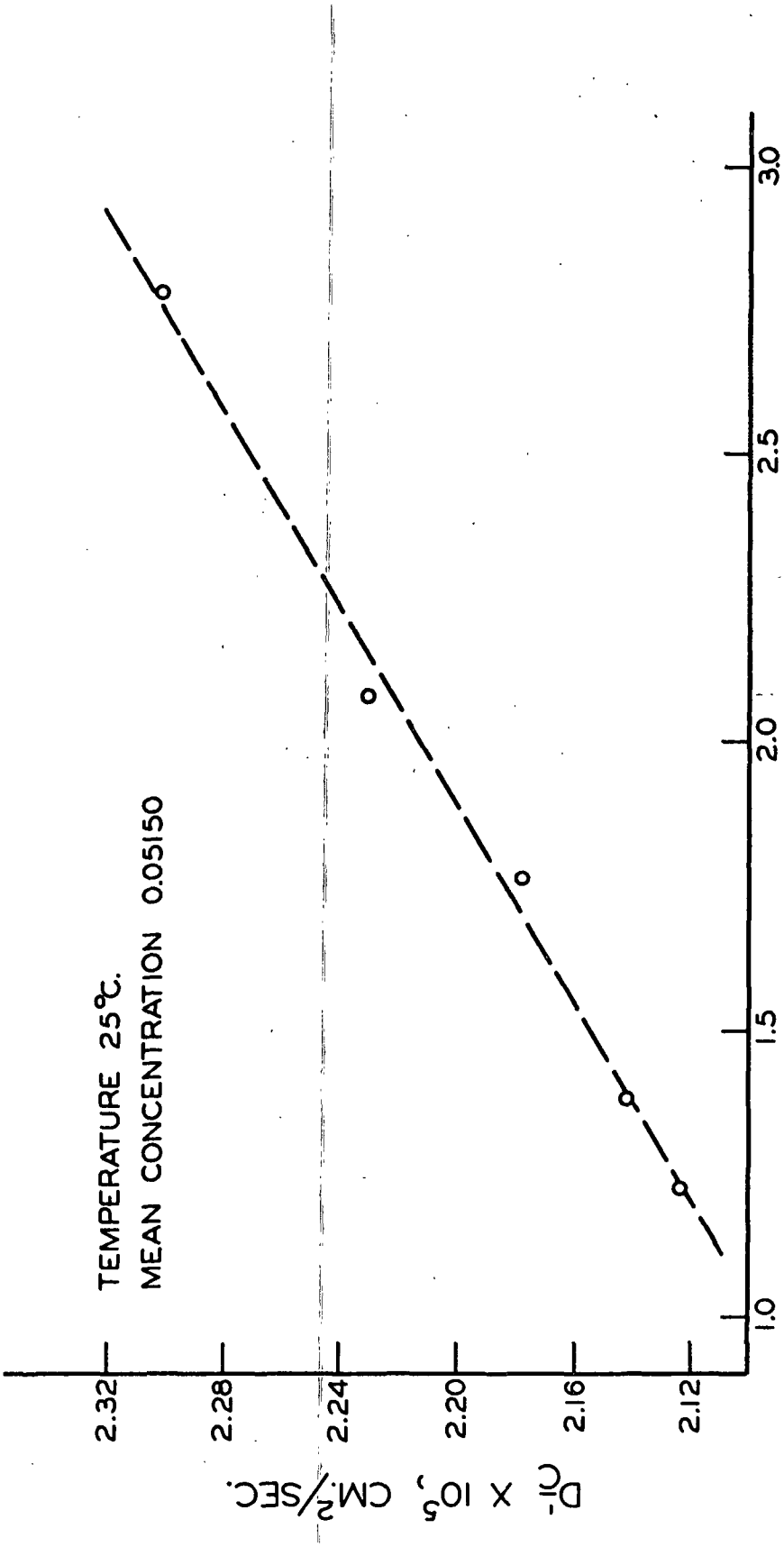

Figure 18. Zero-Time Correction for Diffusion at 25°C. at a Mean Concentration of 0.05150

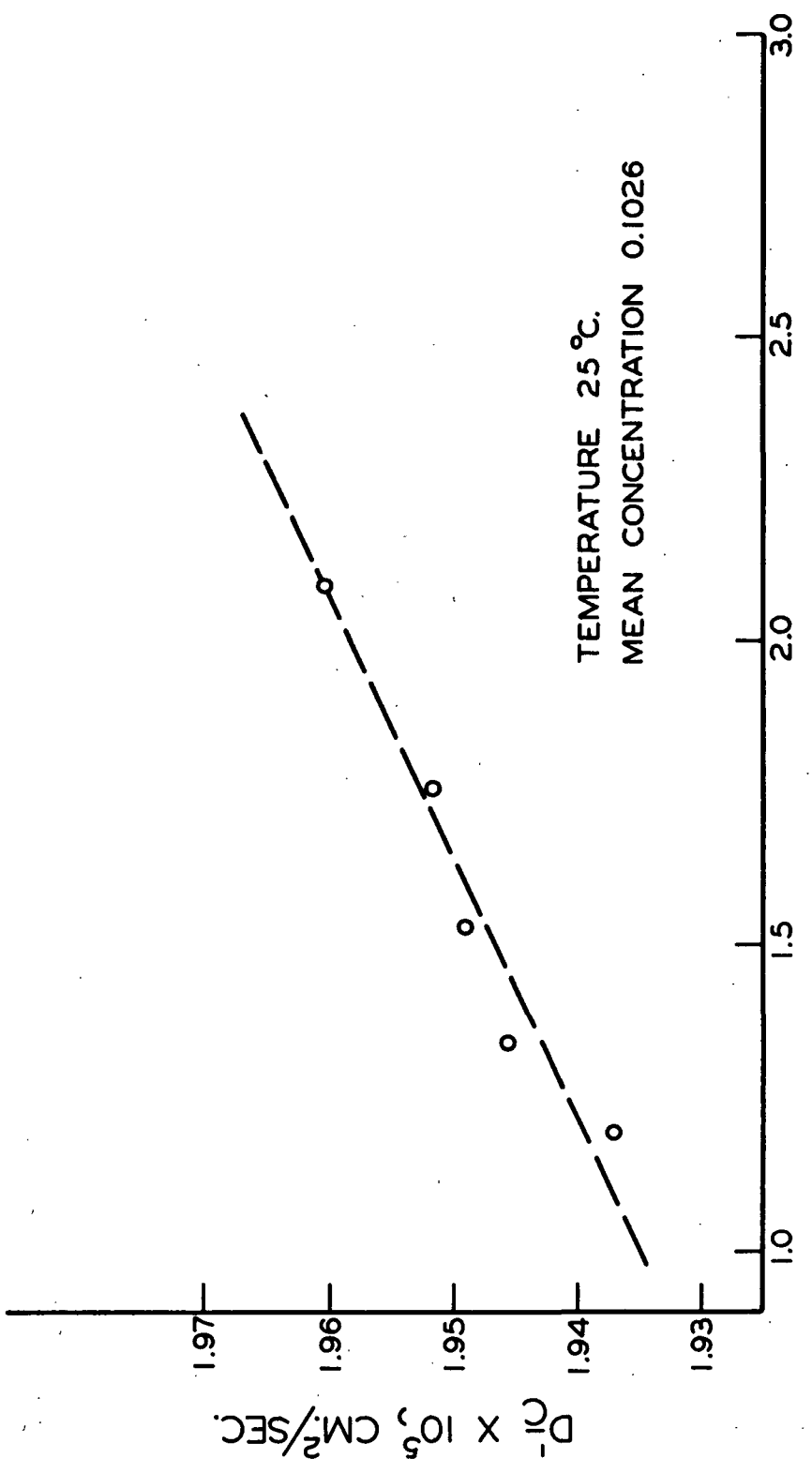

Figure 19. Zero-Time Correction for Diffusion at 25°C. at a Mean Concentration of 0.1026

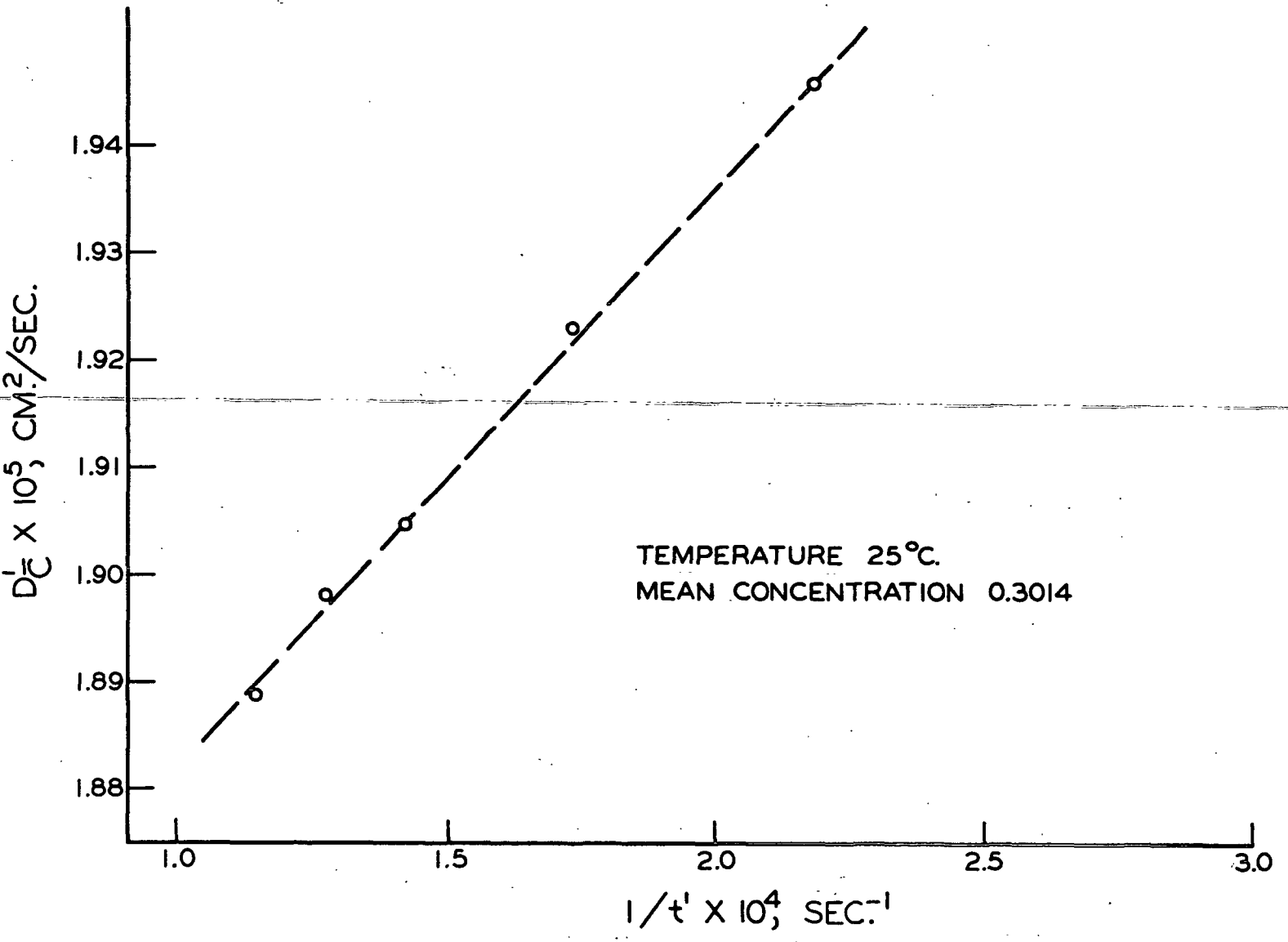

Figure 20. Zero-Time Correction for Diffusion at 25°C. at a Mean Concentration of 0.3014

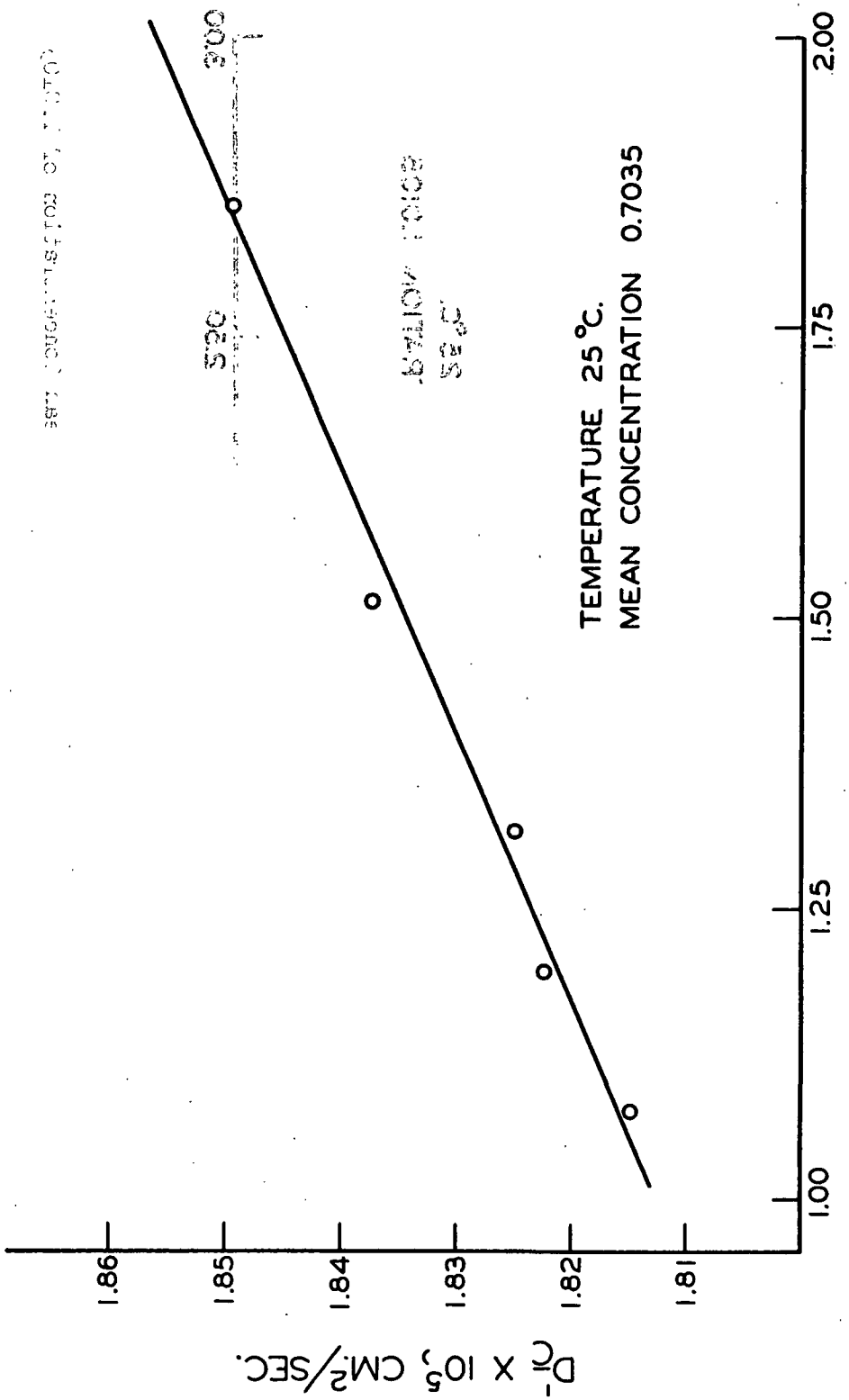

Figure 21. Zero-Time Correction of Diffusion at 25°C. at a Mean Concentration of 0.7035

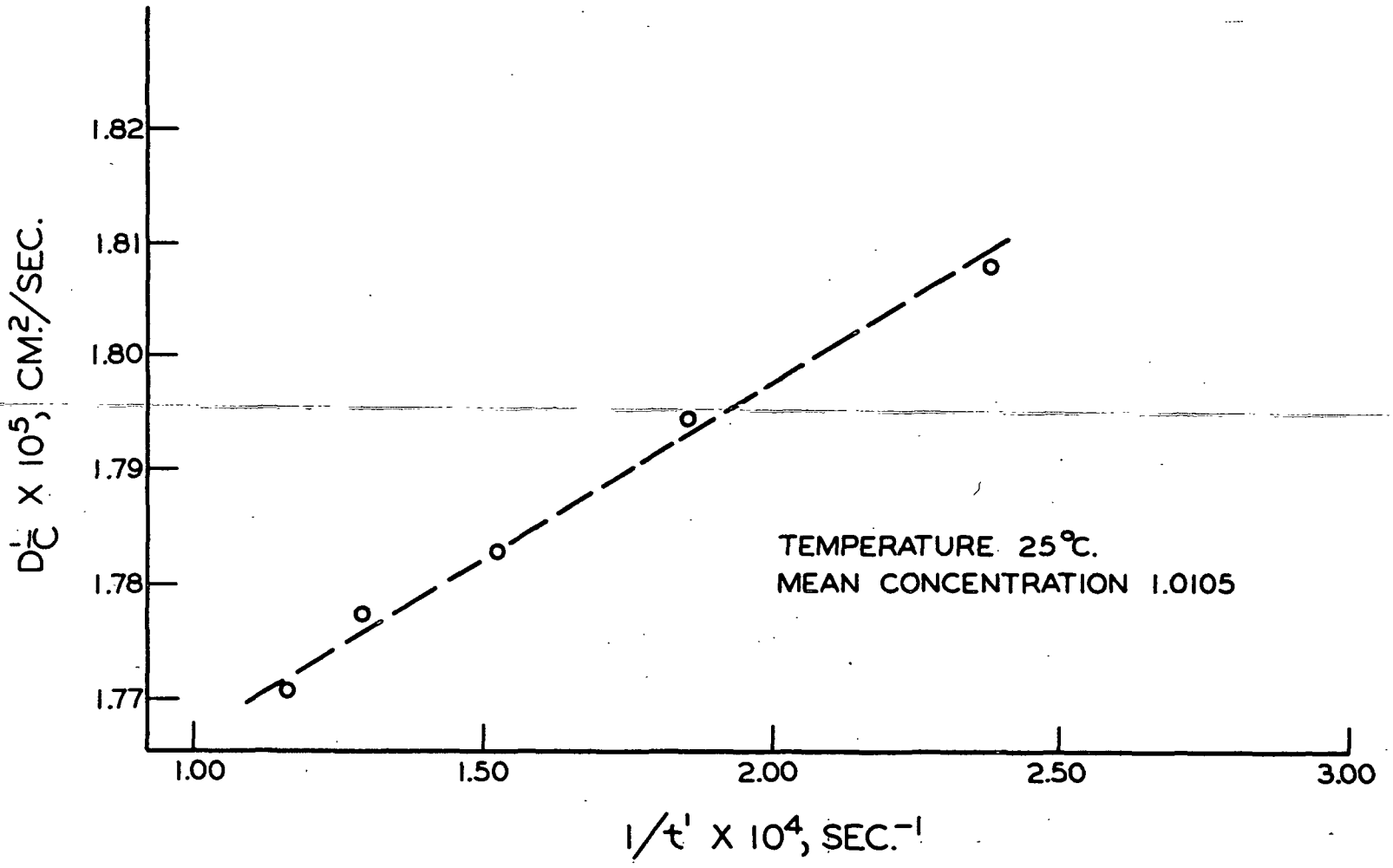

Figure 22. Zero-Time Correction of Diffusion at 25°C. at a Mean Concentration of 1.0105

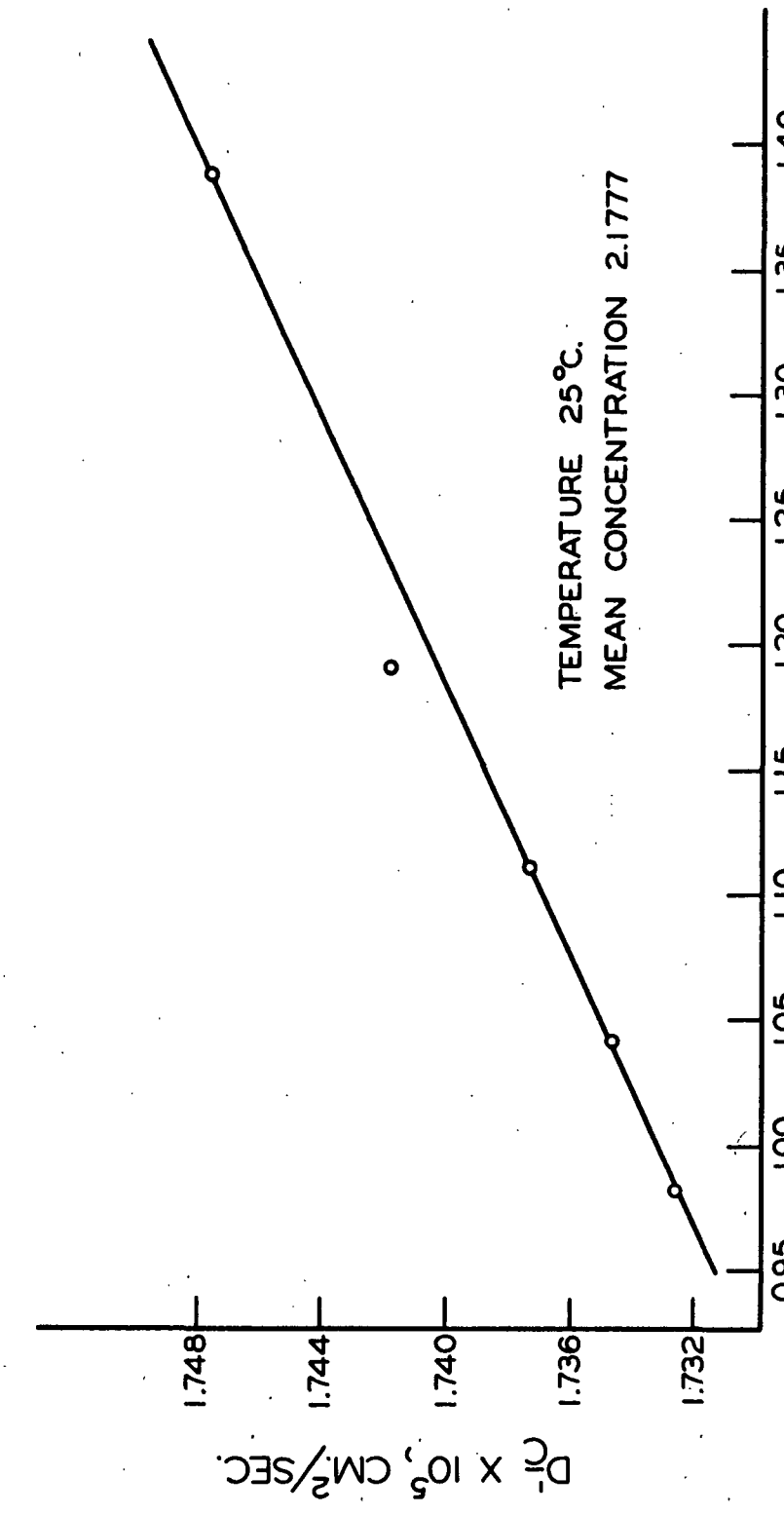

Figure 23. Zero-Time Correction of Diffusion at 25°C. at a Mean Concentration of 2.1777

APPENDIX II

CALCULATION OF DEGREE OF DISSOCIATION FROM CONDUCTIVITY

From the theoretical analysis of Onsager (56), Onsager and Fuoss (2), and Stokes (57), it has been shown that the conductivity of a strong electrolyte is given by

$$\Lambda = \left(\Lambda^{o} - \frac{82.5}{(DT)^{1/2}} \frac{\sqrt{C}}{1 + ba}\right)\left(1 + \frac{\Delta x}{x}\right)\eta_{o}/\eta \qquad (87).$$

The negative quantity in the first parenthesis represents the electrophoretic contribution to the concentration-dependence while the quantity in the second parenthesis represents the relaxation contribution. While the relaxation effect was evaluated by Onsager for dilute solution, it has been more recently evaluated by Falkenhagen, et al. (43) for more concentrated solutions. It has been observed (40, 58) that Equation (87) is applicable to a considerable number of electrolyte solutions up to a relatively high concentration (4-5m) in the form

$$\Lambda = \left(\Lambda^{o} - \frac{B_2\sqrt{C}}{1 + B\mathring{a}\sqrt{C}}\right)\left(1 - \frac{B_1 F\sqrt{C}}{1 + B\mathring{a}\sqrt{C}}\right)\eta_{o}/\eta \qquad (94).$$

In Equation (94), the B's are constants dependent on the temperature, the solvent dielectric constant, the electronic charge, Avogadro's number, and the solvent viscosity. The quantity å is the closest distance of approach of the ions (angstroms) and F is a complex function given by

$$F = [\mathrm{Exp}\ (.2929\ ba) - 1]/.2929\ ba \qquad (95)$$

where b has been previously defined as the reciprocal of the Debye length.

For the case of an electrolyte which tends to form ion-pairs, it has been shown (40) that C in Equation (94) may be replaced by $\alpha \cdot C$, where $(1-\alpha)$ is the extent of ion-pair formation. If this substitution is made, the following

relationship is obtained.

$$\Lambda_e = \alpha \cdot \Lambda_{(\alpha\, C)} \qquad (88).$$

In this equation, Λ_e is the experimentally determined conductivity and $\Lambda_{(\alpha\, C)}$ is the conductivity calculated from Equation (94) with C replaced by $\alpha \cdot C$.

When Equations (94) and (88) were applied to the sodium hydroxide conductivity data of Darken and Meier (44) along with the viscosity data of Hückel and Schaaf (59), it was observed that the results predicted by Equation (94) would fit the observed data only if the adjustable parameter, $\mathring{a}$, were made to equal 5.25 angstroms. In addition, it was observed that even though Equation (94) would fit the conductivity data for $\mathring{a}$ = 5.25 the range of applicability was only up to 0.05M. However, instead of the theory predicting high results as would be the case if ion-pairs existed, the predictions were lower than the experimental values. An additional point is the fact that the 5.25 angstrom value used up to 0.05M is considerably higher than the 3.24 angstrom value predicted empirically from activity data (60).

In reviewing the physical picture of the possible phenomena involved in the conductivity of sodium hydroxide, it was felt that, because of the probability of a Grotthus-type transfer mechanism, certain modifications were necessary to make the conductivity theory applicable. The existence of a Grotthus-type transfer mechanism seems to be quite widely accepted (36, 37) particularly for the hydronium ion, and will be assumed in the succeeding development. Since the two ions involved, sodium and hydroxide, would behave differently in transport due to a Grotthus mechanism, their individual concentration-dependence were evaluated. For the sodium ion the concentration-dependence would be the same as any neutral electrolyte (NaCl, KCl) and would be given by

$$\lambda_{(Na^+)} = \left(\lambda^{o}_{(Na^+)} - \frac{B_2\sqrt{C}}{1 + B\mathring{a}\sqrt{C}}\right)\left(1 - \frac{F\,B_1\sqrt{C}}{1 + B\mathring{a}\sqrt{C}}\right)\eta_o/\eta \qquad (96).$$

However, for the hydroxide there would be no electrophoretic effect or relative viscosity effect since these two effects arise from the viscous drag forces involved in the movement of a particle through uniform media. Thus, the equivalent ionic conductivity of the hydroxide ion would be given by

$$\lambda_{(OH^-)} = \left(\lambda^{o}_{(OH^-)}\right)\left(1 - \frac{F\,B_1\sqrt{C}}{1 + B\mathring{a}\sqrt{C}}\right) \qquad (97)$$

since the relaxation effect would be the only one operating. It is then assumed that the law of Kohlrausch is applicable to ions at finite concentrations with the result being

$$\Lambda_{C,\ NaOH} = \lambda_{C,\ Na^+} + \lambda_{C,\ OH^-} \qquad (98).$$

The use of Kohlrausch's law is supported by the analysis of Stokes (57) for the concentration-dependence of transference numbers in which he evaluated the individual ion effects and then summed them.

Equations (96), (97), and (98) were applied to the sodium hydroxide conductivity data of Darken and Meier (44) and the results of this analysis are shown in Table X. It can be seen that up to approximately 0.4M these equations are quite applicable; even for an å value of 3.24, which is the same as that obtained from activity data (60). Beyond 0.4M, the calculated values of the equivalent conductivity at particular concentrations are greater than the experimental values. Such results are indicative of ion-pair formation and should be amenable to analysis using Equation (88) along with Equations (96), (97), and (98).

TABLE X

RESULTS OF CONDUCTIVITY CALCULATIONS

NaOH Temp. = 25°C. $\underline{\mathring{a}} = 3.24$

$\underline{C}$[a]	α	$\Lambda_{\underline{C}}$[a]	$\alpha \cdot \Lambda_{(\alpha\underline{C})}$
0.0001	1.00	247.70	247.69
0.0003	1.00	246.87	246.85
0.0005	1.00	246.30	246.28
0.0008	1.00	245.64	245.62
0.0010	1.00	245.27	245.25
0.0013	1.00	244.79	244.77
0.0015	1.00	244.50	244.47
0.0018	1.00	244.10	244.07
0.0020	1.00	243.85	243.83
0.0050	1.00	241.13	241.10
0.0075	1.00	239.53	239.50
0.0100	1.00	238.22	238.18
0.0200	1.00	234.39	234.31
0.0500	1.00	227.71	227.36
0.0608	1.00	225.70	224.93
0.09139	1.00	222.40	221.49
0.15173	1.00	216.70	215.70
0.29312	1.00	207.70	207.03
0.44827	0.995	200.00	199.87
0.5665	0.988	195.00	194.98
0.7954	0.969	186.20	186.21
1.1617	0.932	173.80	173.73
1.4737	0.897	164.10	164.05
2.2273	0.806	142.90	142.87

[a]Concentration and conductivity are from Darken and Meier (44).

When Equations (88), (96), (97), and (98) were applied to the conductivity data up to approximately 2.5M, it was found that the degree of ion-pair formation increased fairly rapidly as shown in Table X. It is to be noted that α represents essentially the degree of dissociation and thus $(1-\alpha)$ represents the degree of ion-pair formation. The values of α were determined by trial and error using an IBM 1620-II computer.

APPENDIX III

ZERO-TIME CORRECTION DATA FOR DIFFUSION OF SODIUM HYDROXIDE AT 20, 30, AND 35°C.

The zero-time correction data for all diffusion runs at 20, 30, and 35°C. are shown in Fig. 24 to 39.

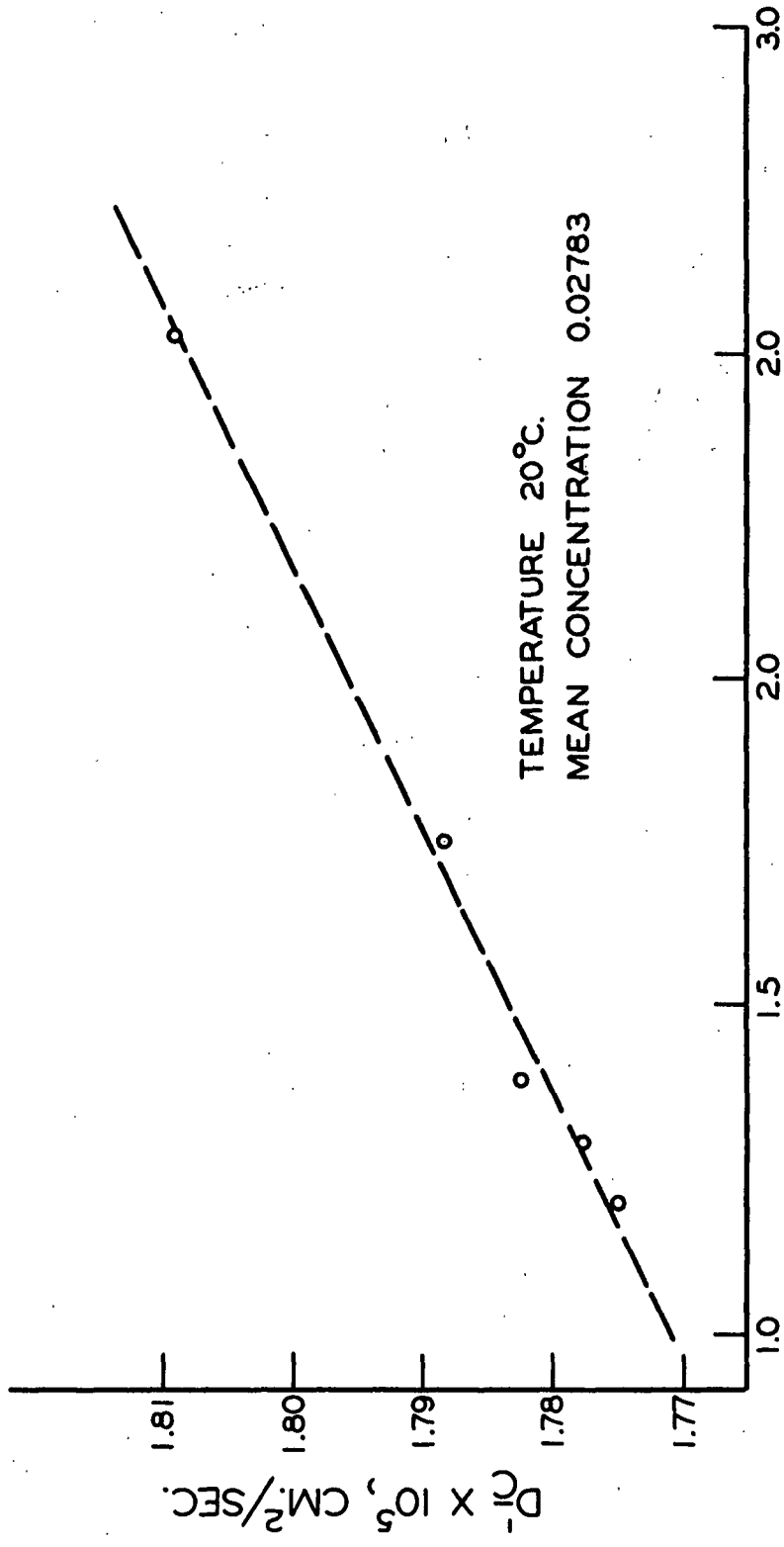

Figure 24. Zero-Time Correction of Diffusion at 20°C. at a Mean Concentration of 0.02783

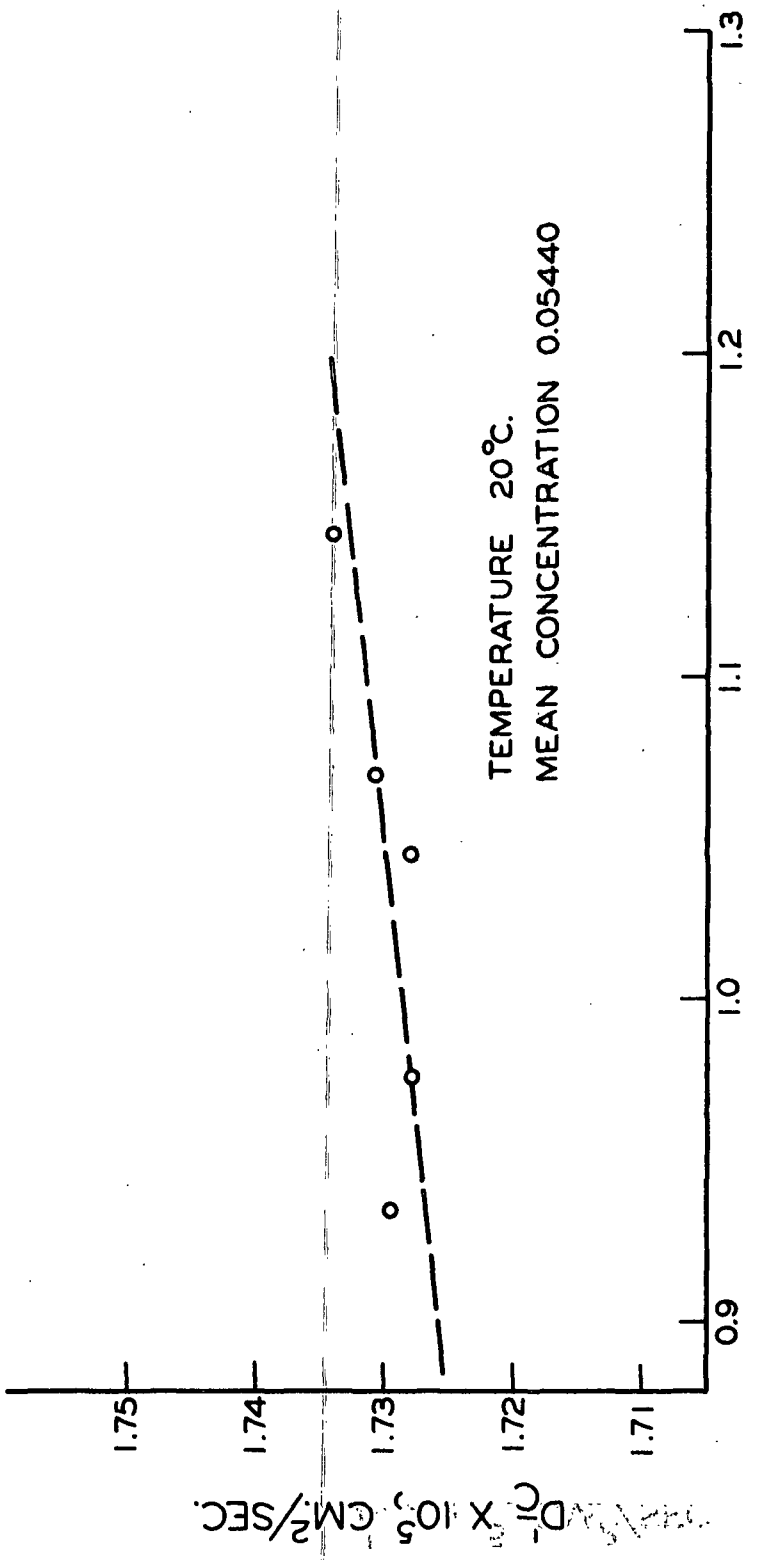

Figure 25. Zero-Time Correction of Diffusion at 20°C. at a Mean Concentration of 0.05440

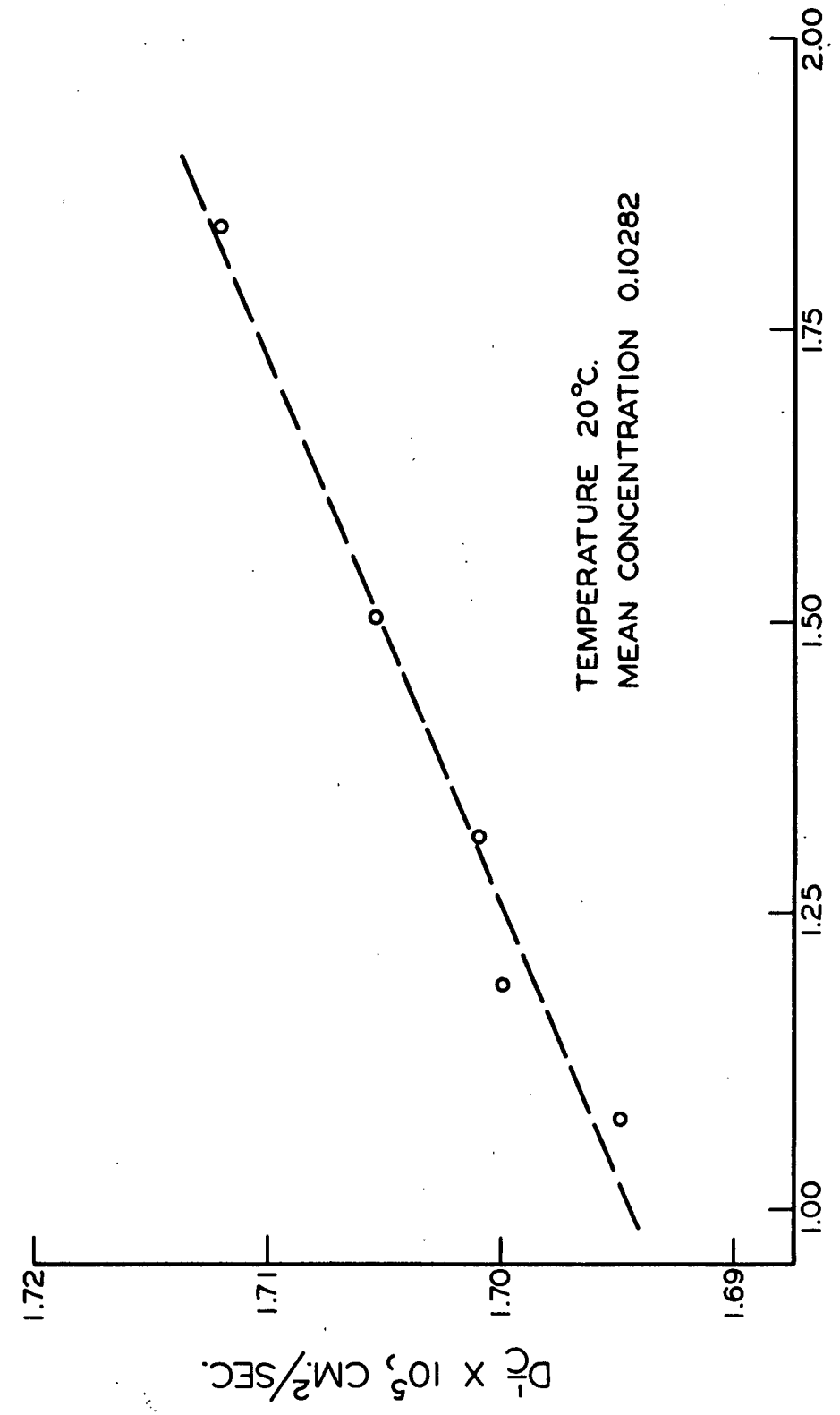

Figure 26. Zero-Time Correction of Diffusion at 20°C. at a Mean Concentration of 0.10282

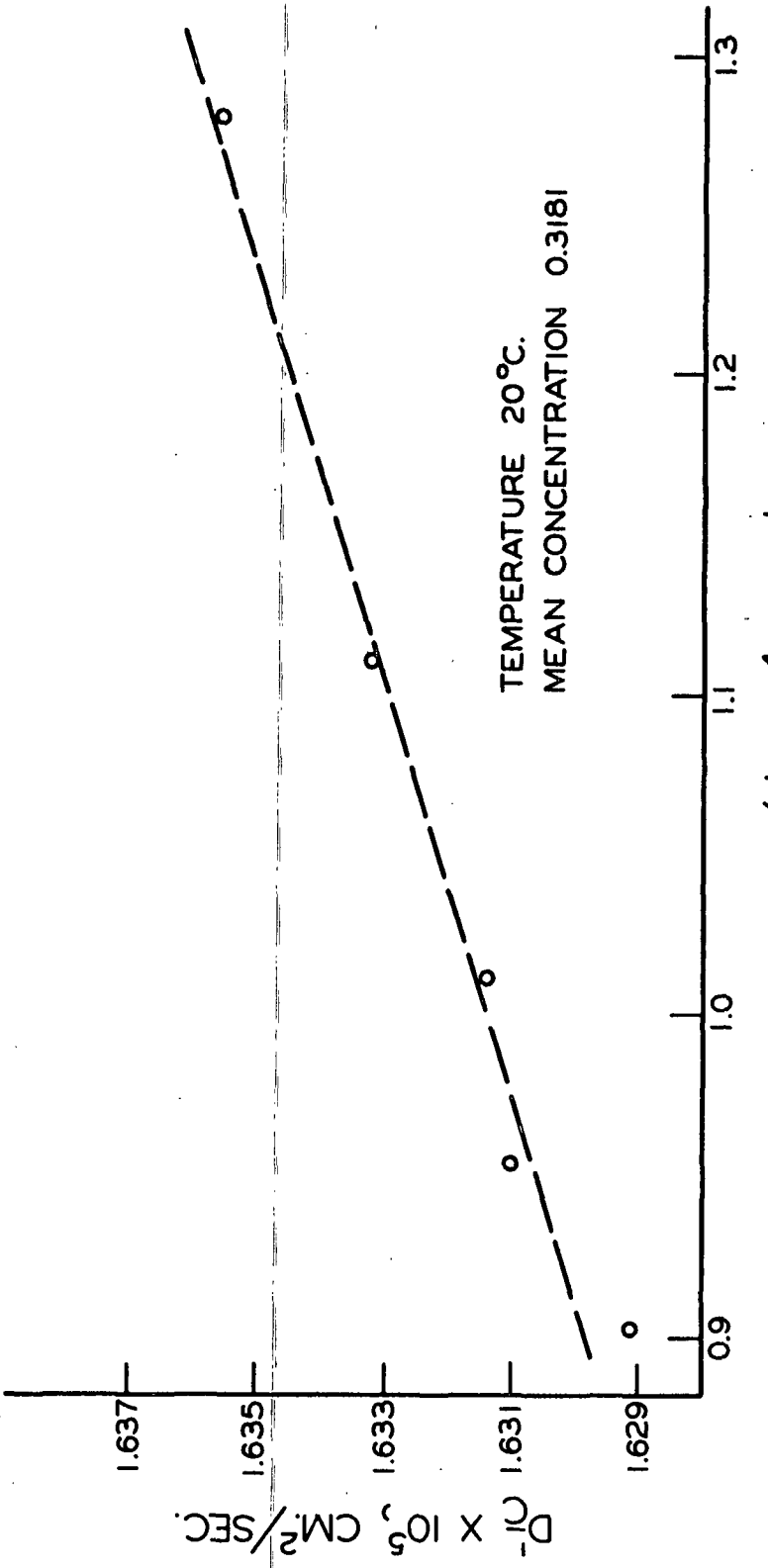

Figure 27. Zero-Time Correction of Diffusion at 20°C. at a Mean Concentration of 0.3181

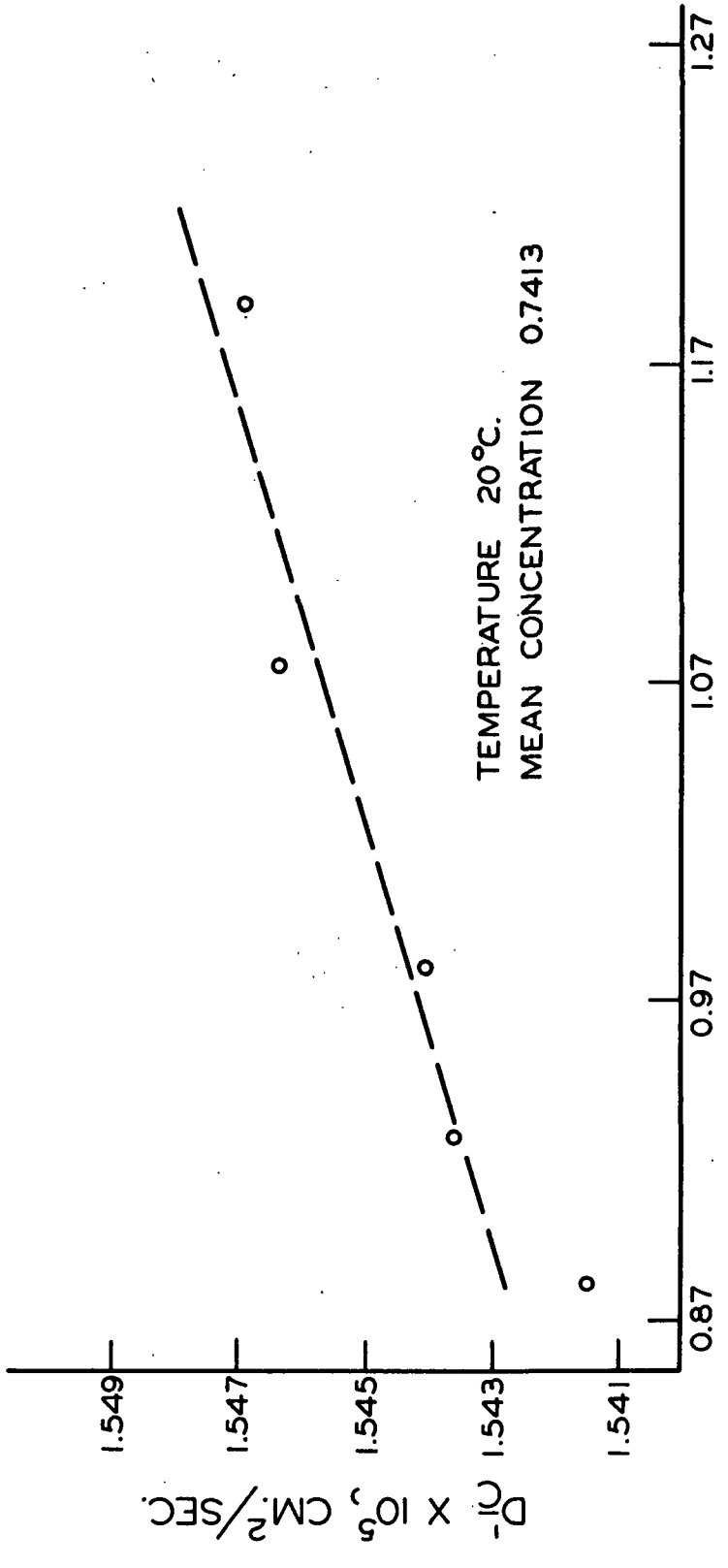

Figure 28. Zero-Time Correction of Diffusion at 20°C. at a Mean Concentration of 0.7413

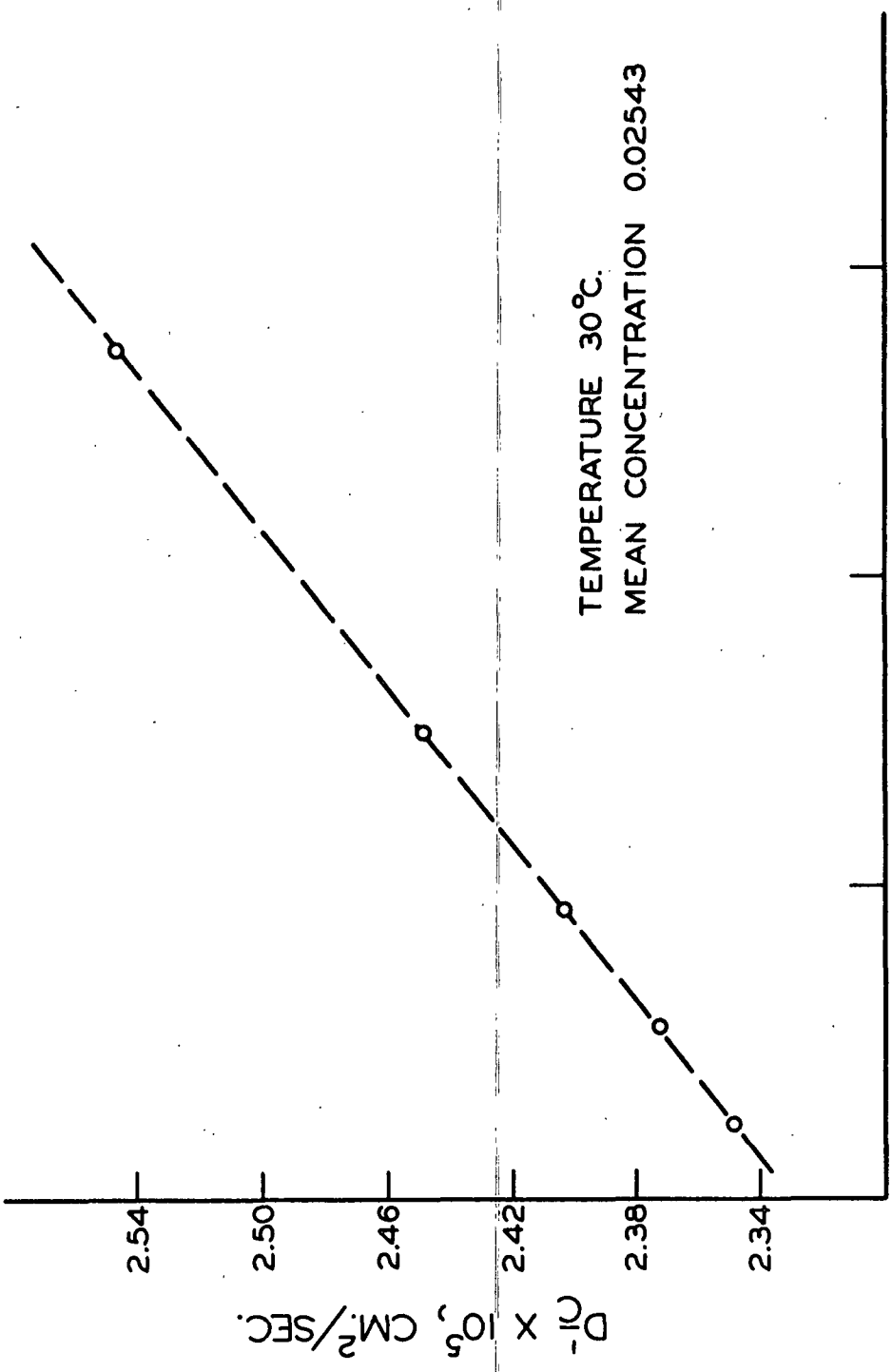

Figure 29. Zero-Time Correction of Diffusion at 30°C. at a Mean Concentration of 0.02543

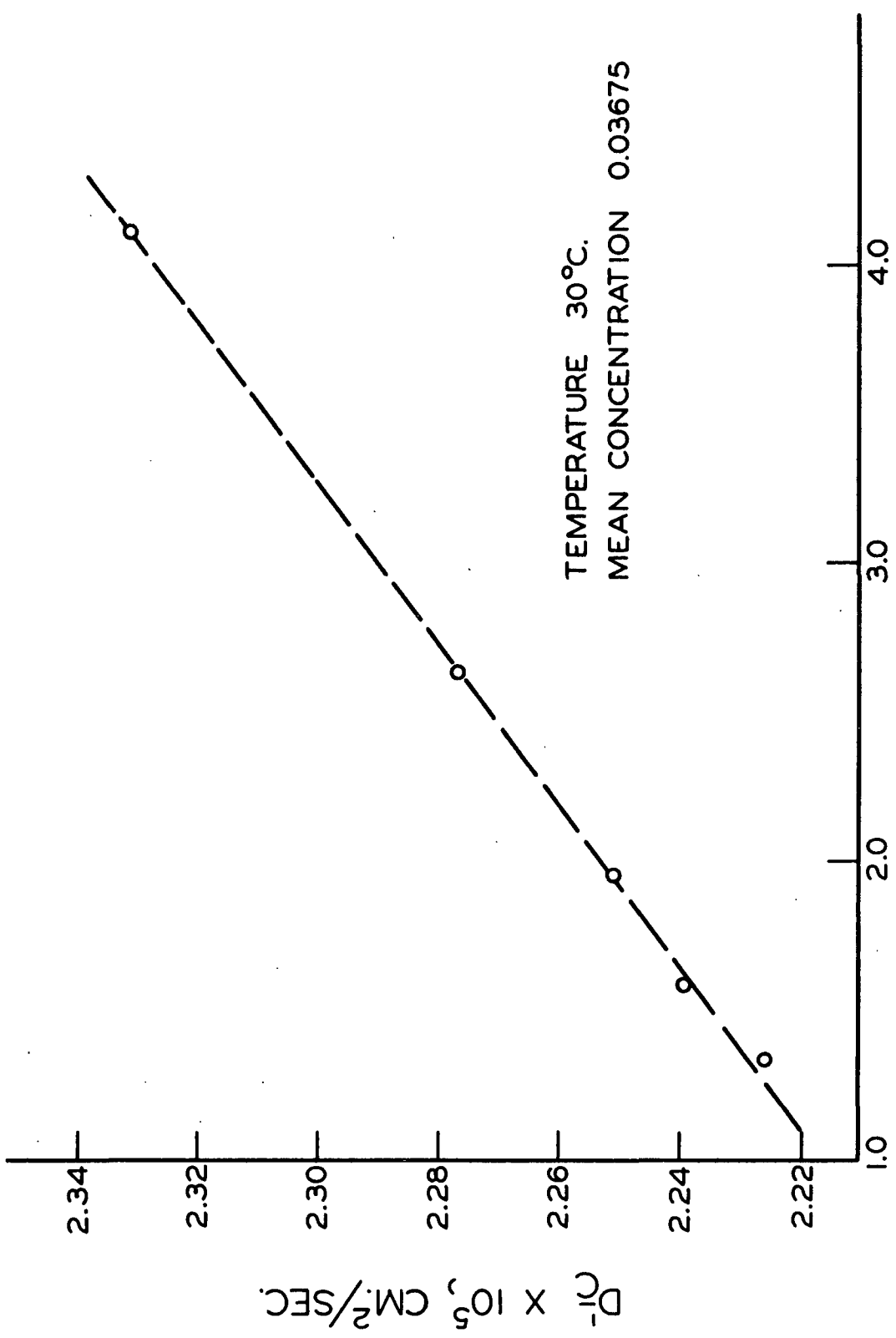

Figure 30. Zero-Time Correction of Diffusion at 30°C. at a Mean Concentration of 0.03675

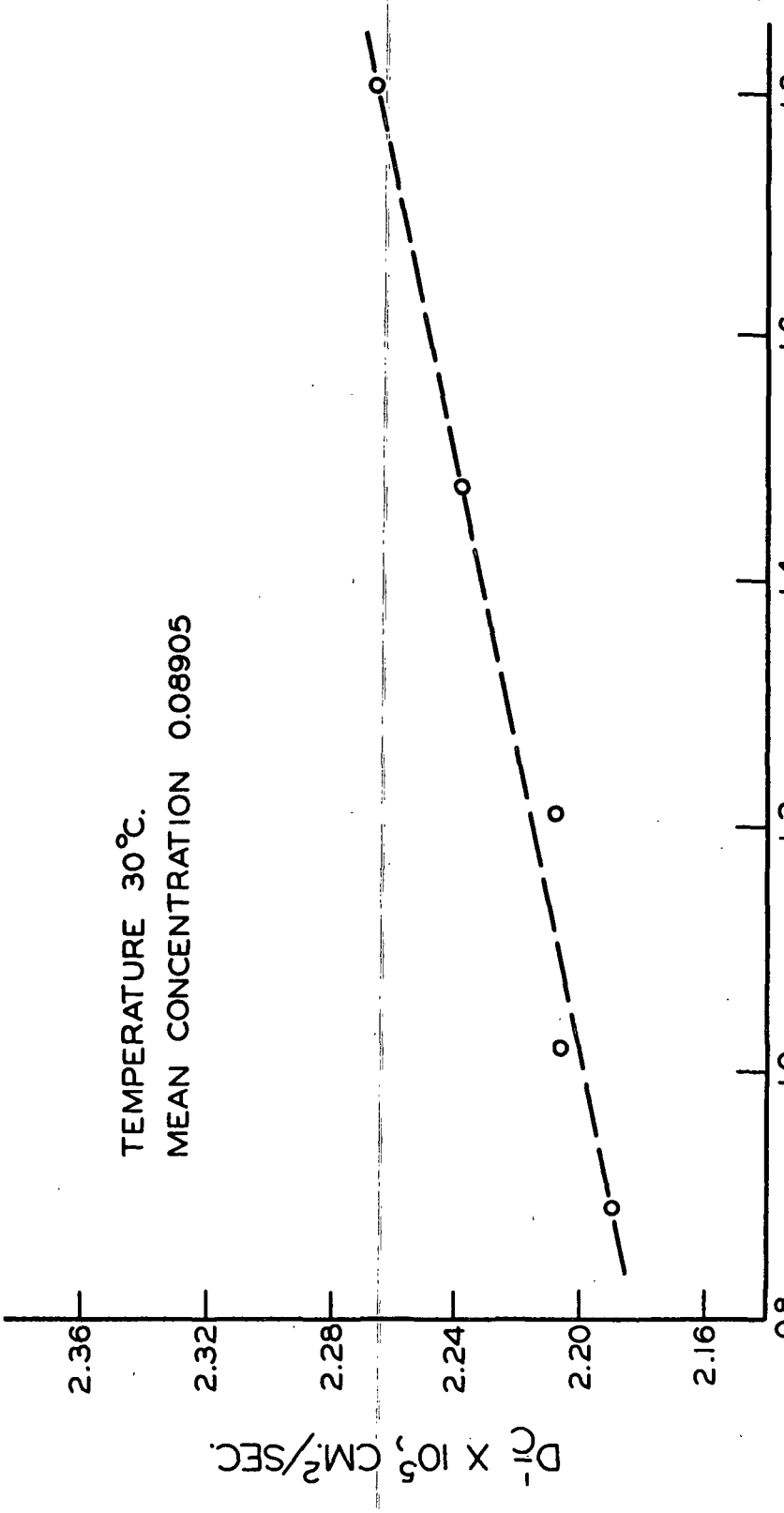

Figure 31. Zero-Time Correction of Diffusion at 30°C. at a Mean Concentration of 0.08905

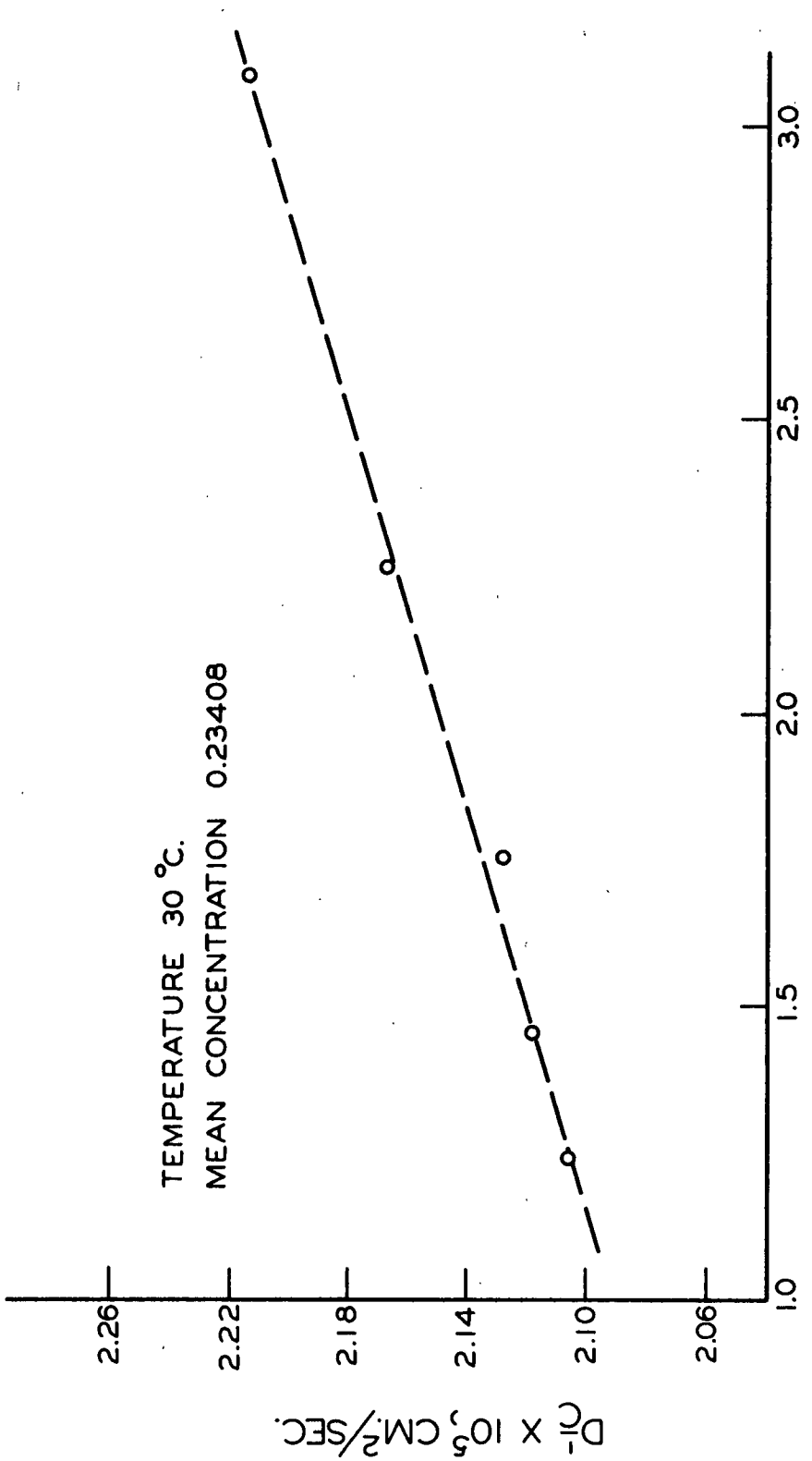

Figure 32. Zero-Time Correction of Diffusion at 30°C. at a Mean Concentration of 0.23408

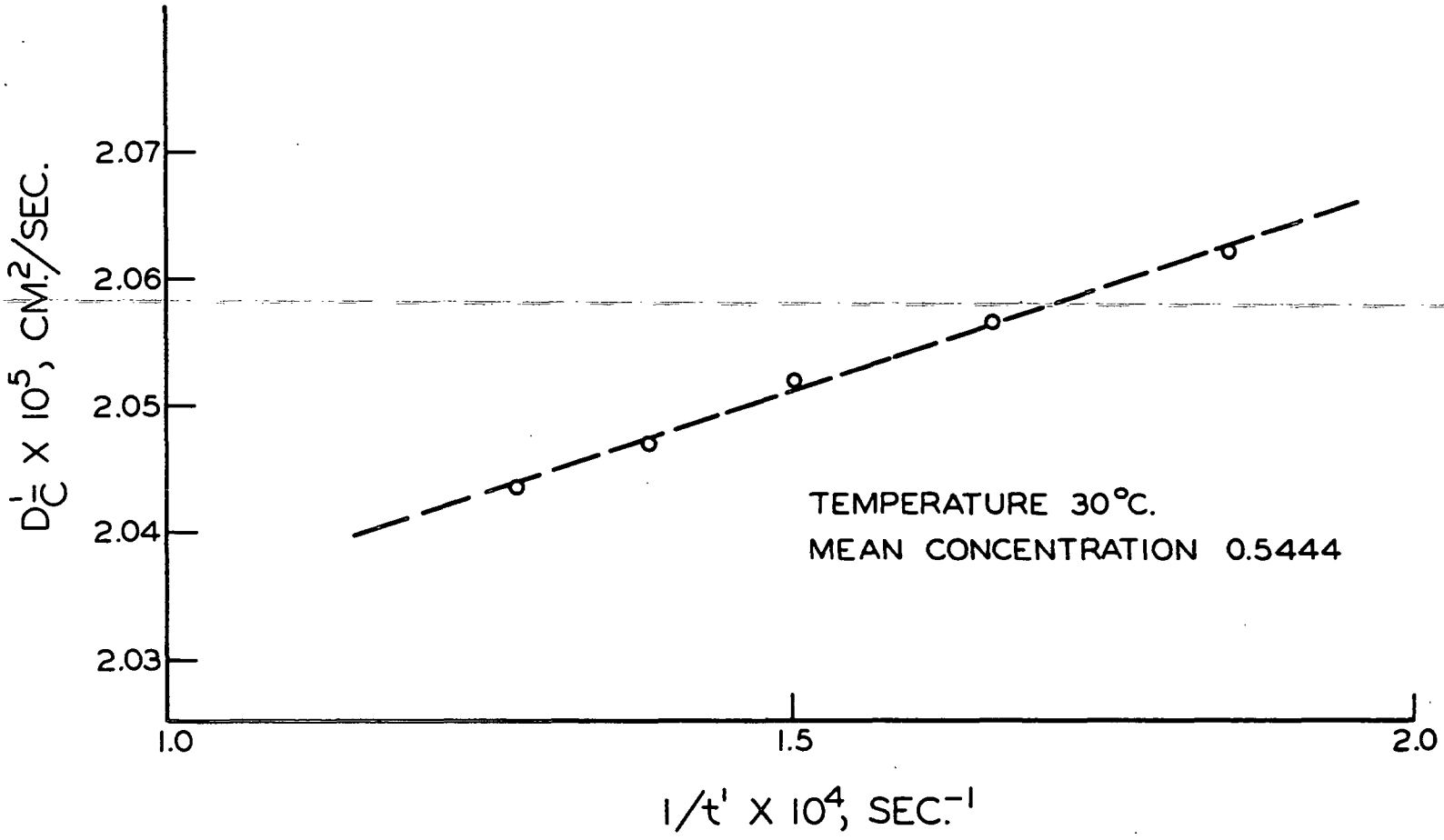

Figure 33. Zero-Time Correction of Diffusion at 30°C. at a Mean Concentration of 0.5444

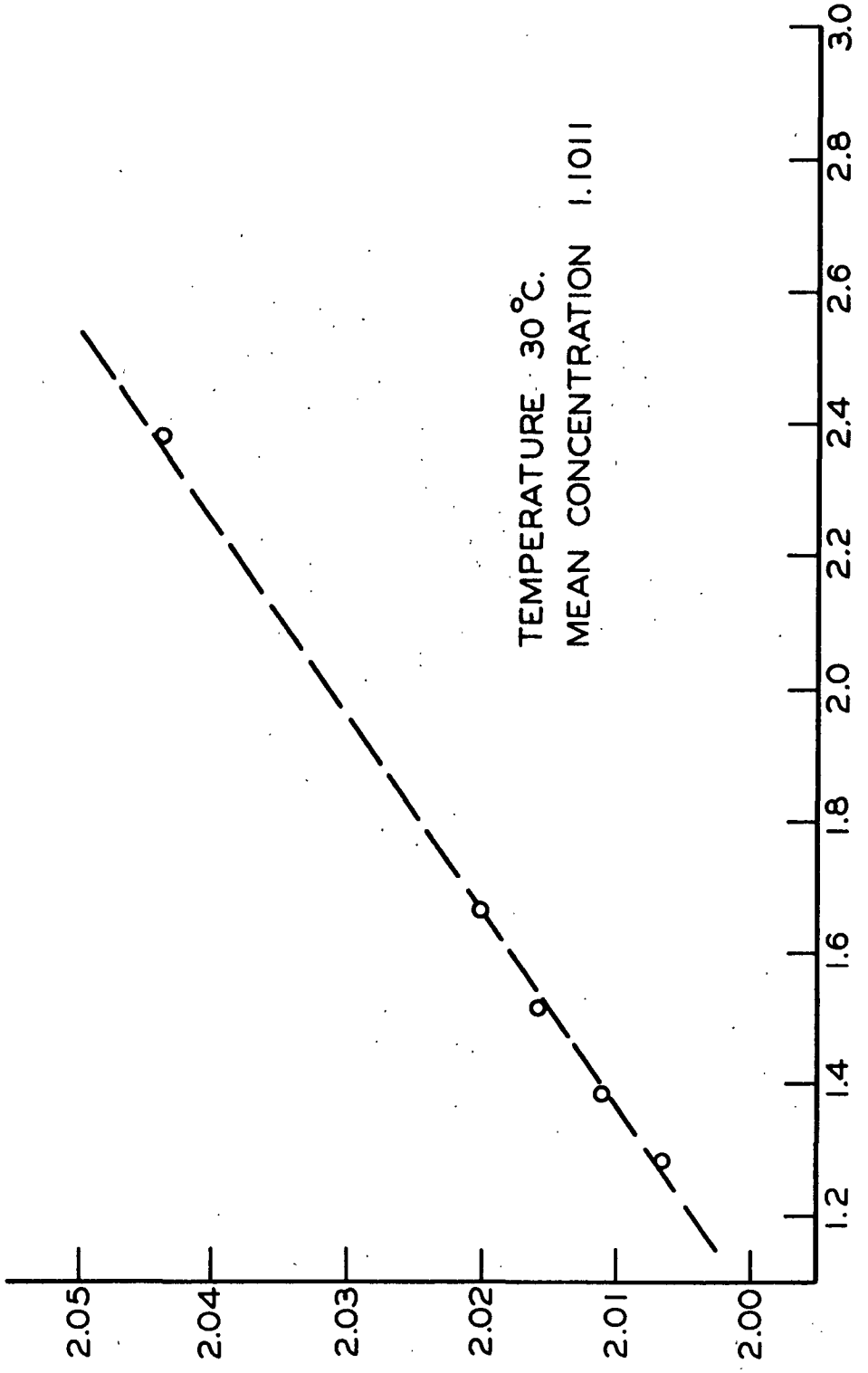

Figure 34. Zero-Time Correction of Diffusion at 30°C. at a Mean Concentration of 1.1011

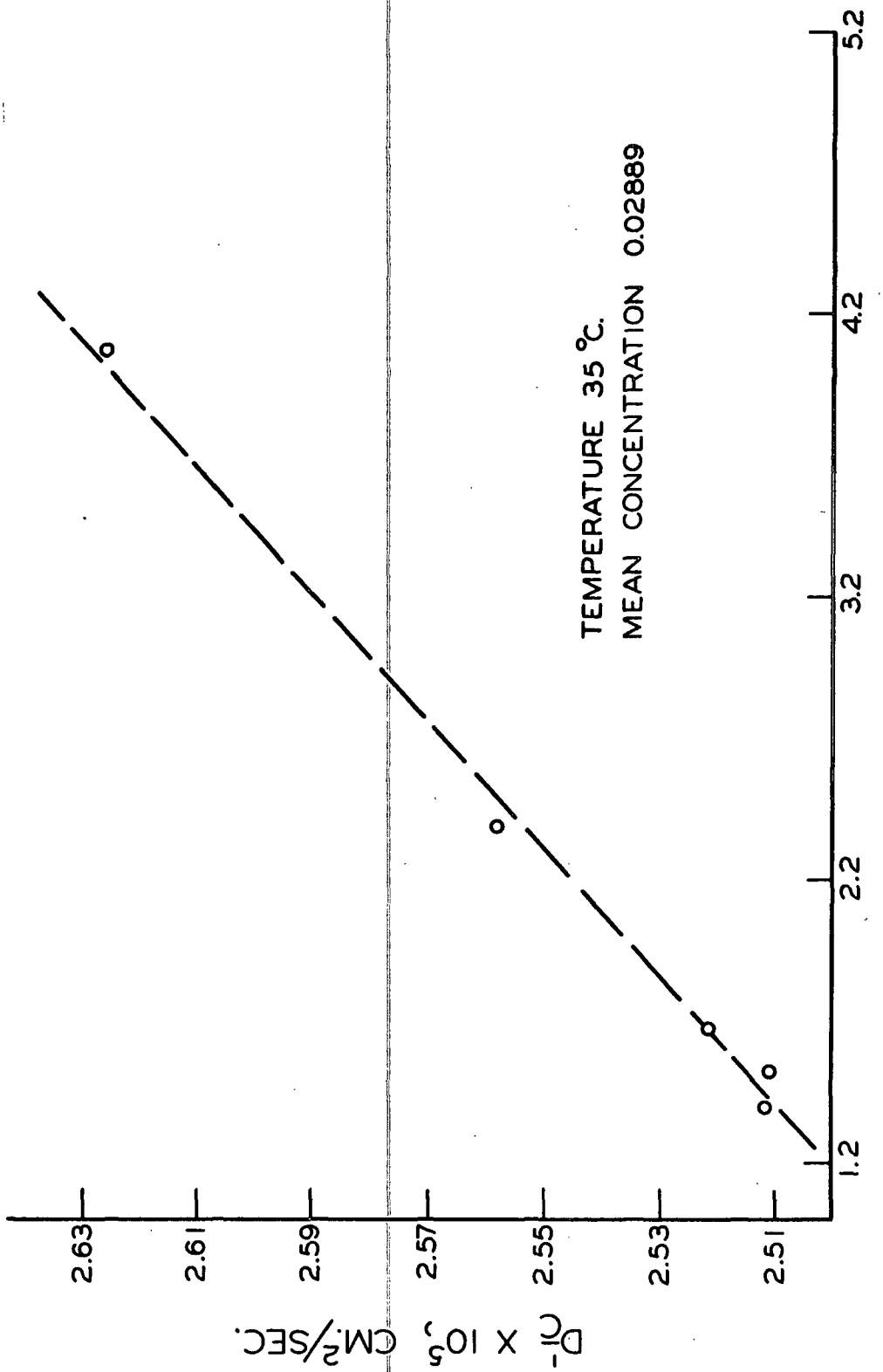

Figure 35. Zero-Time Correction of Diffusion at 35°C. at Mean Concentration of 0.02889

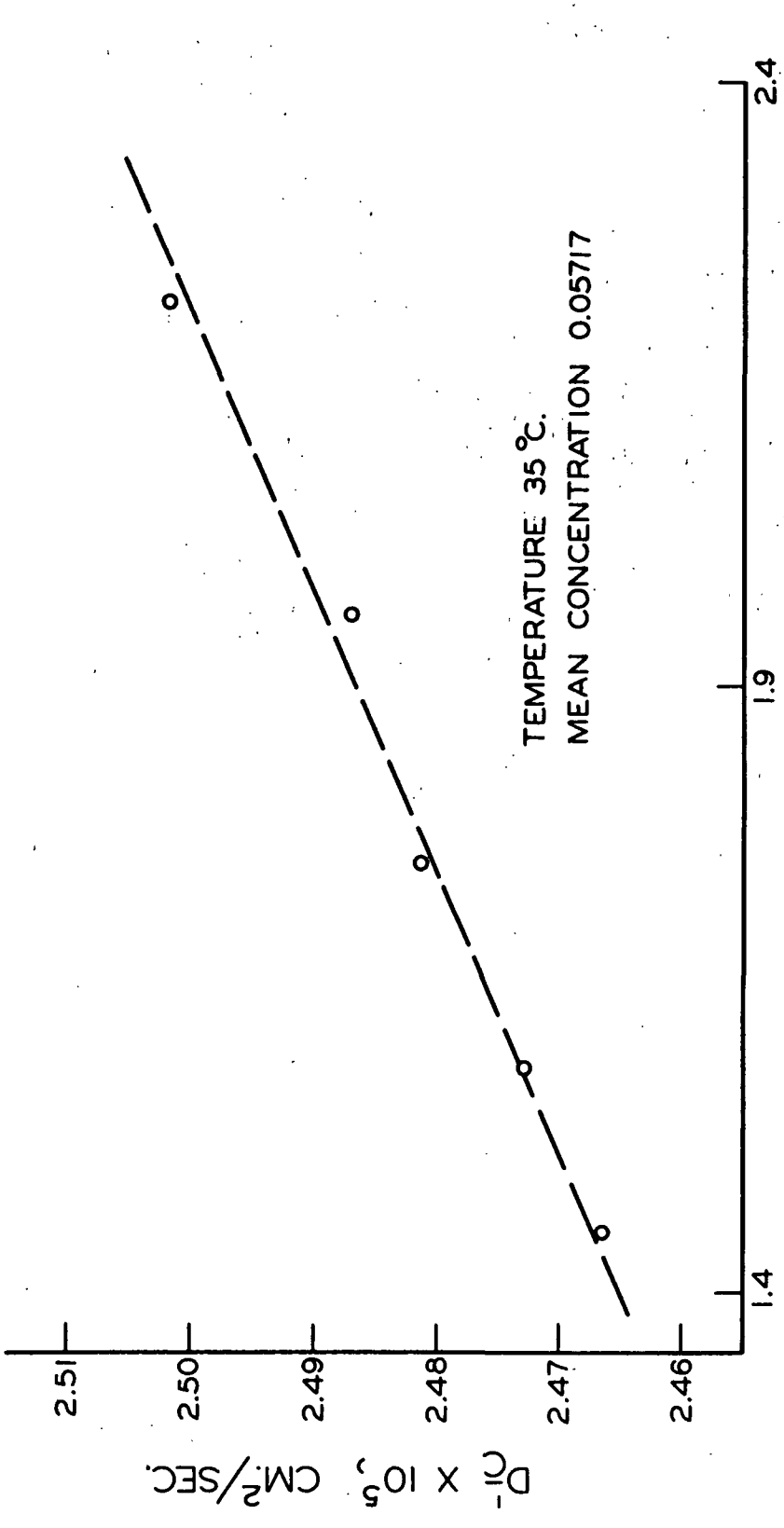

Figure 36. Zero-Time Correction of Diffusion at 35°C. at a Mean Concentration of 0.05717.

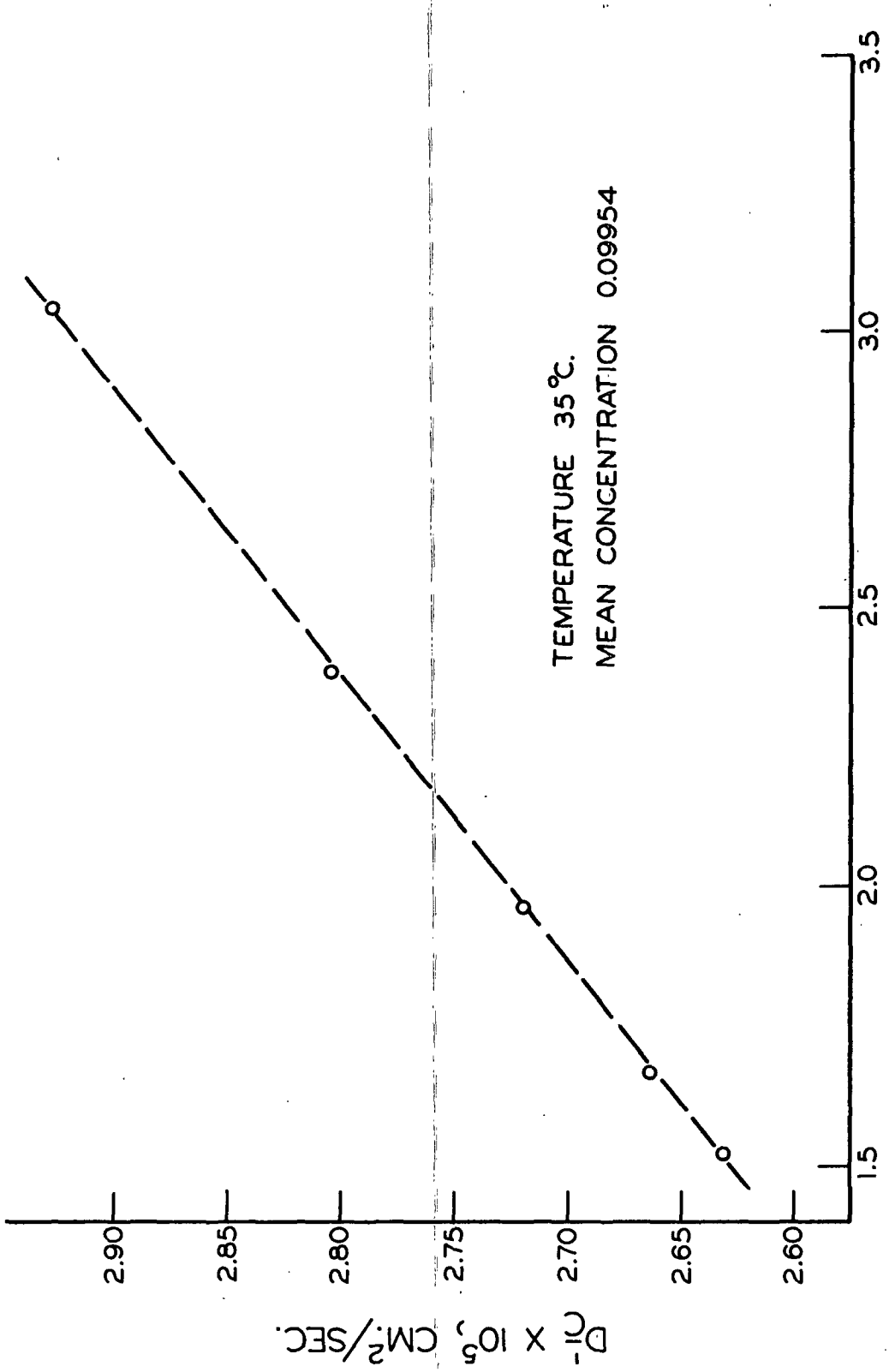

Figure 37. Zero-Time Correction of Diffusion at 35°C. at a Mean Concentration of 0.09954

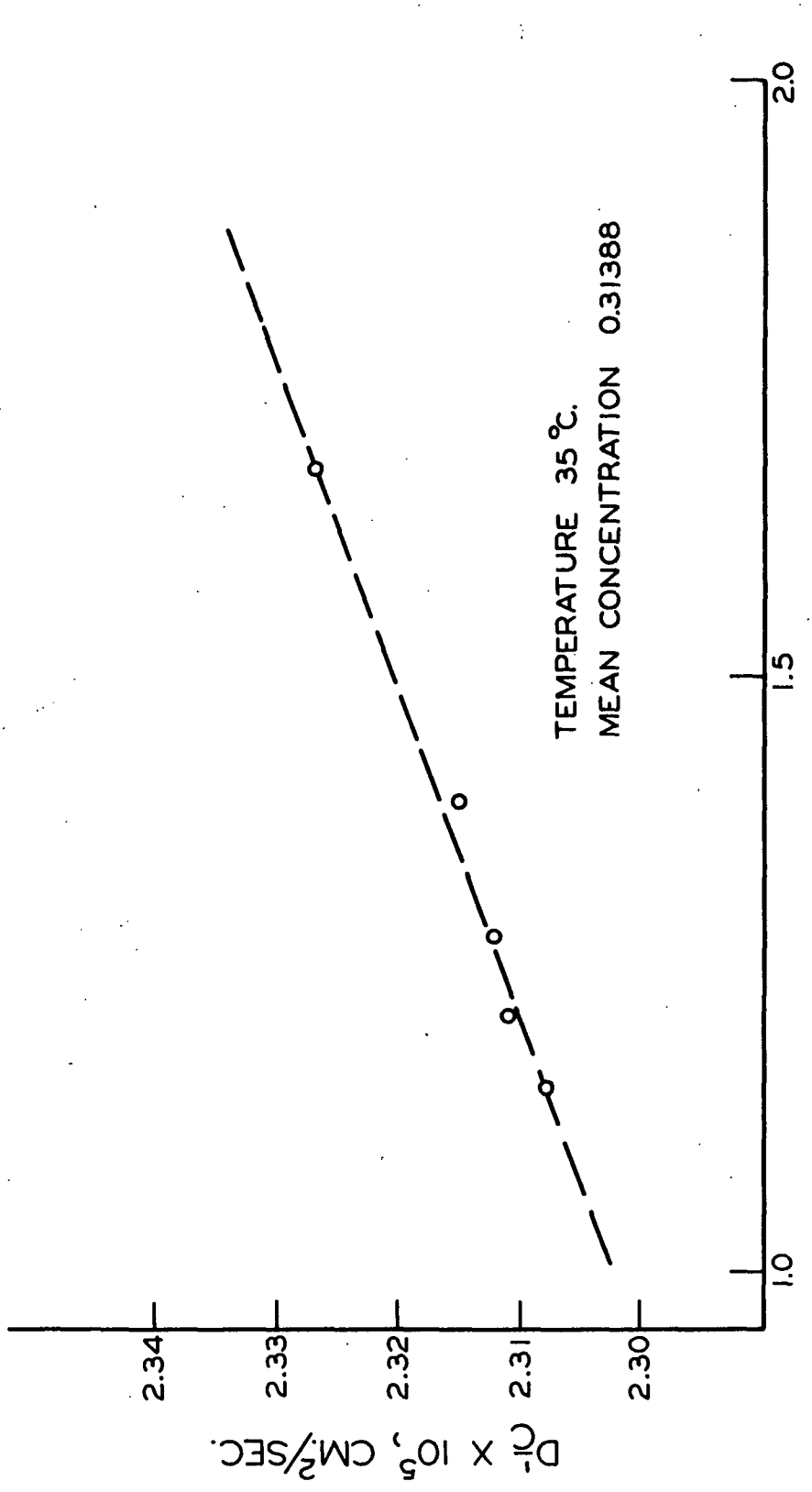

Figure 38. Zero-Time Correction of Diffusion at 35°C. at a Mean Concentration of 0.31388

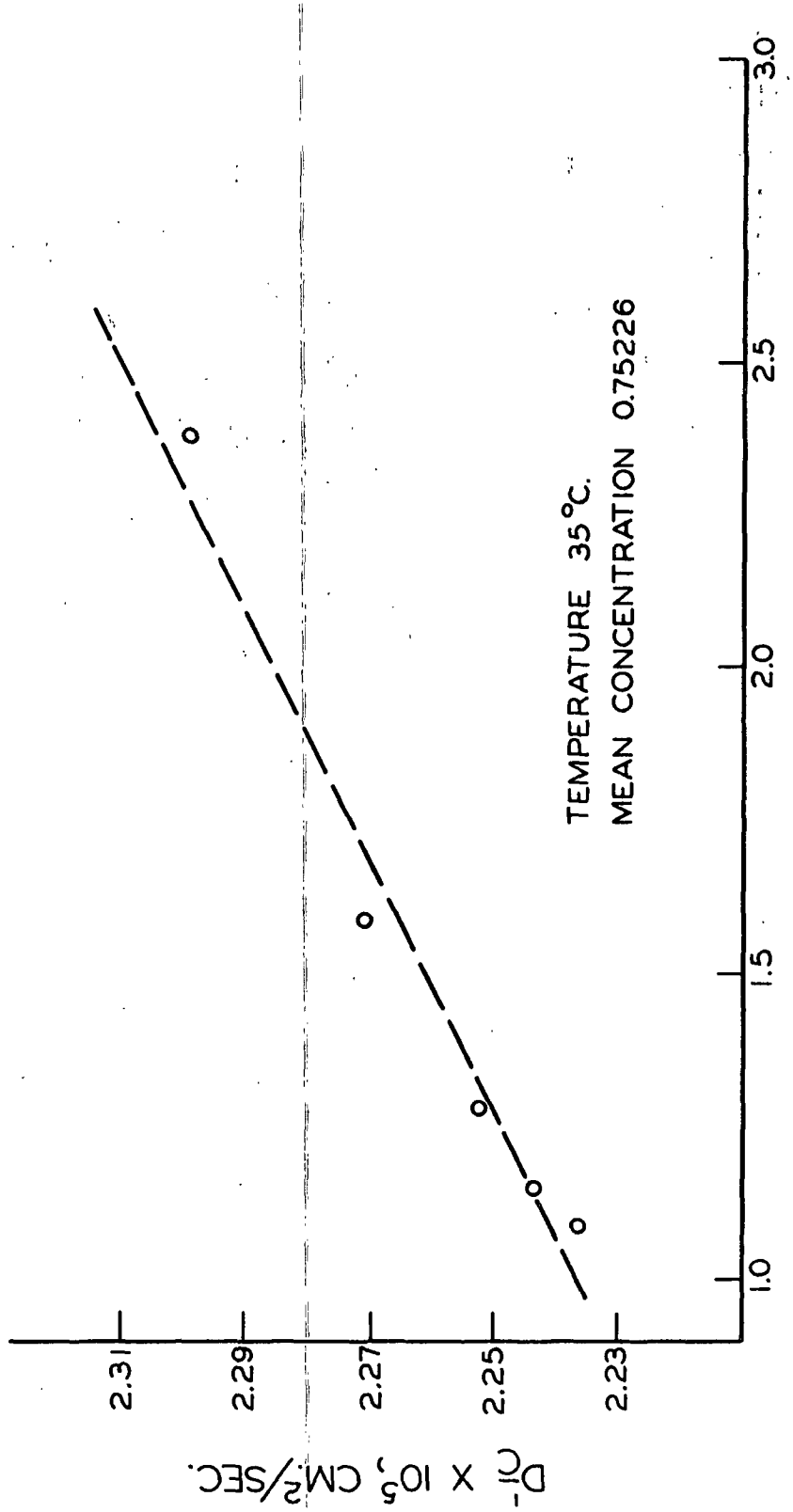

Figure 39. Zero-Time Correction of Diffusion at 35°C. at a Mean Concentration of 0.75226

APPENDIX IV

DIFFUSION OF SODIUM HYDROXIDE IN SUPPORTING ELECTROLYTES

In addition to the experimentation of principal importance to this thesis presented in the previous sections, there were two diffusion runs carried out that are of passing interest. The first of these runs was undertaken to determine whether the hydroxide ion contributed principally to the concentration-dependence of sodium hydroxide diffusion. For this run at 25°C., a solution of 0.1030N sodium hydroxide and 0.2085N sodium chloride was allowed to diffuse into 0.2085N sodium chloride. In essence, this run involved only the diffusion of sodium hydroxide through a solution of sodium chloride with the mean concentration of hydroxide being 0.0515N. Because of the presence of the sodium chloride, one would expect the diffusion coefficient to be lower than would be obtained for the same mean concentration of hydroxide alone. However, the diffusion coefficient for this run in the presence of sodium chloride was 2.146×10^{-5} cm.^{2}/sec. as compared to 1.962×10^{-5} for the diffusion coefficient of sodium hydroxide alone at the same mean hydroxide concentration. While this result was quite unexpected, it is consistent with the effect of potassium chloride on hydrochloric acid diffusion as shown by McBain and Dawson (61). An explanation of these results was not given by McBain and Dawson, and the author has been unable to explain them either.

Thinking that the above results, of sodium hydroxide diffusion in the presence of sodium chloride, were due to some type of common ion effect, it was decided to carry out a second experiment in which the sodium chloride was replaced by potassium chloride. Thus, eliminating any common ion effect, it was expected that the diffusion coefficient of the hydroxide in this case would be below that given above. Once again the result was unexpected as the diffusion

coefficient of the hydroxide was 2.282×10^{-5} cm.^{2}/sec. in this case for a mean hydroxide concentration of 0.0562N and a potassium chloride concentration of 0.2100N. As in the first run above, the result could again not be explained.

Since the above two diffusion runs were of sideline significance in this thesis and the results were not understood, it was decided that additional experimentation would not be possible. However, further investigation concerning diffusion in such mixed electrolyte systems would be quite interesting and the results would be potentially relevant to the kraft pulp process.